#### ABSTRACT

# THE KINETICS OF THE REACTION BETWEEN THE ALKALI METALS AND WATER IN ETHYLENEDIAMINE

By

#### Earl M. Hansen

Since the first direct observation of the hydrated electron in 1962, there has been a great deal of interest shown in the rates of reaction of the solvated electron (1). The rate of the reaction of the hydrated electron with water

$$e_{aq}^{-} + H_2O \longrightarrow H + OH^{-}$$
 (1)

has been measured using the technique of pulsed radiolysis and has a rate constant of  $16 \, M^{-1} \, \mathrm{sec}^{-1}$  (2). Dewald (3) and Feldman (4), using solutions of the alkali metals (mainly cesium) in ethylenediamine, measured the rate of reaction of the solvated electron with water in ethylenediamine.

In the work reported here, the stopped-flow system described by Feldman (4) was slightly modified. The glass stopcocks were replaced with Fischer-Porter greaseless stopcocks and the glass syringes and plungers were replaced with Hamilton gas tight syringes and plungers having Teflon tips.

Provision was made for cooling the photomultiplier tubes to decrease the thermionic noise, thus increasing the signal to noise ratio. An improved data analysis system, utilizing a Varian C-1024 Time Averaging Computer is also described.

The results of this investigation show that the reaction of sodium with water is second order in water at water concentrations greater than 1 M, and the decay of the 660 nm absorption band (V-band) is nearly first order in the absorbance. The reactions of potassium, rubidium and cesium with water are all apparently first order in water, but the decay of the optical absorption during the reaction is not simply first- or second-order in the absorbance.

The data for the reaction of potassium, rubidium and cesium with water are treated in terms of a mechanism involving an equilibrium among the species present (solvated electrons, electron-paired species and "ammonia-like" aggregates) with the slow step being the reaction of any one or all of the reducing species with water. The results are consistent with current models for metal-amine solutions. Improvement in the internal consistency of rate constants is due to improved kinetic control.

The mechanism for the reaction in ethylenediamine is shown to be different from that which is suggested for the same reaction in liquid ammonia (5).

The rates of the reactions:

Cs solutions (1280 nm) + Na<sup>+</sup> 
$$\longrightarrow$$
 V-species (660 nm) + Cs<sup>+</sup> (2)  
Rb solutions (890 nm, 1280 nm) + K<sup>+</sup>  $\longrightarrow$  K solutions (850 nm, 1280 nm) + Rb<sup>+</sup> (3)

were also investigated. These reactions are extremely fast  $(t_{\frac{1}{2}} < 10^{-3} \text{ sec})$  and the results of these studies are of a qualitative nature. The importance of these results in relation to the mechanism described above is discussed.

The mechanism of the formation of molecular hydrogen during the reaction of the alkali metals with water in ethylene-diamine has also been investigated. It is found that not more than 2% of the hydrogen formed in this reaction comes from the  $\alpha$ -position of the solvent. Other possible mechanisms for molecular hydrogen formation are discussed.

The purple color observed in decomposed rubidium ethylenediamine solution is shown to be due to pyrazine anion. The mechanism of its formation is unknown but may be important to the chemistry of metal-amine solutions.

#### REFERENCES

- 1) J. K. Thomas, Rad. Res. Rev., 1, 183 (1968).
- E. J. Hart, S. Gordon and E. M. Fielden, <u>J. Phys. Chem.</u>, 70, 150 (1966).
- 3) R. R. Dewald, Ph. D. Thesis, Michigan State University, East Lansing, Michigan, 1963.

- 4) L. H. Feldman, Ph. D. Thesis, Michigan State University, East Lansing, Michigan, 1966.
- 5) R. R. Dewald and R. V. Tsina, Chem. Commun., 647 (1968).

# THE KINETICS OF THE REACTION BETWEEN THE ALKALI METALS AND WATER IN ETHYLENEDIAMINE

By Earl M. Hansen

#### A THESIS

Submitted to
Michigan State University
in partial fulfillment of the requirements
for the degree of

DOCTOR OF PHILOSOPHY

Department of Chemistry

G62785 7-1-70

To Colleen

#### ACKNOWLEDGMENTS

The author wishes to express his sincere appreciation to Professor James L. Dye for his patience, guidance and encouragement throughout the course of this work.

He also wishes to acknowledge the help of Dr. Vincent A. Nicely and Dr. John Bartelt for help with the computer programs used.

Financial assistance from the United States Atomic Energy Commission is gratefully acknowledged.

# TABLE OF CONTENTS

																					Page
ı.	INTR	ODUCT	ON		•		•	•		•	•	•	•	•	•	•	•	•	•		1
II.	HIST	ORICAI	٠.		•		•	•	•	•	•	•	•	•	•	•	•	•	•	•	3
	В.	Meta: Meta: Radia	L-Am:	ine	Ch	emi	str	Y	•	•	•	•	•	•	•	•	•	•	•	•	3 11 15
III.	EXPE	RIMENT	TAL		•		•	•	•	•	•	•	•	•	•	•	•	•	•	•	21
	B. C. D. E. F.	Solve Metal Solut Cover Solut 1.	Vacuent I Vacuent I L Purice Pring Cion Meta Wate Sali Ded-I Rapic Anai	sswa uri cifi urifi Gas Presi er So Flow clysi nce	are ifi ifi ica ifi pa io	chnication ation in the contraction in the contract	ean iquion n. on fic on on em em ste	in les	g io epepa ts	Pr · · · · · · · · · · · · · · · · · · ·	oc. at at ti	icion	lur	· es						• • • • • • • • • • • • • • • • • • • •	21 21 22 27 28 30 30 34 35 43 46 50 52
IV.	RESU	LTS A	D D	sct	JSS	ION	•	•	•	•	•	•	•	•	•		•	•	•	•	54
	В.	2. 3.	Li Mo Ces: Sod: Rub:	eta] ium ium idiu	Ls • • m	Plus	s W	at • • • •	er • • ss	iu	m	•	•	•	•	•	•	•	•	•	54 76 76 81 92 106
	<b>.</b>	Band 1. 2.	Ces:	Lum	рl	.usˈ	Nad			•	•				•	•			•	•	106 106 108

TABL	<b>E</b> O:	F COI	NTEN	TS –	<b>-</b> c	on	ti	.nu	ed														Page
	D. E.	Sumr	nary gest	ion	·s	fo	·	Fu	ıtu	re	• W	Ior	·k	•	•		•	•	•	•	•	•	114 115
LIST	OF	REFI	EREN	CES	•	•	•	•	•	•	•	•	•	•	•	•	•	•	•	•	•		117
APPE	NDI	CES.		•	•	•	•	•	•	•	•	•	•	•	•	•	•	•	•	•	•	•	117
	Α.	A De	etai the																			•	123
•	В.	Desc Data	~	tio •	n •	of •	•	on	ipu •	te •	r •	Pr •	09	ra •	m	fo.	r •	An	al •	Lyz •	ir •		133
		Obse Rubi																				•	138

# LIST OF TABLES

Page		TABLE
8	Comparison of Experimental and Theoretical Values for Some Properties of the Ammoniated Electron	I.
18	Properties of the Hydrated Electron	II.
53	Results from Tritium Experiment to Check Origin of Molecular Hydrogen in Reaction of Cesium with Water in Ethylenediamine	III.
62	Conductance of Cesium, Sodium and Potassium Hydroxides in "Wet" Ethylenediamine	IV.
80	. Values of $k_{M^-}$ and $k_{e^-}$ Calculated from the Best Fit of Equation 39 to the Data Obtained for the Reaction of Cesium with Water in Ethylenediamine	V.
82	. Values of $k_{\hat{M}}-$ Calculated from the Best Fit of Equation 40 to the Data Obtained for the Reaction of Cesium with Water in Ethylenediamine	VI.
89	. Values of the Rate Constant for the Reaction of Sodium with Water in Ethylenediamine	VII.
96	. Values of k <sub>M</sub> - Calculated for the Reaction of Potassium with Water in Ethylenediamine Calculated Using Equation 39	VIII.
102	. Values of $k_{M^-}$ Calculated from the Best Fit of Equation 40 to the Data Obtained for the Reaction of Rubidium with Water in Ethylenediamine.	IX.

# LIST OF FIGURES

FIGURE	Page
1. First distillation train used for purifying ethylenediamine	23
2. Vessel used for freeze purification of ethylenediamine	25
3. Second distillation train used for purifying ethylenediamine	26
4. Vessel used to prepare metal solutions used in the kinetic studies	29
5. Apparatus used for preparing metal solutions used in the initial kinetic studies of this work [from Dewald (89)]	31
6. Stopped-flow system	36
7. Block diagram of rapid-scan system	37
8. Jig assembly used for the drilling of the quartz flow cells	41
9. aCross section of the four-jet mixing cell showing the nearly tangential entry of the four jets, bFinished flow cell	42
10. Typical oscilloscope trace used for data analysis in the initial studies of this work .	47
11. Block diagram of the CAT data analysis system.	49
12. Apparatus used to measure the conductances of the alkali metal hydroxides in ethylenediamine	51
13. Shape of the IR-band as a function of the initial water concentration and the extent of reaction during the reaction of cesium with water in ethylenediamine	<b>5</b> 6

# LIST OF FIGURES -- continued

FIGURE		Page
14. Decay of the 890 nm absorption of a rubid solution during reaction with water in et diamine. Also shown is the behavior of log(Abs.) and 1/(Abs.) for this push	hylene-	58
15. Plot of specific conductance <u>vs</u> . hydroxide concentration for cesium hydroxide in "we ethylenediamine		64
16. Plot of initial absorbance vs. push number the reaction of cesium, sodium and rubidi with water, in ethylenediamine	Lum	75
17. Comparison of observed decay of the absorwith that given by the best fit of Equation for the reaction of cesium with water in ethylenediamine		78
18. Fit of Equation 39 to observed decay at a ance for reaction of cesium with water who long tail is observed		<b>7</b> 9
19. Plot of $k_{M^-}$ , calculated from Equation 40, sus water concentration for the reaction cesium with water in ethylenediamine	of	84
20. Decay of 660 nm band of sodium during the tion with water		86
21. Plot of $\log \mathcal{K}$ <u>vs</u> . log (water concentration the reaction of sodium with water in ethy diamine. The line drawn has a slope of the solution of the solu	/lene-	87
22. Band shape and position of the 660 nm bar sodium as a function of the initial water centration and the extent of reaction	con-	88
23. Typical spectrum observed for potassium i ethylenediamine, showing the presence of V-band in addition to the R- and IR-bands	a	94
24. Plot of log (Abs.) versus time for the reof potassium with water in ethylenediaming		95
25. Typical spectrum of rubidium solutions us this work		98

# LIST OF FIGURES -- continued

FIGURE	Page
26. Typical decay of the rubidium spectrum during the reaction with water. The decay of both the R- and IR-bands can be seen	99
27. R-band obtained by subtraction of cesium, IR-band from the rubidium spectrum observed in the kinetic studies. Before the subtraction was performed, the absorbances of the two spectra were normalized at 1100 nm	104
28. Comparison of the R-band shape from Figure 27 with that obtained by subtraction of spectrum near the end of the reaction with water from the spectrum observed at the beginning of the reaction	105
29. Spectrum observed after mixing a solution of sodium bromide and cesium in ethylenediamine.	107
30. Optical spectrum observed before and after mixing a solution of rubidium and potassium bromide in ethylenediamine. Curve A is the spectrum observed before mixing and Curve B that observed after the push	109
31. Operational block diagram of program KENANAL .	134
32. EPR spectrum of the pyrazine anion formed in decomposed rubidium-ethylenediamine solutions.	140

#### I. INTRODUCTION

The existence of ammoniated electrons as the colored species in alkali metal-ammonia solutions was first suggested by Kraus in 1908 (27). However, only recently has the existence of the solvated electron in other media been demonstrated (67). Since the discovery of the optical absorption of the hydrated electron by Hart and Boag in 1962 (67), over 600 reactions of this species have been characterized (69).

The properties of metal-ammonia and metal-amine solutions have been studied by a number of investigators and will be discussed in Chapter II. Dewald, Dye, Eigen and DeMaeyer (97) first examined the reactions of "stable" solvated electrons with water by studying the reaction of a dilute cesium solution with water in ethylenediamine using the stopped-flow technique. Feldman (90) continued these studies and suggested that the reaction proceeds via two parallel pseudo-first-order processes with rate constants of  $20\text{M}^{-1}$  sec<sup>-1</sup> and  $5\text{M}^{-1}$  sec<sup>-1</sup>. However, the rate constants measured by Feldman showed a large amount of scatter.

In this research, the earlier studies of Dewald and Feldman were extended. However, the use of a rapid scanning

monochromator and a better data analyzing system showed that the reactions of cesium, rubidium, and potassium solutions with water in ethylenediamine probably do not proceed through parallel first order reactions. Instead the kinetic behavior appears to be complex.

New experimental results, not available to the previous investigators, have drastically altered the interpretation of the behavior of metal-amine solutions. A major goal of this work has been the formulation of a reaction mechanism which is consistent with all available information about metal-amine solutions.

#### II. HISTORICAL

#### A. Metal-Ammonia Chemistry

When alkali or alkaline earth metals are dissolved in liquid ammonia, primary aliphatic amines or certain ethers, metastable blue solutions are formed, with no net chemical reaction. The characteristic blue color of these solutions was first observed in 1864 by Weyl (1), who called them "metal-ammoniums."

Since solutions of alkali metals in these solvents are metastable, extreme care must be exercised to ensure proper cleanliness and purity of materials. Impurities such as water, carbon dioxide, transition metals and surface contaminants are thought to catalyze the decomposition reaction with the solvent,

$$M + NH_3 \longrightarrow MHN_2 + \frac{1}{2}H_2 \tag{1}$$

and can lead to inconclusive results. Kirschke and Jolly (2) and more recently, Schindewolf (3) have shown that the reverse of Reaction 1 can be made to occur to a slight extent under the proper conditions.

The unusual chemical and physical properties of dilute solutions of alkali metals in liquid ammonia have stimulated

the interest of a large number of investigators and have been studied by a variety of experimental methods. These investigations have been extensively reviewed elsewhere (4-11) and will not be discussed in detail here.

In the course of the investigations of the properties of dilute metal-ammonia solutions, several models have been suggested to account for the observed properties. Unfortunately, each of these models is able to account for a few, but not all of the observed properties. Any model which is proposed for dilute metal-ammonia solutions, must be able to account for the following experimental observations:

- 1. A large volume expansion occurs when alkali metals are dissolved in liquid ammonia (12,13,14,15). The report by some investigators (12,14) of a pronounced minimum in the volume expansion of sodium and potassium solutions in liquid ammonia seems to be incorrect (15). However, if this minimum is real, it also must be accounted for by any proposed model.
- 2. All solutions have a single, broad, unstructured, asymmetric optical absorption band which peaks near 1500 nm. This absorption obeys Beer's Law from 400 to 1520 nm. up to metal concentrations as high as 0.03M with a molar extinction coefficient of approximately 4 x 10<sup>4</sup> M<sup>-1</sup>cm<sup>-1</sup> (16-18).
- 3. The molar magnetic susceptibility decreases markedly as the concentration is increased which suggests the

presence of a diamagnetic species in solution (19-21).

- 4. The electrical conductance and transference data show that the negative species in solution carries approximately 80% of the current in dilute solutions and nearly 100% in more concentrated solutions (22, 23). However, the observed mobility of the solvated electron in dilute metal-ammonia solutions is not high enough to be characteristic of a free electron (22).
- 5. Knight shifts for nitrogen and sodium nuclei as well as proton chemical shifts are observed in sodium-ammonia solutions (24,25). The EPR spectrum of metal-ammonia solutions consists of a single narrow line (21).

Before discussing the various aspects of the models which have been proposed for metal-ammonia solutions, it will be useful to examine, in a qualitative way, the various species which are suggested by the above experimental observations.

Since the conductance data indicate that the major current carrier is negatively charged and the EPR data indicate the presence of unpaired electron spins, the major species present in metal-ammonia solutions is probably the solvated (ammoniated) electron. The conductance data also suggest the presence of a non-conducting species in solution. The most likely stoichiometry of this species is M, and it is probably an ion pair formed by the interaction of a solvated metal cation and a solvated electron (26).

As mentioned above, the magnetic susceptibility data suggest the presence of a diamagnetic species in addition to the M unit and the solvated electron. This species could be two electrons in the same cavity with their spins paired. However, optical and volumetric data suggest the presence of ion-paired species such as  $M^-$  ( $e^- \cdot M^+ \cdot e^-$ ) and  $M_2$  ( $M^+ \cdot M^-$ ). The models discussed below include some or all of these species. However, none of these models adequately describes all of the observed physical and chemical properties of metal-ammonia solutions.

The first model for metal-ammonia solutions was that suggested by C. A. Kraus (27). He proposed that solvated metal ions and solvated electrons as well as undissociated metal atoms were present in dilute metal-ammonia solutions. In 1946, Ogg (28) postulated that the solvated electron occupies a spherical cavity in which it is trapped by the surrounding ammonia molecules. Assuming the electrons to be confined in this cavity by an infinite potential well created by the surrounding solvent molecules, Ogg estimated the cavity radius and the enthalpy of solution of the solvated electron. The cavity radius calculated in this manner was too large (10Å) and the calculated heat of solution was smaller than the experimental value.

The original cavity model of Ogg has been refined and improved by a number of investigators (29-33). The most extensive treatment of a refined cavity model is due to

Jortner (33). Jortner has applied this treatment to solvated electrons in liquid ammonia and in other solvents.

The treatment of Jortner involves application of Landau's polaron theory (34). In this type of treatment, the electron is considered to be trapped in a cavity by the polarization forces of the solvent. The electrostatic potential which results from this polarization is assumed to be constant within the cavity and continuous beyond the cavity boundary. This treatment does not restrict the electronic wave function to the cavity but allows the charge distribution to extend beyond the cavity boundary. Using this approach, Jortner obtained reasonable agreement with the experimental values for the heat of solution and optical transition energy of metal-ammonia solutions (see Table I). Jortner, Rice and Wilson (35) refined this type of calculation by using a self consistent field treatment but obtained no improvement in the agreement with existing experimental data. In fact, the agreement actually worsened.

The cluster, or BLA model has also enjoyed considerable popularity. The basis for this model was originally suggested by Coulter (37) and was later expanded by Becker, Lindquist and Alder (36). According to the cluster model, the species in dilute solutions are the metal cation and a solvated electron. As the metal concentration is increased, these two species are thought to associate into "monomer" units according to

TABLE I

COMPARISON OF EXPERIMENTAL AND THEORETICAL VALUES
FOR SOME PROPERTIES OF THE AMMONIATED ELECTRON

Reference	Cavity Radius Used	Heat of Solution (eV)	Optical Transition Energy (eV)	Oscillator Strength
Jortner (33)	3.2	1.60	0.81	0.65
JRW (35)	3.2	0.92	0.93	0.70
Land and O'Reilly (43)	3.05	3.4	1.02	0.98
Exp't. (33)		1.7±0.7	0.80	0.72

$$M_{am}^{+} + e_{am}^{-} \xrightarrow{K_{1}} M_{am}$$
 (2)

At higher metal concentrations, the model allows for the association of two monomer units to form a dimer according to

$$2M_{am} \xrightarrow{K_2} (M_2)_{am}$$
 (3)

This dimer is thought to be held together principally by exchange forces. The "cluster" or "BLA" model was used with some success in fitting conductivity and magnetic susceptibility data (38,39).

Douthit and Dye (16) and Gold, Jolly and Pitzer (26), have suggested that the monomer unit of the "cluster" model is actually an ion pair between a solvated metal cation and a solvated electron. These authors also suggested that the metal ion and solvated electron forming such an ion pair retain their individual characteristics. The "BLA" dimer is pictured as a quadrupolar assembly of two solvated electrons and two metal cations. Using these modifications, Gold, Jolly and Pitzer obtained qualitative agreement with volumetric, optical and Knight shift data.

In spite of the apparent agreement, the set of equilibrium constants for Reactions 2 and 3 calculated from conductivity data do not agree with those calculated from magnetic data. The agreement can be improved somewhat by the introduction of a third equilibrium and another species  $(M^-)$ ,

$$M_{am} = \frac{K_3}{M_{am}} + e_{am}$$
 (4)

Arnold and Patterson (39,40) and Golden, Guttman and Tuttle (41) have suggested a model which includes the species of the "cluster" model, but adds M as an additional species. The models of these authors consider M to be a diamagnetic species.

Arnold and Patterson calculated the equilibrium constants  $K_1$ ,  $K_2$ , and  $K_3$  using conductivity, magnetic susceptibility and transference number data. Although these calculations give reasonably good agreement with experiment, the calculation involves the use of three adjustable parameters to fit the data. No assumptions about the detailed nature of the various species are made in the treatment of Arnold and Patterson.

The model of Golden, Guttman and Tuttle also assumes  $M^-$  as an additional species and further assumes the dimeric species,  $M_2$ , to be an ion pair between a solvated metal cation and a solvated metal anion  $(M^+ \cdot M^-)$ . These investigators used only one adjustable parameter in fitting this model and obtained reasonable agreement with optical, Knight shift and vapor pressure data. However, Jolly (42) has pointed out that the correlation with optical data may be in error.

Recently, Dye (100) has attempted to correlate all of the experimental data for dilute metal-ammonia solutions with the stoichiometries implied by the above models. The new conductance data of Dewald and Roberts (101), which showed the earlier data to be in error in the dilute region, were used in this correlation. Dye concluded that the use of distinct species of stoichiometry  $M^+$ ,  $e^-$ , M,  $M^-$  and  $M_2$  with concentrations determined by equilibrium constants was inconsistent with the available data. He suggested that electron-electron interactions were long range in nature and could not be described by equilibria among distinct "species."

#### B. Metal-Amine Chemistry

Metal-amine solutions are more complicated than metal-ammonia solutions. It appears that in addition to the solvated electron and "loosely bound" aggregate "species" which may be present in metal-ammonia solutions, new species, which more directly involve the alkali metal, are present in metal-amine solutions. Optical and EPR studies (44-48) indicate that the species in metal-amine solutions which contain the alkali metal are more than simple ion pairs.

The optical spectra of solutions of alkali metals in ethylenediamine show one to three absorption bands (44).

One of these bands appears in the visible at about 660 nm (V-band), one in the near infrared region at 850 nm to 1030 nm (R-band), and one in the infrared (IR-band) at 1280 nm.

The V-band has been observed in ethylenediamine solutions of sodium, lithium, potassium and occasionally rubidium and cesium. The position and shape of the V-band are independent of the metal. The R-band is observed in solutions of

potassium (850 nm), rubidium (890 nm) and cesium (1030 nm) in ethylenediamine. Solutions of all the metals except sodium exhibit the IR-band. The shape and position of the infrared band are independent of the metal used.

Pulse radiolysis studies of amines (49) show the presence of a transient which has a broad optical absorption in the infrared region. The correlation of this fact with conductivity and solubility studies in ethylenediamine have led to the assignment of the IR-band to the solvated electron and its loose "ammonia-like" aggregates (see Part A, this Section).

The V-band and the non-reproducibility associated with its study has been a most troubling phenomenon (50-53). It now appears that the V-band puzzle has been solved. Hurley, Tuttle and Golden (54), have recently investigated the V-band observed in solutions of potassium in ethylamine. Analysis of metal solutions prepared in Pyrex vessels showed the presence of enough sodium to account for the V-band observed in the optical spectrum. They also found that solutions prepared in fused silica vessels exhibited no V-band and contained no sodium. DeBacker (55) has recently confirmed these observations for potassium solutions in ethylene-It now seems likely that the V-band is characteristic only of sodium solutions and that the observation of a V-band in other metal-amine solutions indicates the presence of sodium in the solution. Although the exact mechanism for the contamination of the solutions by sodium from Pyrex

glass is unknown, the metal solutions and/or the solvent, evidently leach sodium or sodium ions from the glass surface or take part in ion exchange phenomena. Although these experiments have revealed the origin of the V-band in metal-amine solutions, the detailed nature of the sodium species responsible for the V-band is still unknown.

The exact nature of the R-band remains a mystery. It has been observed that the magnitude of the R-band decreases relative to that of the IR-band as the solution is diluted or decomposed (56). This implies that the species responsible for the R-band can dissociate. Also, since the position of the R-band is metal dependent, it seems reasonable that the species responsible for this band contains the metal cation.

Dye and Dewald (56) suggested that the R-species is a solvated alkali metal dimer, similar to those found in the gas phase. They also suggested that the optical absorption arises from a  ${}^2\Sigma_u \longleftarrow {}^1\Sigma_g^{\dagger}$  transition. However, now that it has been shown that the V-band is due to the presence of sodium, it is likely that the species responsible for the R-band is of the same type as that which is responsible for the V-band observed in sodium solutions and in other metal solutions contaminated by sodium ions. Since the  ${}^1\pi_u \longleftarrow {}^1\Sigma_g$  transition is also an allowed transition which is easily observed for the gaseous alkali metal dimers, the absence of a second absorption band in sodium solutions makes it

unlikely that the species responsible for the R-band is the solvated diatomic molecule,  $(M_2)$ . Because of the strong metal dependence of the R-band, it probably does not originate from a simple ion pair such as  $M \cdot e^-$  or  $e^- \cdot M^+ \cdot e^-$ . Recently Matalon, Golden and Ottolenghi (102) have concluded that the V-band (and hence also the R-bands) can be attributed to a species  $M^-$ . They reached this conclusion by comparing the shift of the optical absorption with solvent and temperature to that of the charge-transfer-to-solvent (CTTS) band of  $I^-$ . They also showed that the variation of the peak position with metal is consistent with that expected on the basis of reasonable radii for the alkali metal anions.

The conductivity data of Dewald and Dye (50) and of Dewald and Roberts (103) show that the species responsible for the V-band in sodium solutions in ethylenediamine and in methylamine is very different from the solvated electron. Indeed, the small variation of equivalent conductance with concentration is unlike the behavior of any known system in solvents of such low dielectric constant.

EPR studies of metal-amine solutions show the presence of nuclear hyperfine splitting by the alkali metal nucleus (45-48). These studies have shown that a monomer species of stoichiometry M exists in some metal-amine solutions but only as a minor constituent (48). These workers (45-48) have also shown that the hyperfine splitting exhibited by metal-amine solutions is strongly dependent on the solvent and the temperature.

In summary, it appears that metal-amine solutions are indeed more complex than metal-ammonia solutions. Two different optical absorptions are observed. One (IR-band) has been assigned to the solvated electron and its "ammonia-like" aggregates such as  $(M^+, e^-)$ ,  $(e^- \cdot M^+ \cdot e^-)$  and  $(M^+ \cdot M^-)$ . The exact nature of the other optical absorption (R-band) is still unknown. It may be due to an alkali metal dimer or a metal anion which is not simply an ion pair. It could also be the absorption of a completely different species.

#### C. Radiation Chemistry

The chemical reactions which result from the action of ionizing radiation on matter have been studied for about seventy years. Debierne (57) suggested in 1914 that free radicals were responsible for the overall chemical effects observed in aqueous solutions of radium salts.

Lea (58) suggested in 1947 that electrons escaped from the parent ions during the radiolysis of water. Stein in 1952 (59), and Platzman (60) in 1953 suggested that these electrons could become solvated. Up until this time, it was thought that the irradiation of water produced only H-atoms and OH radicals as primary products and that the subsequent reactions of these species were responsible for the overall chemical effects (61).

The first experimental evidence for the possible existence of the hydrated electron came in 1959. Barr and Allen (62) showed that the H-atom produced during the radiolysis of aqueous solutions containing hydrogen ions, oxygen and hydrogen peroxide reacted faster with oxygen than with hydrogen peroxide. However, the H-atoms produced in solutions containing only oxygen and hydrogen peroxide reacted equally fast with the oxygen and the hydrogen peroxide.

They suggested that one of these H-atom species was probably atomic hydrogen and the other a basic or acidic form of the H-atom, as expressed by the following:

$$e_{aq}^{-} \xrightarrow{H^{+}} H \xrightarrow{H^{+}} H_{2}^{+}$$
 (5)

Further evidence for the existence of the hydrated electron came from several investigators (63-68). The most direct evidence came from the kinetic salt-effect studies of Czapski and Schwartz (65). They studied the effect of ionic strength on the rate constant ratios for reaction of the reducing species with  $H_3O^+$ ,  $O_2$  and  $NO_2^-$  to that with  $H_2O_2$ . These studies showed that the reducing species in neutral and slightly acidic solutions has a unit negative charge. These results were verified by Collinson, Dainton et al. (66), who studied the ionic strength dependence of the rate constant ratios of the reaction of the reducing species with  $Ag^+$  and acrylamide. Their studies showed that at a pH of 4, the reducing species has a unit negative charge, but that in acidic solutions (pH = 2), it is uncharged. This suggests that in acidic solutions the major reducing species is

probably the H-atom, rather than the solvated electron.

The first direct observation of the hydrated electron came in 1962 (67,68), when Hart and Boag observed a broad transient absorption band, with a maximum at about 7200  $^{\circ}A$ , after pulsing deaerated water with a beam of 1.8 MeV electrons. The observed spectrum was similar in shape to the absorption band observed in metal-ammonia solutions and its intensity was decreased by the addition of small amounts of known electron scavengers such as  $N_2O$  and  $H_3O^{\dagger}$ . Since this "discovery" of the hydrated electron, a number of its properties have been measured. These are listed in Table II.

With the advent of linear accelerators, the technique of pulse radiolysis has been extensively used to study the kinetics of hydrated electron reactions. The rates of over 600 different reactions involving the hydrated electron have been studied (69). The reaction of the hydrated electron with water,

$$e_{aq}^{-} + H_{2}O \xrightarrow{k_{1}} H + OH^{-}$$
 (6)

is important to the understanding of the nature of the hydrated electron and in comparing its properties with those of solvated electrons in other media. The kinetics of both the forward (70) and reverse (71,72) rates of Reaction 6 have been studied. The currently accepted value for  $k_1$  is  $16 \ \underline{M}^{-1} \ \text{sec}^{-1}$ , but Anbar has suggested that this may only be the upper limit for this rate constant (73). The reverse

TABLE II

PROPERTIES OF THE HYDRATED ELECTRON

Quantity	Value	Ref.
$\lambda_{ extsf{max}}$	7200 Å (1.72 eV)	82
Molar extinction coefficient at $7200\ \text{\AA}$	15,800 <u>M</u> -1 <sub>Cm</sub> -1	82
Oscillator strength	0.65	83
Solvation energy	∼40 kcal mole <sup>-1</sup>	84
Equivalent conductance	177 ohm <sup>-1</sup> cm <sup>2</sup>	85
Partial molal volume	-5.5 to -1.1cc.mole	86
$G(e_{aq}^{-})$ , $\gamma$ -ray yield in neutral water	2.6 ions/100 eV	87
$t_{\frac{1}{2}}$ in pure water at pH = 7	230 µsec	83
Diffusion constant 4	$.75 \times 10^{-5}$ cm <sup>2</sup> sec <sup>-1</sup>	85
$E^{0}(e_{aq}^{-} + H_{3}O_{aq}^{+} \longrightarrow \frac{1}{2}H_{2} + H_{2}O)$	$\leq$ 2.67 v.	84
Calculated mean radius of charge distribution	2.5-3.0 Å	88
$pK (e_{aq} + H_2O \longrightarrow H + OH^-)$	9.7	84

rate constant,  $k_{(OH^-+H)}$ , has a value of 2.2 x  $10^7 \underline{\text{M}}^{-1} \text{sec}^{-1}$ . Using these rate constants, a pK<sub>a</sub> value of 9.7 has been calculated for the H-atom.

Of particular interest to the radiation chemist has been the mechanism of molecular hydrogen production in irradiated water. It has been unambiguously demonstrated that most of the molecular hydrogen is not produced by the recombination of H-atoms but rather is produced directly by the bimolecular reaction (74):

$$e_{aq}^{-} + e_{aq}^{-} \xrightarrow{H_2O} H_2 + 2OH_{aq}^{-}$$
 (7)

Hydrated electrons can apparently also be generated in solution without exposure to high energy radiation. Walker (75,76) has recently found evidence for the presence of hydrated electrons in the reaction of sodium amalgams with water and also in the electrolysis of water.

Observations of the solvated electron in a number of liquids other than water have also been reported. Ahrens, Suryanarayana and Willard (77) reported observing a reversible increase in the electrical conductivity of liquid ammonia during exposure to  $\gamma$ -irradiation. An optical spectrum similar to that observed in alkali metal-ammonia solutions has been observed in the pulse radiolysis of liquid ammonia (78) and Ward (79) has recently reported rate constants for the reactions of the solvated electron with a variety of solutes in liquid ammonia. Sauer, Arai and Dorfman (80) investigated

the optical spectra and measured the yields of solvated electrons in several aliphatic alcohols. The existence of solvated electrons in other solvents has also been discussed by Dorfman (81).

#### III. EXPERIMENTAL

#### A. General Laboratory Procedures

#### 1. Glassware Cleaning Procedure

All glassware was first rinsed in a hydrofluoric aciddetergent cleaning solution (5% HF, 33% HNO3, 2% acid soluble
detergent, 60% distilled water). This was followed by at
least ten rinses with distilled water. The glassware was
then immersed in boiling aqua regia and then rised at least
ten times in doubly distilled conductance water. Vessels
which were to contain the metal solutions were subsequently
filled with conductance water and heated gently. For later
runs, this steaming process was followed by a washing with
anhydrous liquid ammonia. In these cases, all other solution
vessels were also washed with liquid ammonia prior to solution preparation.

### 2. Vacuum Techniques

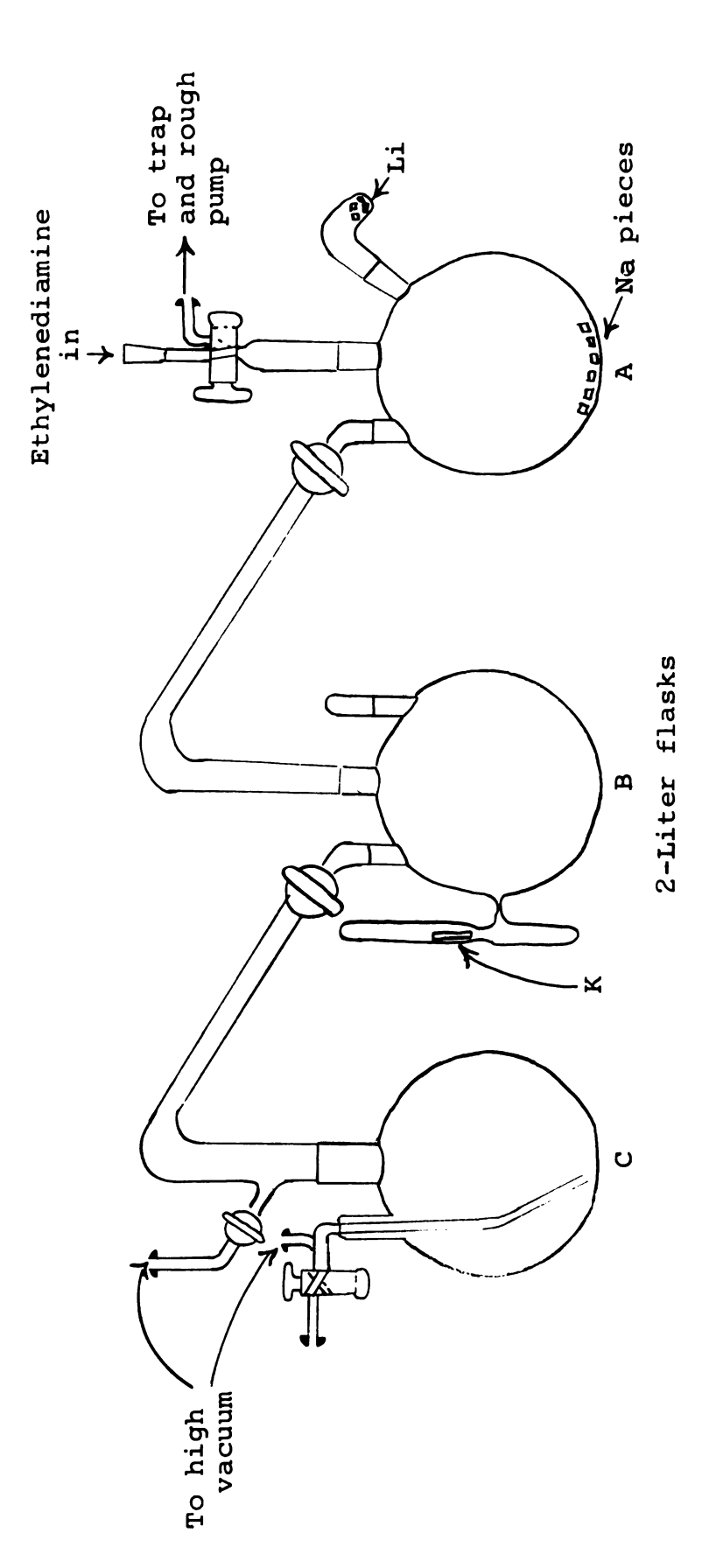
High vacuum techniques were used wherever possible.

Pressures of 10<sup>-5</sup> torr were obtained using either two-stage mercury vapor diffusion pumps or two-stage oil diffusion pumps. Pressure measurements were made using a calibrated Veeco RG75P ionization gauge with a Veeco RGLL-6 power supply.

Dow Corning high vacuum silicone grease was used on all stop-cocks which came into contact with liquid. Apiezon W wax was used on all joints and tapers. In later work Fischer-Porter "quick opening" Teflon valves and "Solv-Seal" Teflon joints were used on the stopped-flow system and on all solution vessels and Delmar-Urry Teflon valves were used on the freeze-purification vessels. Breakseals were used on solution vessels and on ampoules containing metal and solute samples.

#### B. Solvent Purification

Ethylenediamine (Matheson, Coleman and Bell 98-100% or Dow Chemical 98-100%) was purified in one of two ways. the first method, the ethylenediamine was first poured into an evacuated five liter separatory funnel. It was slowly frozen. A core was then melted from the center and this portion was discarded. The remaining solvent was thawed and slowly refrozen. This procedure was repeated at least six The ethylenediamine was then poured into an evacuated vessel which contained pieces of sodium and lithium (Figure 1, Flask A). The resulting blue solution was degassed twice by slowly freezing it with an ice-water bath. After degassing, the solvent was vacuum distilled into Flask B which contained a potassium mirror. Any hydrogen formed by the decomposition reaction was periodically pumped off. The solvent was distilled into storage Flask C, covered with nitrogen and



First distillation train used for purifying ethylenediamine. Figure 1.

used as needed. It was discovered that this storage vessel was not vacuum tight and another purification scheme was devised.

The freeze-purification procedure was carried out as described above with two exceptions. Instead of using a separatory funnel with large greased stopcocks, a five liter round-bottom flask equipped with Delmar-Urry Teflon valves was used (Figure 2). The freeze-purification procedure was repeated at least eight times. Attempts to prepare a stable metal solution using only the freeze-purified solvent were unsuccessful. The distillation train was also redesigned (Figure 3). The freeze-purified ethylenediamine was admitted to Flask A which contained sodium-potassium alloy with an excess of potassium. The solvent was then distilled through a coarse fritted glass filter into storage vessels equipped with breakseals. The purpose of the coarse glass filter was to prevent any possible splash-carry-over of the metal. The solvent was thoroughly degassed by repeated freeze-pump-thaw cycles until the pressure after any two consecutive cycles was less than  $1 \times 10^{-6}$  torr. These vessels were then sealed off under vacuum. The solvent in these vessels was used as needed by breaking the breakseal with a magnet encased in glass and the solvent distilled as needed. Both of the above techniques are extremely slow due to the low volatility of the ethylenediamine and because hydrogen formation from the decomposition reaction during the distillation slowed the distillation considerably.

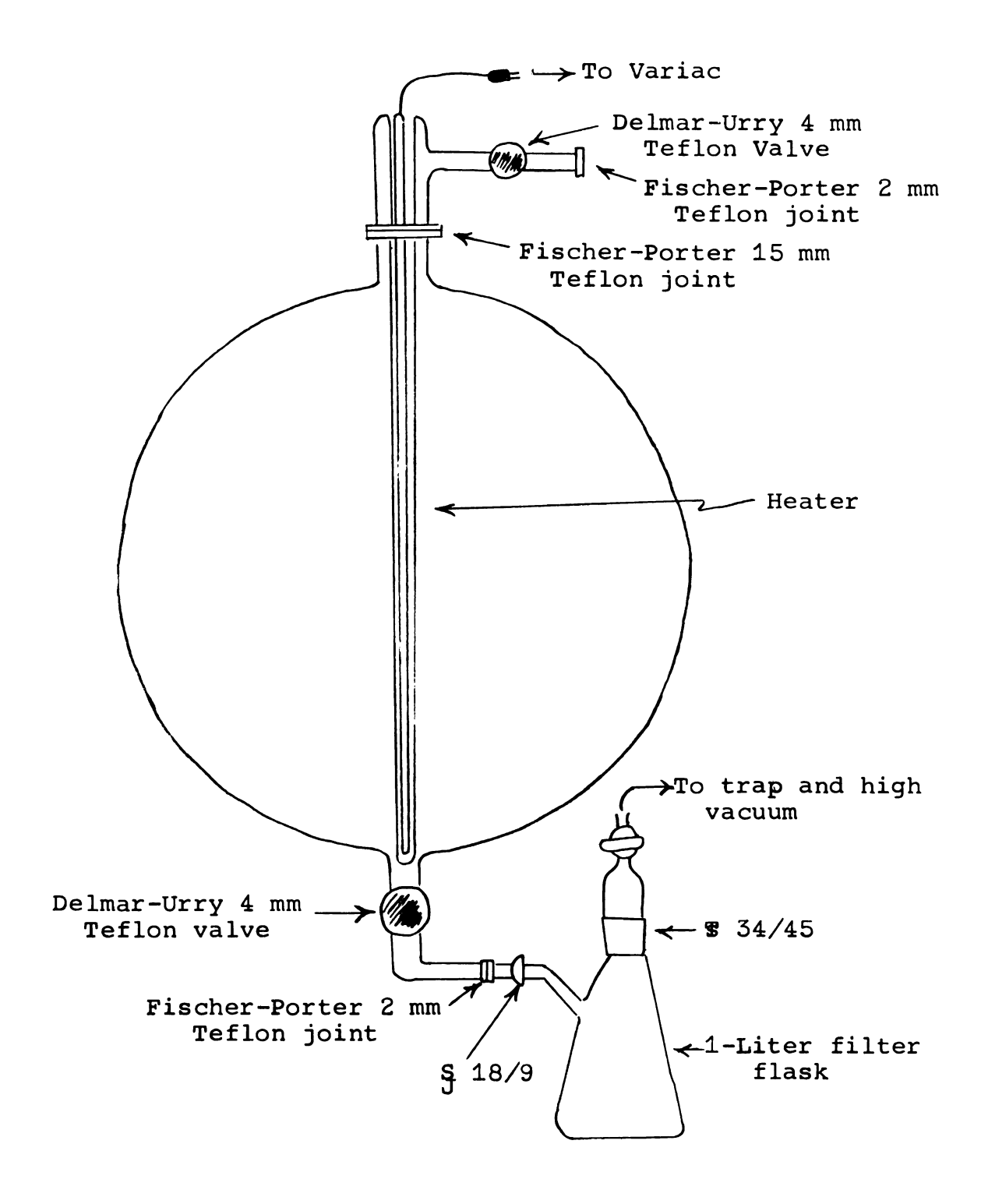
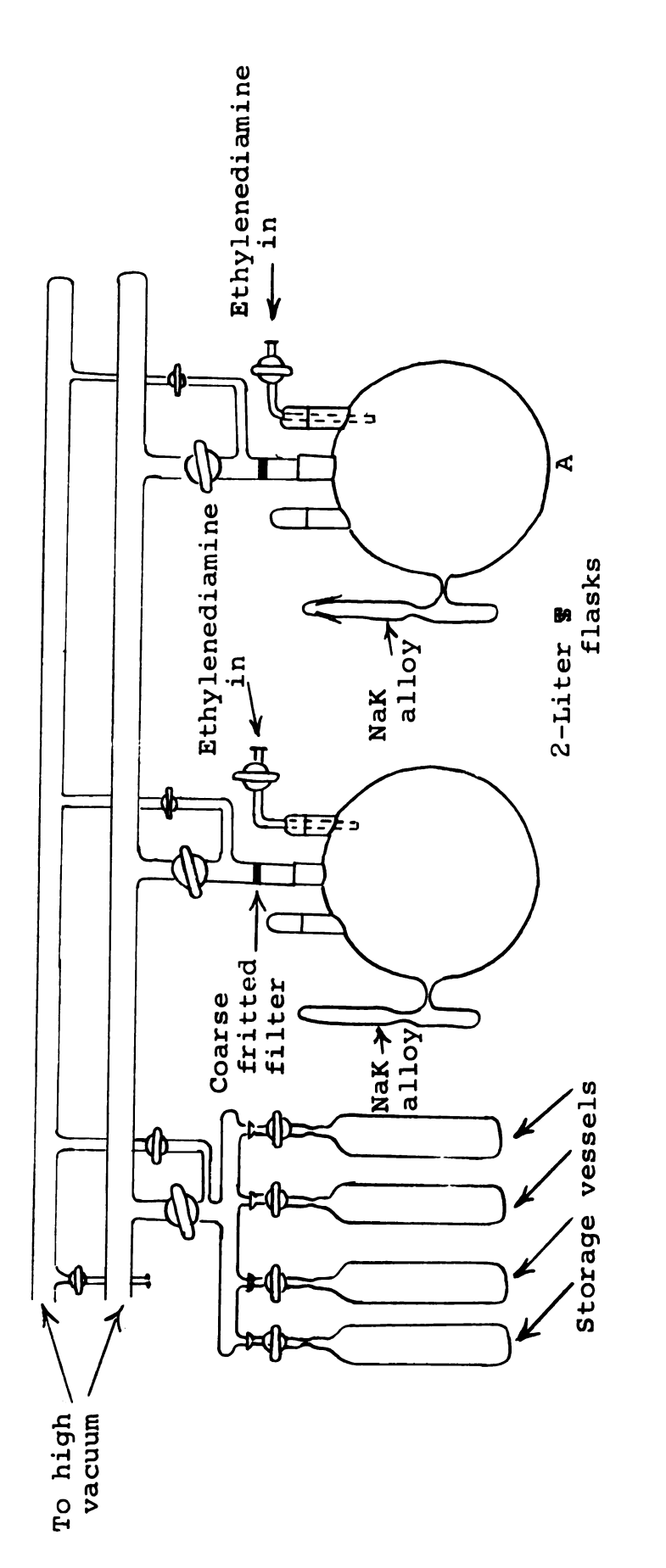


Figure 2. Vessel used for freeze purification of ethylene-diamine.



Second distillation train used for purifying ethylenediamine. Figure 3.

An alternate procedure was tried with the hope of eliminating the distillation step. This consisted of drying the solvent with anhydrous calcium hydride for approximately 24 to 72 hours before the freeze-purification procedure. The freeze-purification was repeated as before using a cylindrical five liter vessel equipped with Delmar-Urry Teflon valves. Attempts to prepare stable metal solutions using solvent purified in this way were also unsuccessful. However, this method does show promise in that the metal solutions prepared using solvent purified in this way were more "stable" than those prepared with solvent that had only been freeze-purified. This method seems to be very efficient for removing the residual water which is the major impurity found in the ethylenediamine.

#### C. Metal Purification

Alkali metals of the highest purity commercially available were obtained from the following sources: Sodium, J.

T. Baker Co.; Potassium, Fisher Chemical Co.; Cesium, a gift from the Dow Chemical Co.; and Rubidium, Fairmount Chemical Company. The final metal purification was carried out in two ways. In the first method, the metals were vacuum-distilled twice and stored in sealed ampoules. For solution preparation, these ampoules had to be broken and dropped into a sidearm sealed to the metal solution makeup vessel. This brief exposure to the atmosphere led to difficulties in

degassing the metal prior to vacuum-distillation into the metal solution makeup vessel. Several metal solutions decomposed because of this problem. The second procedure which eliminated this problem was then used. This method involves vacuum-distillation of the metal into ampoules which were equipped with breakseals. These ampoules were then sealed directly to the metal solution makeup vessels (Figure 4). The breakseals were not broken until the vessel had been evacuated to less than  $1 \times 10^{-5}$  torr.

#### D. Solute Purification

Water was purified in the following manner. Conductance water was thoroughly degassed by repeated freeze-pump-thaw cycles. It was then vacuum-distilled into weighed fragile glass ampoules, or into weighed ampoules equipped with breakseals. These vessels were used as needed for solution preparation.

Absolute methanol was placed in a vessel containing concentrated sulfuric acid and 4-5 grams of 2-4-dinitro-phenyl-hydrazine (105). The methanol was then distilled, keeping the middle fraction. It was thoroughly degassed by repeated freeze-pump-thaw cycles and vacuum-distilled into ampoules equipped with breakseals and used as needed.

The reagent grade salts KBr and NaBr were recrystallized three times from conductance water and then weighed into breakseal ampoules. The salts were flamed under vacuum prior

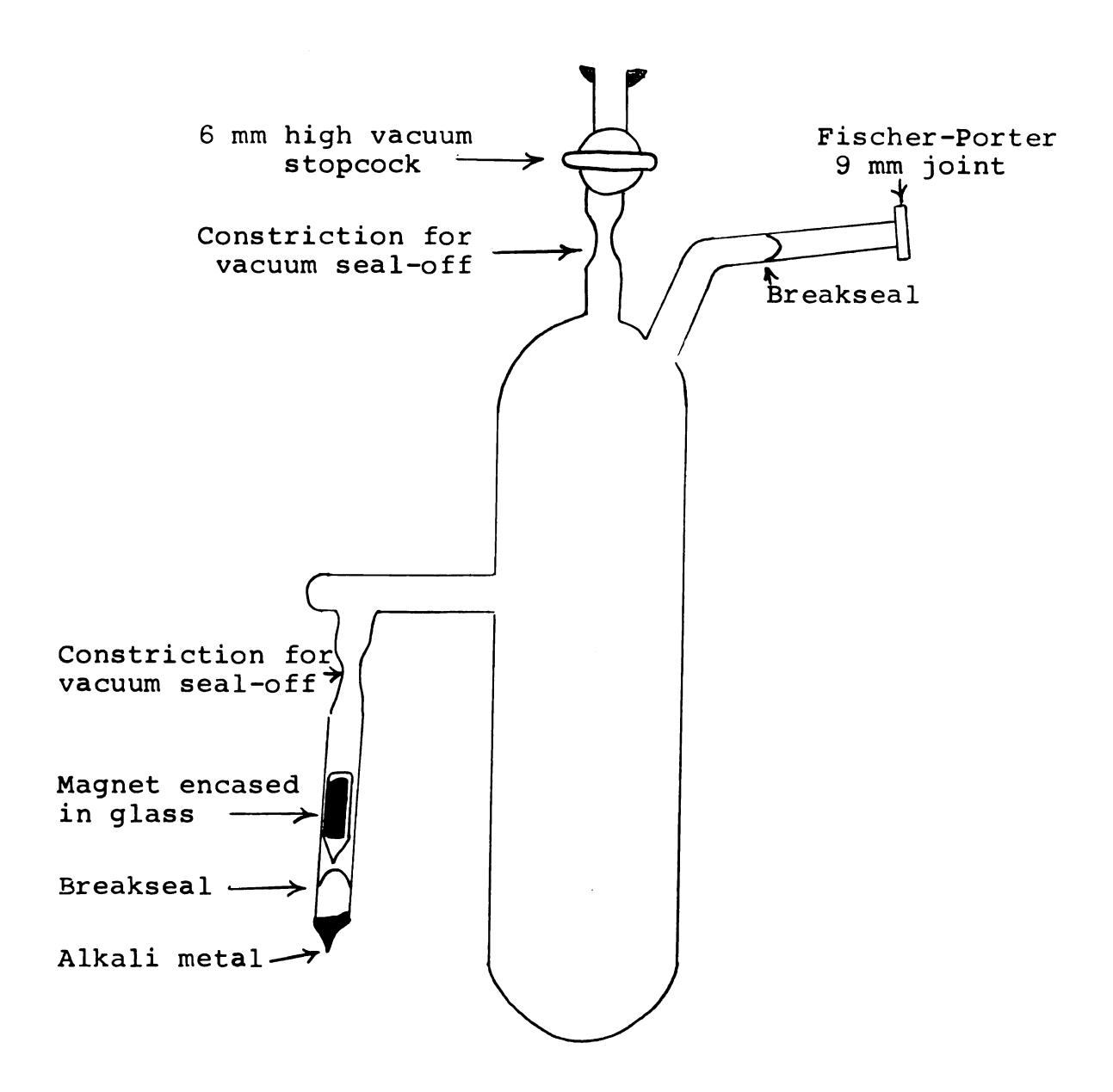


Figure 4. Vessel used to prepare metal solutions used in the kinetic studies.

to use. Rubidium chloride was used as the reagent grade salt without further purification.

The metal hydroxides were prepared by vacuum-distilling conductance water into a vessel which contained the appropriate metal mirror. Concentrated sodium and potassium hydroxide solutions were made up using reagent grade chemicals (0.77% carbonate) and conductance water.

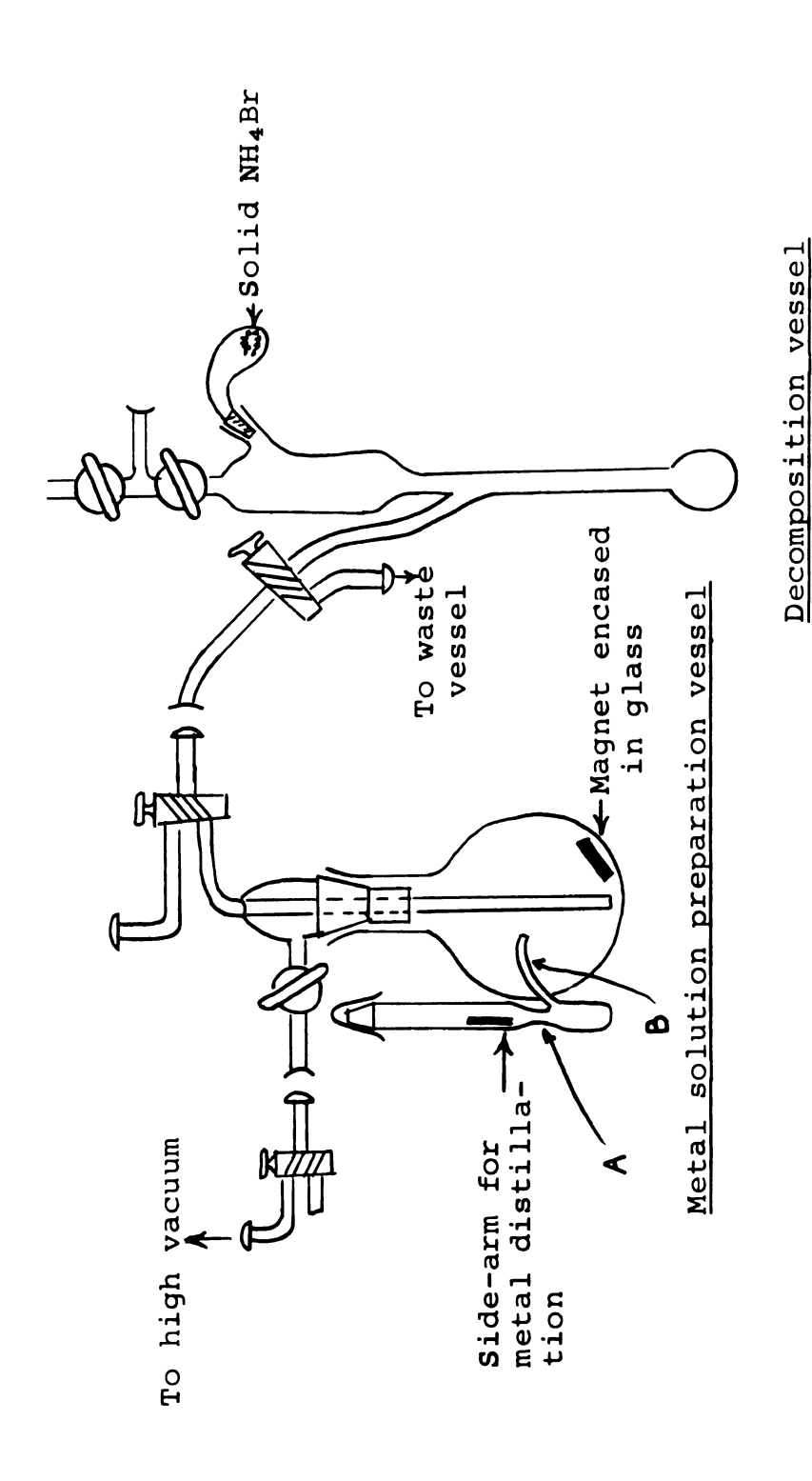
#### E. Covering Gas Purification

In earlier preparations, nitrogen (Matheson, pre-purified) was used as a covering gas. It was further purified by passing it over copper turnings in a tube furnace, through an Ascarite column and finally through a silica gel column at  $77^{\circ}$ K. It was then stored in two liter bulbs on the vacuum line. Some problems were encountered with the metal solution preparation using nitrogen as a covering gas and in later preparations, helium purified as above was used as the covering gas.

#### F. Solution Preparation

# 1. Metal Solution Preparation

Two different methods were used to prepare metal solutions. In the first method, the solutions were prepared immediately prior to use. The apparatus used for this purpose is illustrated in Figure 5. An ampoule containing the appropriate amount of metal was broken and dropped into the sidearm of the metal solution preparation vessel. The sidearm



Apparatus used for preparing metal solutions used in the initial kinetic studies of this work [from Dewald (89)]. Figure 5.

was capped and the vessel evacuated and flamed until the pressure stablized at less than  $1 \times 10^{-5}$  torr. The metal was melted down and degassed and the sidearm was sealed at A. The metal was then distilled into the vessel and the remaining seal-off made at B. Solvent was then poured under vacuum into the vessel containing the metal mirror. In most cases the blue solution formed immediately. The solution was stirred using the magnet sealed in glass and any hydrogen produced was pumped off. The solution was then covered with nitrogen or helium and five to ten milliliters were run into the waste compartment of the analysis vessel. From twenty to thirty milliliters of the solution were then run into the calibrated bulb of the analysis vessel and were analyzed at a later time. The metal solution vessel was removed from the vacuum line and attached to the stopped-flow system. metal concentration was determined by measuring the amount of hydrogen collected from a solution decomposed with ammonium bromide according to the reaction:

$$NH_4Br + M_{(en)} \longrightarrow \frac{1}{2}H_2 + MBr + NH_3$$

The second method used to prepare metal solutions did not involve pouring the solvent from one vessel to another. The metal samples were stored in ampoules equipped with a breakseal. One of these ampoules, containing the appropriate amount of metal, was sealed to the solution preparation vessel (Figure 4). The vessel was attached to the vacuum

line and evacuated and flamed until the pressure stabilized at less than  $1 \times 10^{-5}$  torr. Liquid ammonia was then condensed in the vessel. The ammonia was distilled back into a storage vessel containing sodium-potassium alloy. The metal solution preparation vessel was opened to the high vacuum line until the pressure again stabilized at less than 1 x  $10^{-5}$ torr. This procedure was repeated four more times. Thoroughly degassed solvent was then vacuum-distilled into the solution makeup vessel at -78°C. When the desired amount of solvent had been added, the distillation was stopped and the frozen solvent allowed to melt. A final degassing using a freezepump-thaw cycle was carried out and the solvent was frozen at -78°C until the metal solution was prepared. Just prior to a run the breakseal on the sidearm was broken, using the magnet encased in glass, the metal was distilled into the vessel containing the frozen solvent and the sidearm was sealed off. Helium purified as described above, was admitted until a pressure of about 1 torr was obtained. The vessel was then sealed off, the solvent was melted using a warm water bath and the solution was prepared by allowing the solvent to contact the metal mirror. In most cases, a blue solution formed immediately (see Appendix C). The solution was thoroughly mixed by tipping the vessel back and forth. The vessel was then attached to the stopped-flow system, the connecting tubes were evacuated and the remaining breakseal was broken.

#### 2. Water Solution Preparation

Water solutions were also prepared by two different methods. In the first method, dilute  $(10^{-2} \text{ M})$  and intermediate (~0.5 M) water solutions were prepared using fragile ampoules which contained a known amount of water. Ampoules containing the desired amount of water were placed in 500 ml. round bottom flasks and these flasks were weighed. The solution preparation vessels were then attached to the vacuum line via storage Flask C (Figure 1) and evacuated until the pressure stabilized at less than  $1 \times 10^{-5}$  torr. The fragile ampoules were broken using a magnet sealed in glass and solvent was added from storage Flask C and the solution was thoroughly mixed using a magnet sealed in glass. Helium or nitrogen was then added as a covering gas. The vessels were disconnected from the vacuum line, reweighed to determine the amount of solvent added and attached to the stopped-flow system. More concentrated (5 to 10 M) water solutions were prepared by vacuum distilling an amount of degassed conductance water directly into a weighed and volumetrically calibrated preparation vessel. The vessel was then disconnected from the vacuum line and reweighed to determine the amount of water added. The vessel was again connected to the vacuum line and ethylenediamine was added until the total volume of solution reached a calibration mark on the preparation vessel, so that the total volume of solution was known. Nitrogen or helium was added as a covering gas and the vessel

was disconnected from the vacuum line and attached to the stopped-flow system.

The second method of water solution preparation involved vacuum distilling degassed conductance water into weighed ampoules equipped with breakseals. These ampoules were then sealed off and reweighed to determine the amount of water added. One of these ampoules was then sealed to the solution preparation vessel. The necessary amount of solvent was distilled in, the breakseal on the sidearm was broken and the water and ethylenediamine were mixed. The rest of the procedure was the same as that for the metal solution preparation which is described above.

# 3. Salt Solution Preparation

The ampoules containing the salts which were purified as described above, were sealed to solution preparation vessels. The solution preparation procedure was the same as that for metal and water solution preparation.

# G. Stopped-Flow System

The stopped-flow apparatus used in this work, illustrated in Figures 6 and 7, is generally similar to those described by Dewald and Feldman (89,90). As before, only one concentration of metal solution could be used, but up to three different stock concentrations of solute could be used for each run. Appropriate dilutions of these stock concentrations were made,

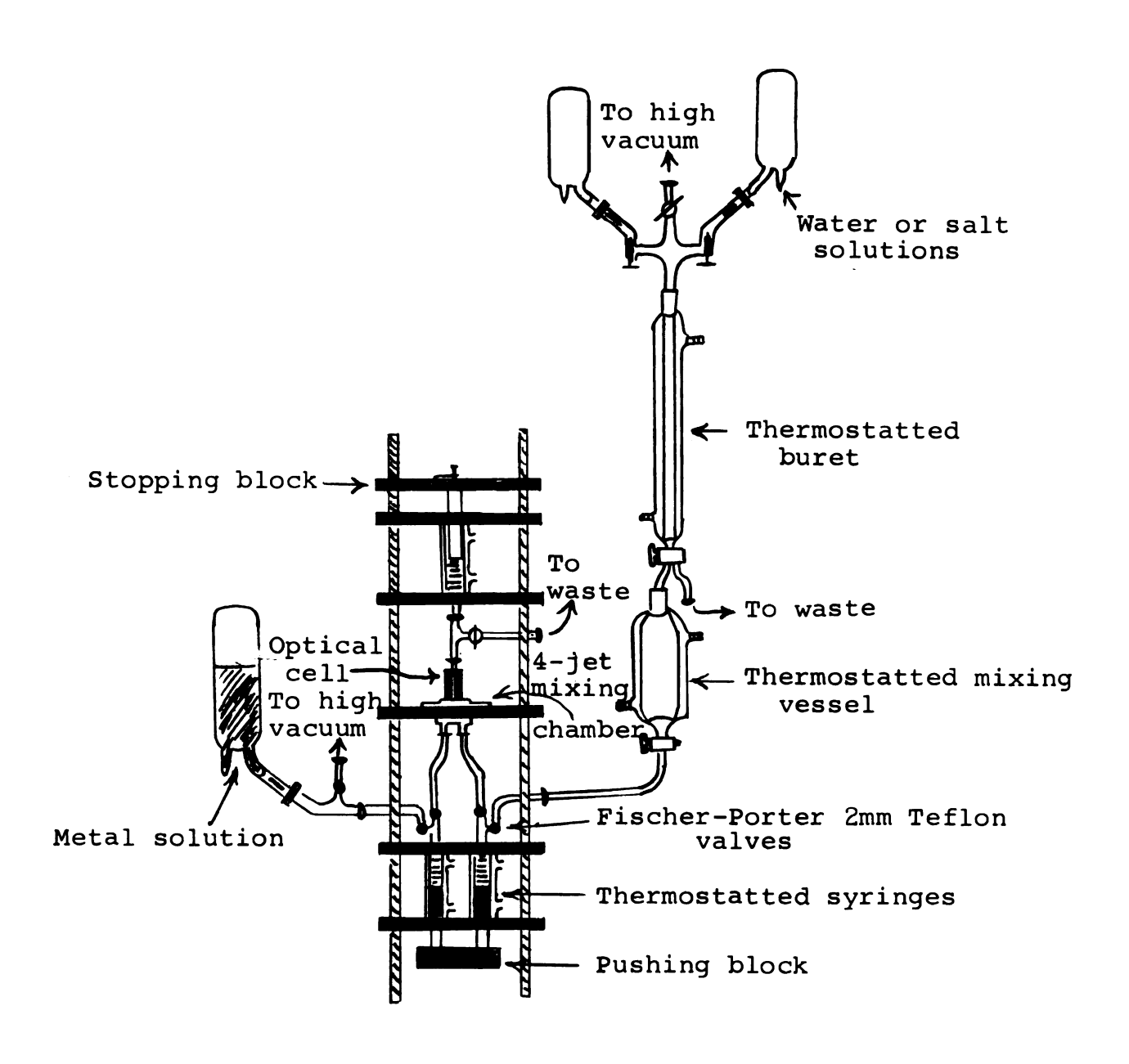


Figure 6. Stopped-flow system.

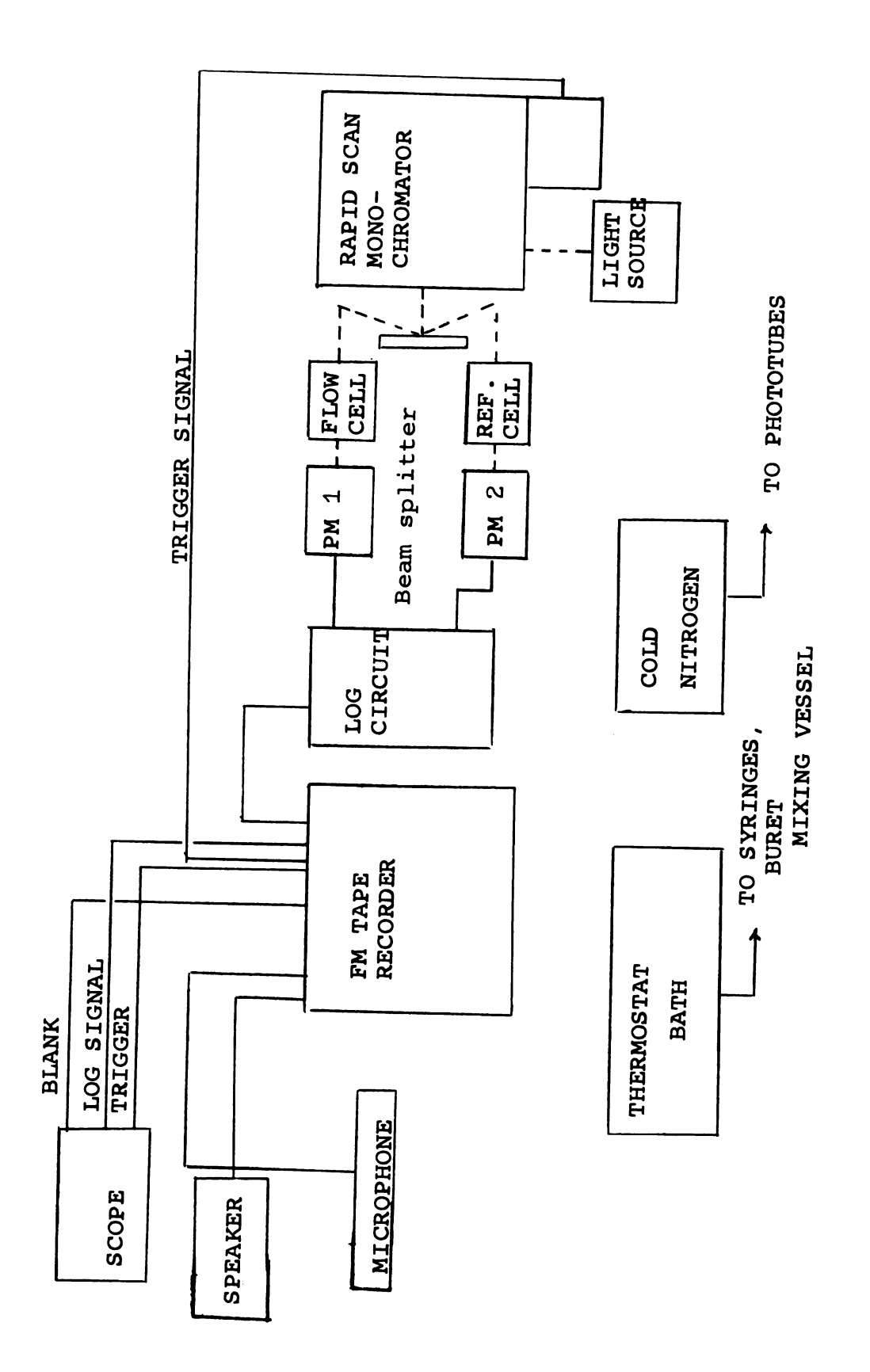


Figure 7. Block diagram of rapid-scan system.

either by diluting any one of them with pure solvent or by diluting one stock solution with another. These solutions were thoroughly mixed in a thermostatted mixing vessel using a Teflon coated magnet. The whole system could be evacuated to less than  $1 \times 10^{-5}$  torr. Flow was stopped when the plunger of a third syringe reached a metal plate (see Figure 6).

Two types of syringes and stopcocks were used on the stopped-flow system during the course of this work. Early kinetic investigations employed glass syringes (Sure-Fit, Richard Allan and Co., Evanston, Illinois) with glass plungers as well as all glass stopcocks (H. S. Martin and Co.). The major drawback to the use of all glass syringes and stopcocks was that it was necessary to grease them (using Dow Corning Silicone grease). Both ethylenediamine and the metal solutions slowly attacked the silicone grease and left deposits of silica throughout the flow system. These deposits could not be removed and it is possible that they acted as sites for catalytic decomposition. Since the metal solutions are metastable, the elimination of all sites for rapid catalytic decomposition is a necessity in any kinetic study.

A second problem encountered in the use of the greased stopcocks was that during the course of a run the slow attack of the metal solution and solvent on the silicone grease made the stopcocks very difficult to turn. They often had to be regreased several times during the course of a given run.

This regreasing procedure necessitated opening the flow system

to the atmosphere. The possibility for contamination of the flow system and also the possibility of breakage due to the difficulty in turning the stopcocks led to the elimination of the glass stopcocks and syringes.

A system of greaseless Teflon plungers, stopcocks and high vacuum joints was constructed. The greaseless plungers were made by mounting Teflon tips on plungers taken from Hamilton glass syringes. These tips had lips machined on them to insure a vacuum-tight liquid seal. Fischer-Porter 2 mm "Solv-Seal" joints were sealed via uranium glass graded seals to the Hamilton syringe barrels. These joints employ a Teflon insert with 2 Viton-A O-rings as a greaseless vacuum seal. The stopcocks were constructed using Fisher-Porter 4 mm quick opening valves and 2 mm i. d. heavy walled capillary tubing.

Four-jet mixing cells of both Pyrex and quartz were used. The Pyrex cells were constructed as previously described. Quartz cells had been previously constructed commercially, however, the cost of commercial fabrication of these cells was very high and a cheaper, more efficient method was devised. The starting materials were 7.7 cm lengths of heavy-walled 1 mm i.d. (Thermal American Co.) quartz capillaries which were polished flat on two sides (Precision Glass Products Co., Oreland, Pa.). The drilling of the inlets was accomplished using an Airbrasive unit (White Dental Supply, Bloomfield Hills, Mich.). This instrument utilizes a high speed stream

helium gas containing finely divided alumina to drill the holes. The lengths of capillary were mounted in a jig which could be accurately positioned using an indexing head in a horizontal drill (see Figure 8). Using this device, holes were drilled which entered the central bore of the capillary almost tangentially and at an angle of about 105° to it. The jig was rotated 90° between successive holes until all four holes had been drilled. To prevent unwanted drilling of the capillary wall opposite a hole being drilled, a length of polyethylene medical tubing was inserted in the central bore of the capillary tube while the inlet holes were being drilled. This drilling procedure yielded a coneshaped hole, tapered from the outside surface of the capillary to the central bore. A 0.5 mm diameter tungsten rod was then coated with a mixture of mineral oil and the abrasive powder and used in a drill press to enlarge the holes to a minimum diameter of 0.5 mm. To complete the construction of the inlet tubes, the appropriate vacuum joints (Fischer-Porter, 2 mm "Solv-Seal" joints) were sealed to these lengths of capillary (see Figure 9).

The syringes on the flow system were thermostatted by means of Plexiglas jackets which were sealed with Viton-A O-rings. The thermostatting fluid was a 50:50 mixture of water and Prestone antifreeze and was circulated by means of a Lab-Line Hi-Lo Tempmobile.

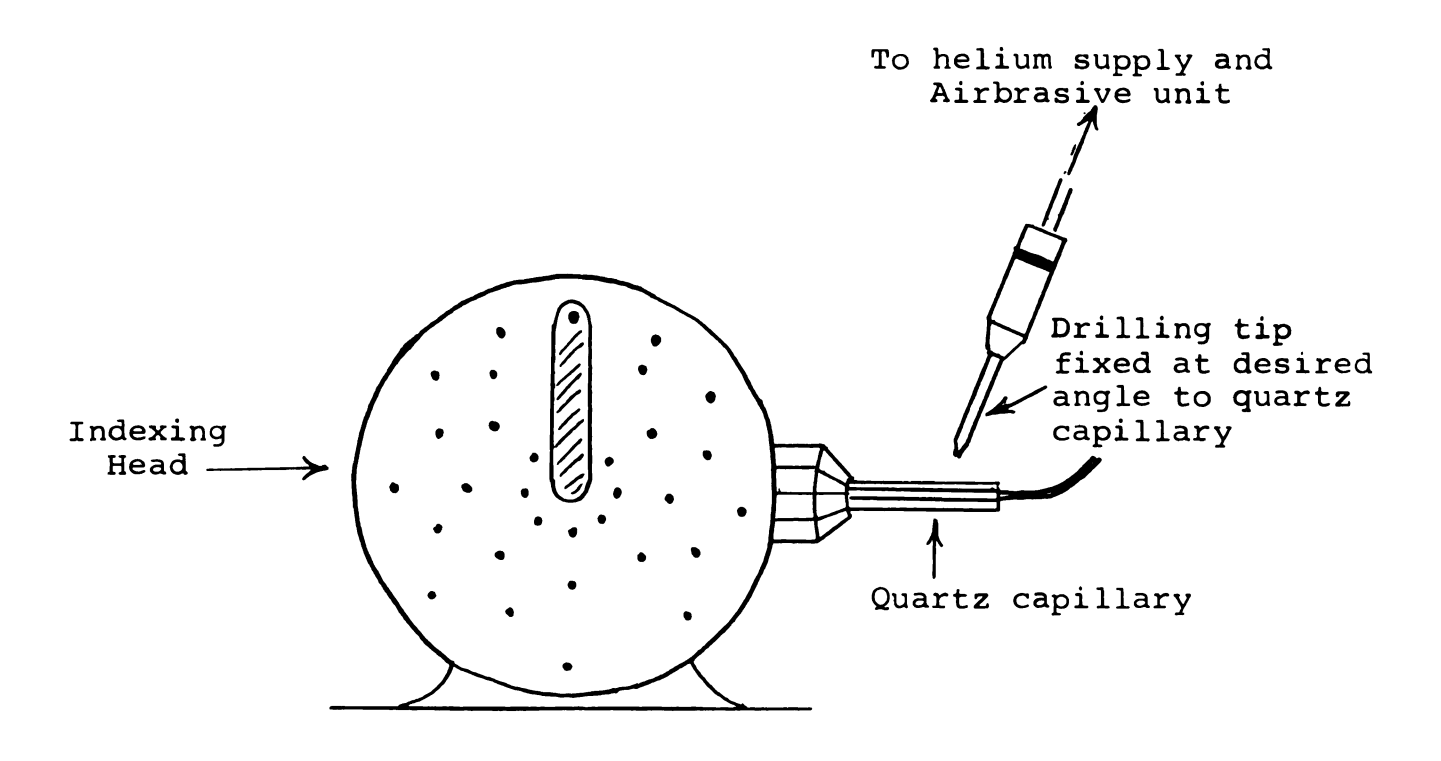


Figure 8. Jig assembly used for the drilling of the quartz flow cells.

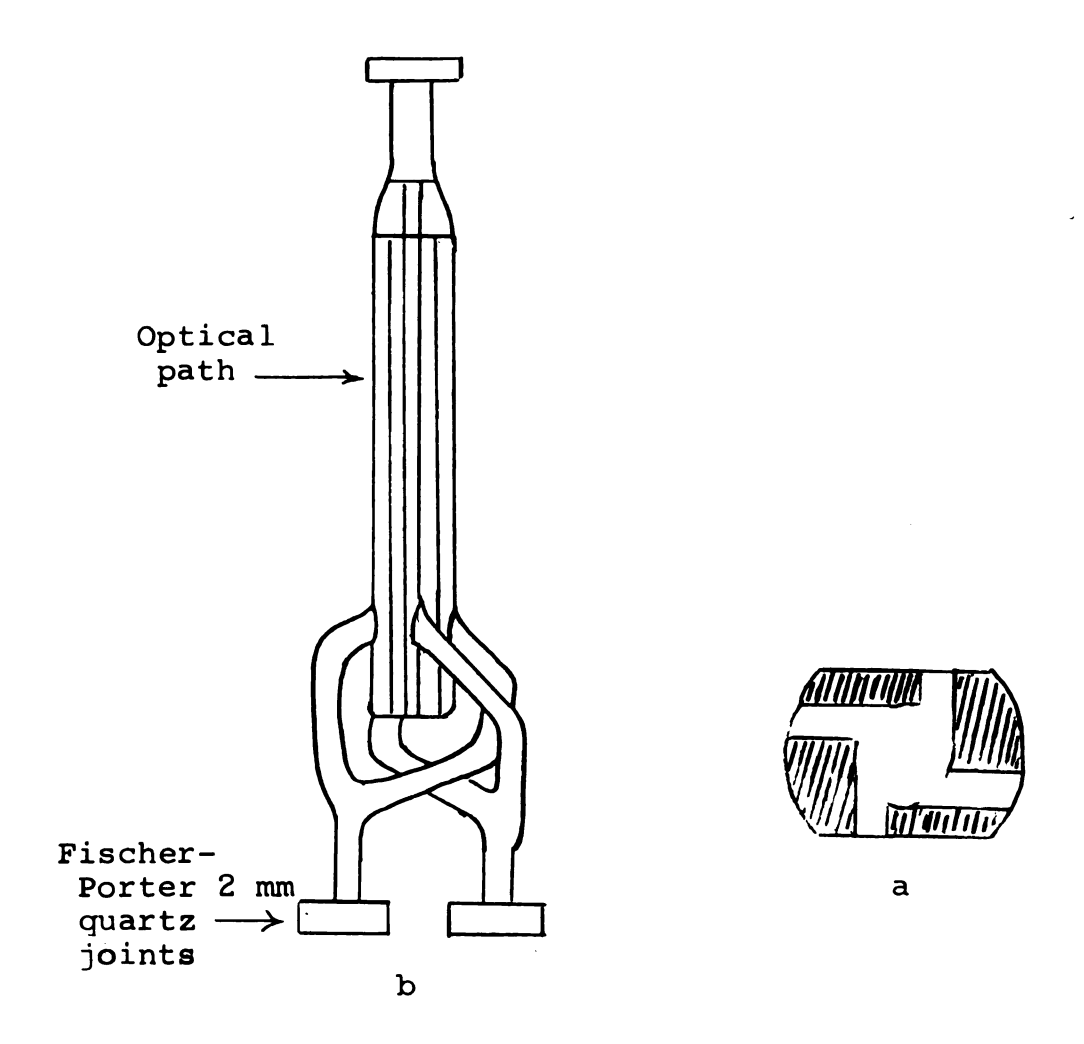


Figure 9. a--Cross section of the four-jet mixing cell showing the nearly tangential entry of the four jets.

b--Finished flow cell.

#### H. The Rapid-Scan System

The main component of the optical system illustrated in Figure 7 is a Perkin-Elmer Model 108 Rapid-Scanning monochromator. The spectral scan of this instrument is generated by a double pass Littrow system with a rotating tilted mirror. It is capable of scanning a selected spectral region between 300 and 1100 nm with from 3 to 150 scans per second. The scanning speed may be changed either by interchanging gears or by a two-position switch on the instrument. The two-position switch permits selection of two scanning speeds for each set of gears.

A trigger circuit consisting of a small neon light, a slotted wheel which rotates at the same speed as the rotating mirror of the monochromator, and a cadmium sulfide photocell was used to generate a trigger signal at the beginning of each scan. The intensity of this trigger signal is a function of the scanning speed and is adjusted by means of a potentiometer.

A Bausch and Lomb source employing a tungsten-iodine lamp with a quartz envelope was used for this work. As shown in Figure 7, the light, after leaving the monochromator, strikes a stacked mirror beam splitter (from a Bausch and Lomb Spectronic 505 Spectrophotometer). The beams are then focussed on the centers of the flow and reference cell (in the case that a reference cell is used) and then passed through two quartz lenses used for focussing the light into

the photomultiplier tubes (RCA 6199 or RCA 7102). These phototubes were cooled to  $-50^{\circ}\text{C}$  using a stream of dry nitrogen that had been passed through a copper condenser immersed in liquid nitrogen. This was done to reduce the thermionic or "shot" noise and also to reduce the dark current of the phototubes. The anode currents of the phototubes, balanced as well as possible over the spectral range of interest, were then fed into a logarithmic amplifier. This circuit, using Philbrick operational amplifiers (PL1-P and P-25), produces an output voltage which is proportional to the logarithm of the ratio of the current from the reference phototube ( $I_0$ ) to that of the sample phototube (I). This voltage is then proportional to the absorbance.

The output of the rapid scanning monochromator is not linear in wave number about the center of scan. Because of this fact, the spectral range investigated in each run was calibrated using a Didymium or a Holmium oxide glass filter. Both of these filters have well-defined optical spectra.

Each rotation of the mirror actually gives two scans of the spectral region of interest. One-half of the total scan is simply the mirror image of the other half. It is important that the two halves of the scan be symmetric if all the spectral data are to be used reliably for kinetic studies. The symmetry between the two halves of the scan is a function of the slit width, position of the light source with respect to the slit and the presence of stray light from the first

pass of the light beam through the optical system of the monochromator. The slit width and the position of the light source were adjusted prior to each run to give the best symmetry of the spectrum of the Didymium glass filter. The instrument was checked for internal stray light and appropriate masking was used to eliminate it.

In early work using the rapid-scanning monochromator, the linearity of the absorbance was not checked prior to The adherance of a permanganate solution to Beer's each run. law showed that the output voltage of the Philbrick logarithmic amplifier was linear in absorbance up to an absorbance of about 1.5, but that it became non-linear above this value. For this reason, calibrated neutral density filters (Oriel Co., Stamford, Conn.) with absorbances ranging in value from 0.3 to 3.0 absorbance units were used to check the system during each of the later runs. These filters were calibrated in the wavelength range 400 to 1000 nm. Intermediate absorbance values could be obtained using two of these filters. In this way, the absorbance range 0.3 to 3.0 was then calibrated using the ten readings 0.3, 0.5, 0.8, 1.0, 1.3, 1.5, 2.0, 2.3, 2.5, and 3.0. The details of this calibration are qiven in Appendix B, which deals with the computer programs used in this work.

All pertinent data taken during the course of a run were recorded on magnetic tape using an Ampex SP-300 FM tape recorder equipped with 4 record/reproduce heads. All information concerning solute concentrations, scanning speed and

other of th

from Stora

first

nel o

and 3

permi trigge

from 1

of the

scope

by us: A typ:

were

time (

analy:

noted

tion :

be use If one

 $\mathtt{gecg}^{\lambda}$ 

other instrumental settings was recorded on the audio channel of the tape recorder.

# I. Data Analysis

Data analysis was carried out by two methods. In the first method, the signal from the log circuit was played back from the tape recorder into the positive input of a Type 564 Storage Oscilloscope with Types 2A63 Differential Amplifier and 3B4 Time Base plug-in units. The output of a blank channel on the tape recorder was played into the negative input to permit common-mode noise rejection. The oscilloscope was triggered externally in the normal mode by the trigger signal from the monochromator which was recorded in a third channel of the tape recorder.

The decay of the spectrum was displayed on the oscilloscope in the storage mode and this display was photographed by using a Polaroid camera and Type 146L transparency film. A typical display is shown in Figure 10. These photographs were then enlarged and traced on graph paper and the absorbance-time data were taken from these traces. The data were then analyzed with the aid of a CDC 3600 computer. It is to be noted here that since one looks at the decay of the absorption spectrum with time, every scan recorded on tape cannot be used in the kinetic analysis of a relatively slow reaction. If one tries to use every scan, only the envelope of the decay is obtained.

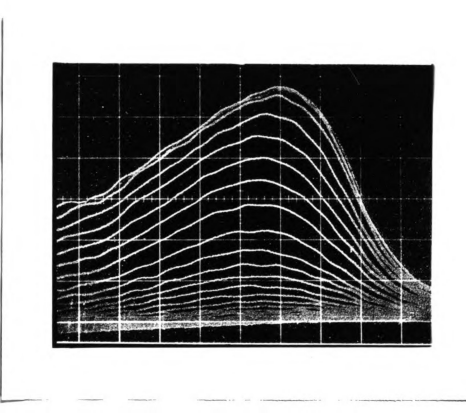


Figure 10. Typical oscilloscope trace used for data analysis in the initial studies of this work.

could not
seemed to
carried c
conversic
a new dat
main comp
Average T
used is s
The
the output
positive s
signal from
as an input
fier. The

The s
the normal
A gate pul
loscope, was
equipped w

taneously

scope and

by the 5452 (Wavetek, 1

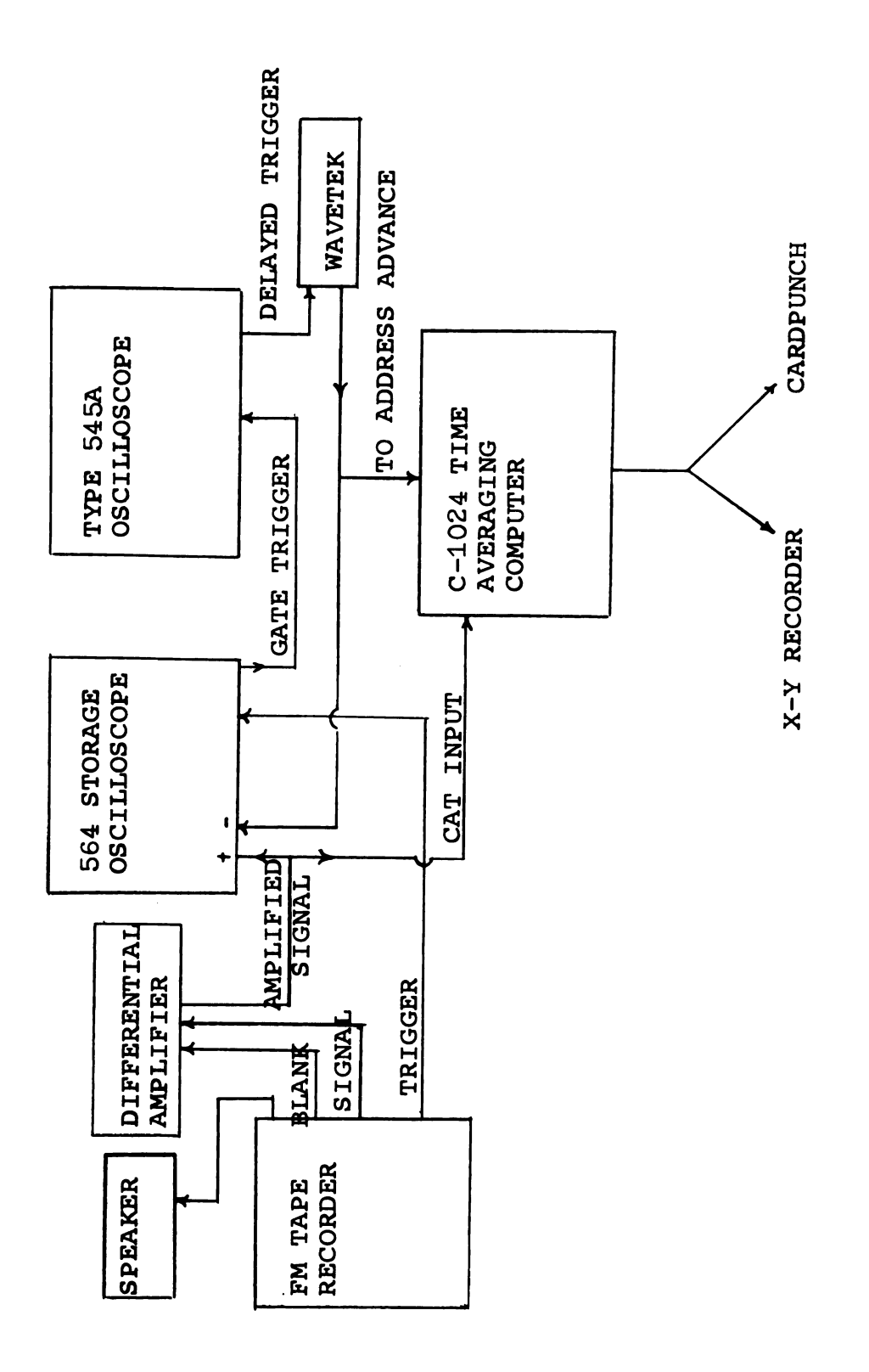
between the

gate trigge

Since in the above method, many of the data recorded could not be used, a more efficient data analysis system seemed to be in order. Also, since final data reduction was carried out with the aid of the computer, analog to digital conversion of the data was desirable. To achieve these ends, a new data analysis system was designed and assembled. The main component of this system is a Varian C-1024 Computer of Average Transients (CAT). A block diagram of the system used is shown in Figure 11.

The signal from the tape recorder channel containing the output of the log circuit was used as an input to the positive side of a calibrated differential amplifier. The signal from the blank channel of the tape recorder was used as an input to the negative side of this differential amplifier. The output signal of this amplifier was then simultaneously fed into the positive input of the storage oscilloscope and into the CAT.

The storage oscilloscope was triggered externally in the normal mode by the trigger signal from the monochromator. A gate pulse, generated at the end of each sweep of the oscilloscope, was input to a Tektronix type 545-A Oscilloscope equipped with a time delay unit. A gate trigger generated by the 545A Oscilloscope was input to a waveform generator (Wavetek, Model 116, San Diego, Calif.). The length of time between the signal input to the 545A Oscilloscope and the gate trigger output of this scope could be varied by means



Block diagram of the CAT data analysis system. Figure 11.

to examine the designment to the designment to

of the

the port
CAT has a

reaction
to advance
fed into

monitorin Havi:

into CAT, tion on ar The card p

an IBM key coupler.

are discus

The a
were prepa:

conductance

ly that des is shown in

of the time delay circuit within the scope. This corresponds to examining a given portion of the recorded spectrum.

The frequency of the waveform generator was adjusted to the desired value. From 16 to 256 trigger cycles could be used to analyze any given scan. This corresponds to defining the portion of a given scan with 16 to 256 points. Since the CAT has a total of 1024 channels, a given kinetic trace can consist of up to 64 different absorbance values over the total reaction time. The output of the waveform generator was used to advance the address register of CAT. This signal was also fed into the negative input of the storage oscilloscope for monitoring purposes.

Having read the absorbance data as a function of time into CAT, in this manner, one can then display this information on an X-Y recorder and/or punch it directly on cards. The card punching was completely automatic and was done with an IBM keypunch (type IBM 526) equipped with a Varian C-1001 coupler. The computer programs used to analyze these data are discussed in detail in Appendix B.

#### J. Conductance Measurements

The alkali metal hydroxides used in these measurements were prepared as described in the preceding Section D. The conductance apparatus used in these measurements in essentially that described by Keskey and Spleet (91). This apparatus is shown in Figure 12. After each sample of the hydroxide

Fischer-2mm Teflovalve

To high v

1 m.1

Pigure 12.

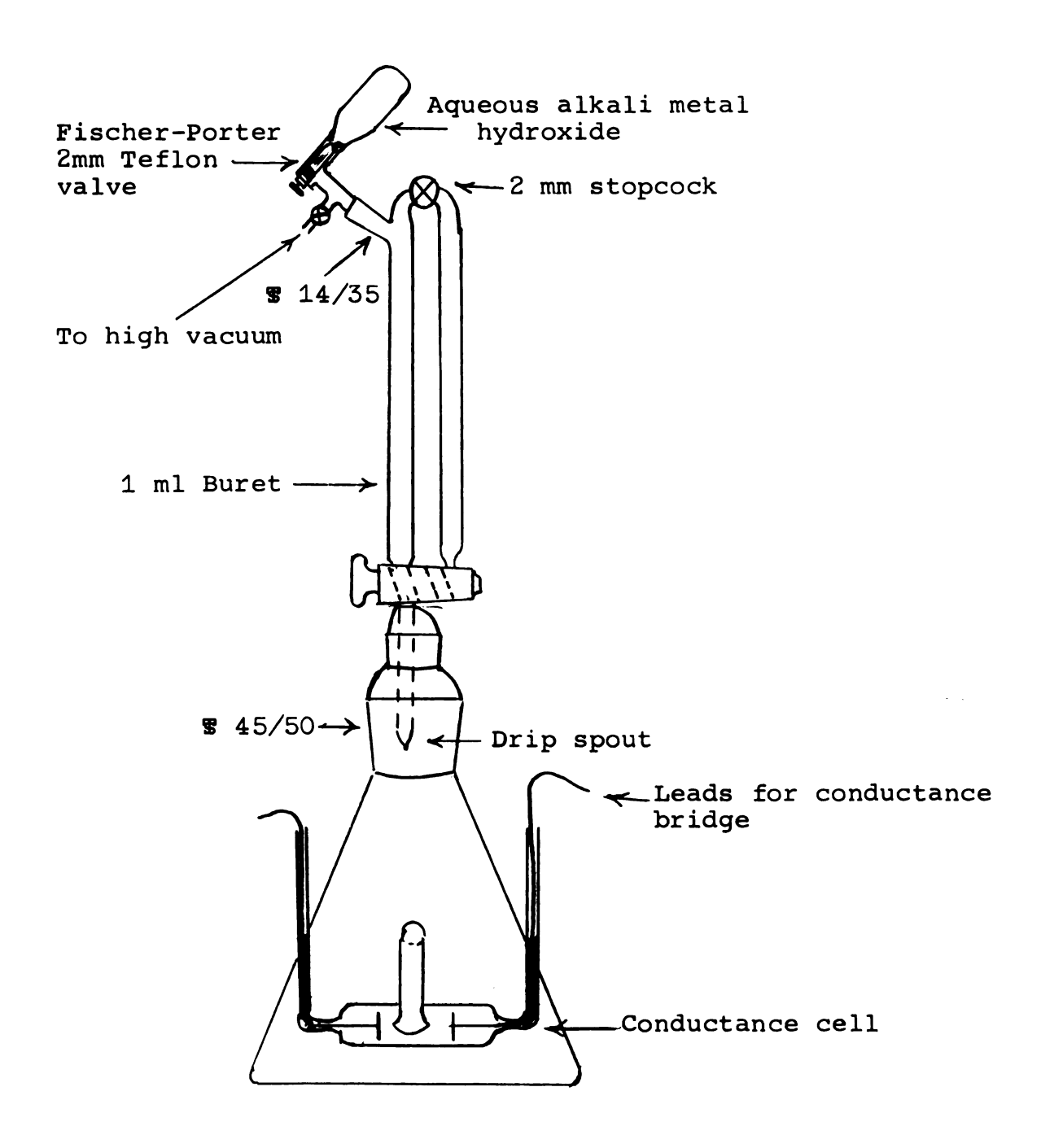


Figure 12. Apparatus used to measure the conductances of the alkali metal hydroxides in ethylenediamine.

resistandescribed these concell used

For

solution

labelled
was obtai
chloride.
diamine w
solutions
solvent.
water solutions
a modified
produced w
introduced

A sidearm
was condens
filled wit:

and this t

<sup>hydrogen</sup> t

was measure

solution was added, the solution was shaken until a constant resistance reading was obtained. Helium, purified as described in this Section, was used as the covering gas in these conductance experiments. The cell constant for the cell used was 0.25.

## K. Tritium Experiments

For these experiments a 1 mCi sample of ethylenediamine labelled at the  $\alpha$ -position ( $H_2N-CT_2-CT_2-NH_2$ ) was used. It was obtained from New England Nuclear Corp. as the hydrochloride. This was first dissolved in 20 ml of pure ethylenediamine which was then distilled once prior to use. Cesium solutions (7 ml samples) were prepared using this labelled solvent. These metal solutions were mixed with concentrated water solutions and the hydrogen produced was collected using a modified Van Slyke apparatus. The volume of the hydrogen produced was measured at atmospheric pressure. It was then introduced into a vessel containing 1-2 g of silver oxide and this vessel was heated to  $100^{\circ}$ C for 1 hr to burn the hydrogen to water via the reaction

$$Ag0 + H_2 \xrightarrow{100^{\circ}C} Ag + H_2O$$

A sidearm of the vessel was then cooled to 77°K and the water was condensed. The vessel was then opened and the sidearm filled with scintillation liquid. The activity of this liquid was measured using a Tri-Carb Scintillation counter. Any

hydroge itself any act samples Table I cussed

RE

Experiment

1

۷

3

hydrogen produced by decomposition of the metal solution itself was also collected, burned to water and tested for any activity. No appreciable activity was observed in these samples. The results of three such experiments are given in Table III. The significance of these results is also discussed in Section IV.

TABLE III

RESULTS FROM TRITIUM EXPERIMENT TO CHECK ORIGIN
OF MOLECULAR HYDROGEN IN REACTION OF CESIUM
WITH WATER IN ETHYLENEDIAMINE

Experi-	Volume H <sub>2</sub> collected (ml)	Average number counts	Percent of total hydrogen active
1	0.75	244	2.3
2	0.83	269	2.38
3	0.65	225	2.06

in ethy
Feldman
follow sereaction

Th

peting p graphica Thi.

analyze o

V-band in that the 1

react inde

contaminat conversion the glass

the presen

## IV. RESULTS AND DISCUSSION

## A. Introduction

The reactions of dilute metal solutions with water in ethylenediamine were first studied by Dewald (89) and Feldman (90). Feldman showed that the reaction rate did not follow simple first-order kinetics. He suggested that the reaction with water could be described in terms of two competing pseudo-first-order reactions and analyzed his data graphically on this basis.

This parallel first-order reaction scheme was used to analyze the kinetic data for two reasons. First, Dewald had observed a very slow (minutes) interconversion of the IR- and V-band in solutions of lithium in ethylenediamine, suggesting that the two kinds of species in metal-amine solutions could react independently (89). If, as Hurley, Tuttle and Golden report (54), the 660 nm absorption (V-band) is due to sodium contamination from the Pyrex container, then the slow interconversion of the optical bands results from reaction with the glass and not from a homogeneous reaction. Studies in the present work (to be described later) of reactions of the

type

Cs

Rb

 $(t_{\frac{1}{2}} > 10)$ 

cannot be kinetics.

nm band d

is contrar

type

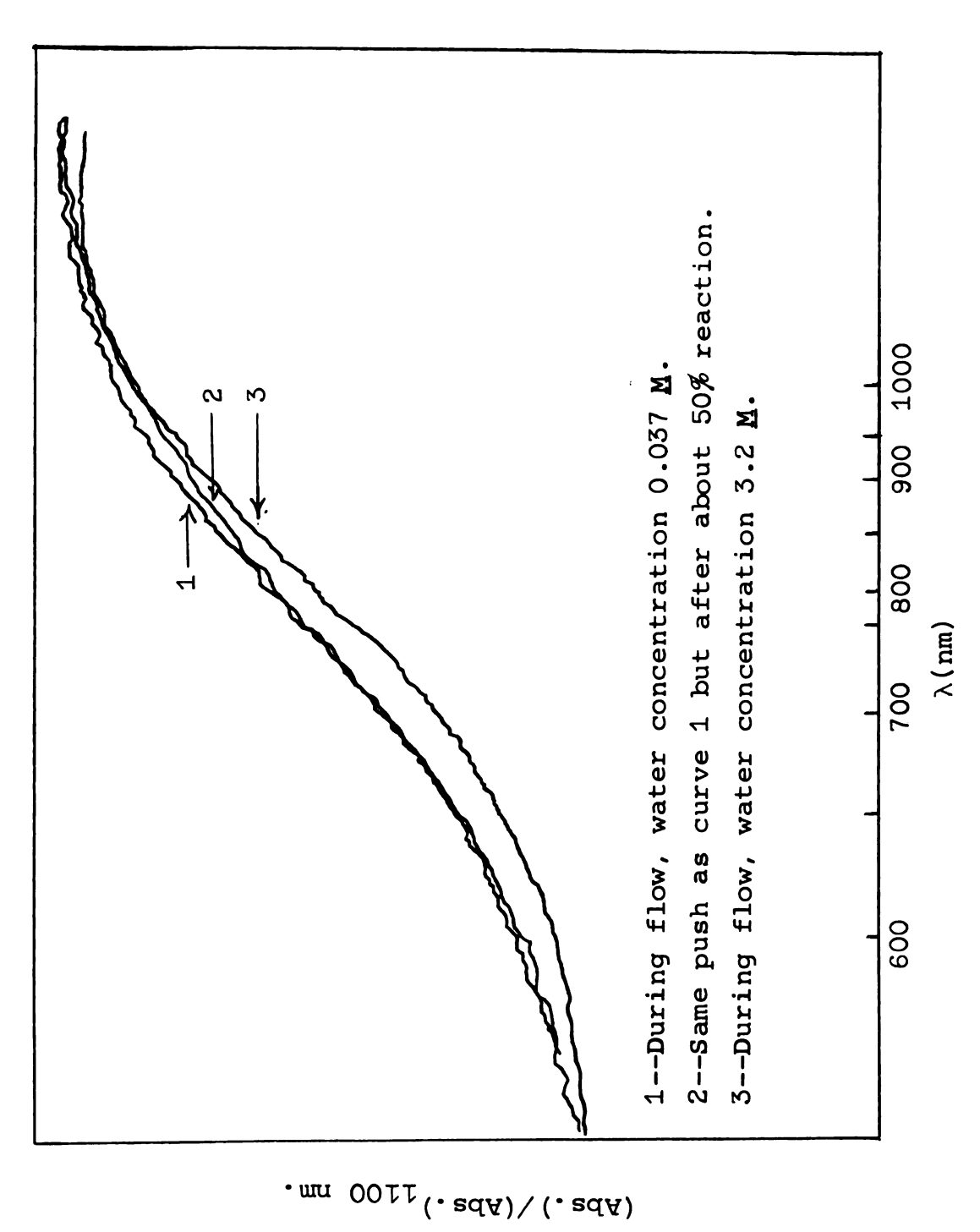
Cs solution (1280 nm) + Na<sup>+</sup> 
$$\longrightarrow$$
 "V-species" (660 nm)  
+ Cs<sup>+</sup> (1)

and

Rb solution (890 nm, 1280 nm) + Na<sup>+</sup> 
$$\longrightarrow$$
 "V-species" (660 nm) + Rb<sup>+</sup>

in ethylenediamine show that these reactions are fast  $(t_{\frac{1}{4}} > 10^{-3} \text{ sec})$ . This information, not available to Feldman, proves that independent decay of the different optical bands cannot be the explanation of the deviations from first order kinetics. The second reason for the parallel first order treatment was the conclusion reached by Feldman that the 1280 nm band decayed before the 1030 nm band when a dilute cesium solution reacted with water in ethylenediamine (90a). is contrary to the order of decay expected for equilibrium among the species (see Section II). However, re-examination of the same kinetic data of Feldman using the CAT data analysis system, shows that there is no change in shape of the cesium spectrum during reaction with water. Also, there is no dependence of the spectral shape on the initial water concentration. These two observations are illustrated in Figure 13. Apparently, difficulties with the triggering circuit of the monochromator (see Section III, Part H) led Feldman to an erroneous conclusion.

The consistency of the values of  $K_{\!\stackrel{}{A}}$  obtained from the above analysis was not good and the scatter among rate



Shape of the IR-band as a function of the initial water concentration and the extent of reaction during the reaction of cesium with water in ethylenediamine. Figure 13.

constan In some kinetic them gav optical tained i Feldman tem wher log(Abs.) strictly 890 nm al ing the r the behav kinetic p It is ism for th diamine is

for the sa

reaction o

minutes to

action wit

(98) · If }

diamine, ti

Whe

constants was larger than the expected experimental error. In some cases, oscilloscope traces taken from different kinetic pushes were nearly superimposable but analysis of them gave rate constants which were not the same (90).

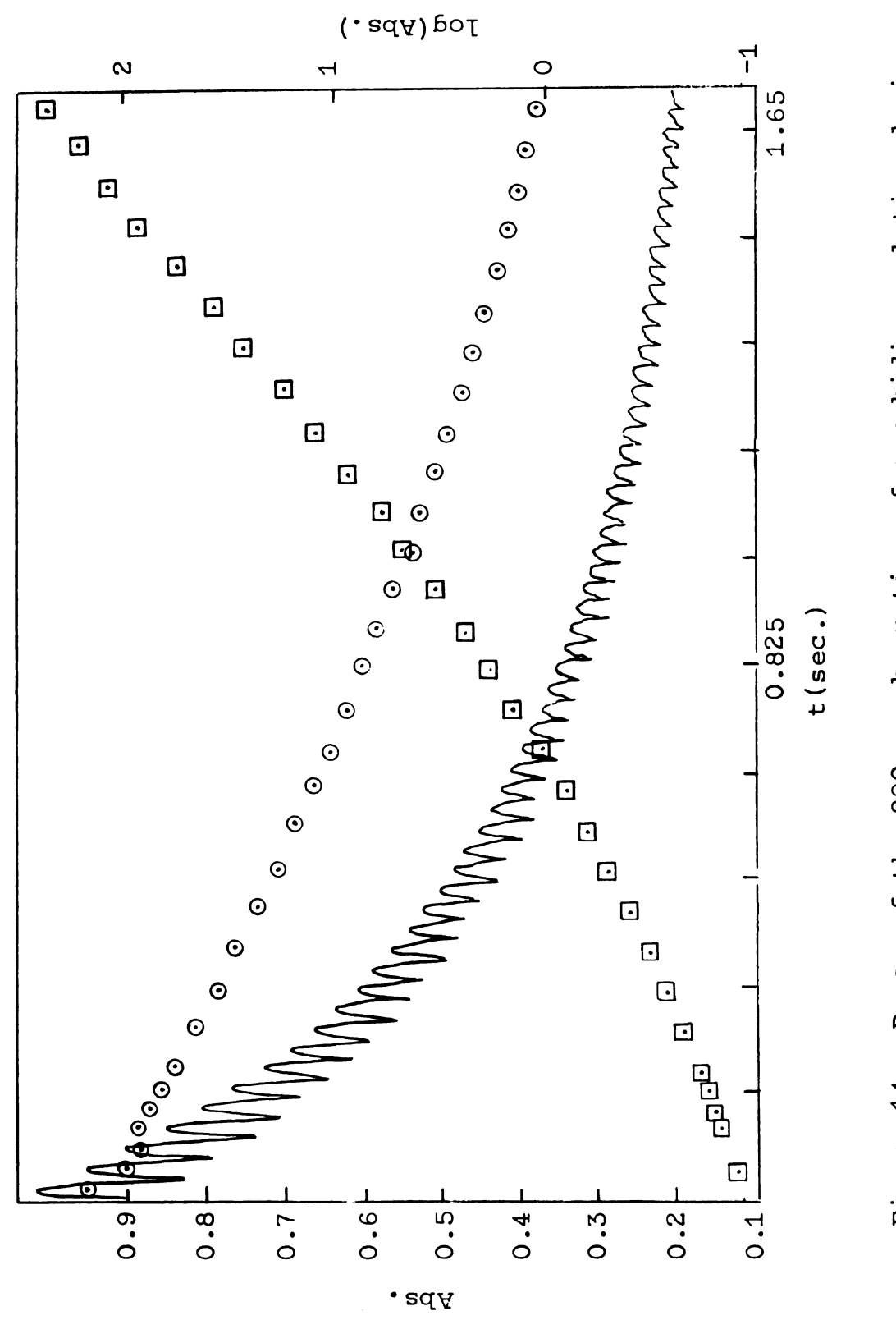
When it became obvious that independent decay of the optical absorptions could not occur, the kinetic traces obtained in the present study and also those of Dewald and Feldman were carefully examined, with the aid of the CAT system where possible. This analysis showed that plots of log(Abs.) versus time are, in fact, smooth curves and have no strictly linear portions. Figure 14 shows the decay of the 890 nm absorption of a rubidium-ethylenediamine solution during the reaction with water. Also shown in this Figure is the behavior of log(Abs.) and l/Abs. versus time for this kinetic push.

It is necessary to ask at this point whether the mechanism for the reaction of alkali metals with water in ethylene-diamine is different from the mechanism which is operative for the same reaction in liquid ammonia. In ammonia, the reaction of dilute metal solutions is slow (half-times of minutes to seconds at  $-34^{\circ}$ C) and is thought to involve reaction with the ammonium ion produced by solvent dissociation (98). If this same mechanism were operative in ethylenediamine, the necessary reactions would be:

$$H_2O + RNH_2 \xrightarrow{k_1} RNH_3^+ + OH^-$$
 (3)

© 0

0.9 H 8.0



Decay of the 890 nm absorption of a rubidium solution during reaction with water in ethylenediamine. Also shown is the behavior of log(Abs.) and  $1/({\rm Abs.})$  for this push. Figure 14.

followe

and

weak aci Reaction measured (90a).

Cor

Using the

represent

d[R

which yiel

[RNE

Substituti

Measu!

ethylenedia

followed by

$$e_{sol}^{-} + RNH_3^{+} \xrightarrow{k_3} H + RNH_2$$
 (4)

and

$$M^{+} + OH^{-} \xrightarrow{k_{4}} MOH(s)$$
 (5)

Conductivity studies (91) show that water acts as a weak acid in ethylenediamine with  $K = k_1/k_2 < 10^{-12}$  for Reaction 3. The rate constant of Reaction 4 has been measured in ethylenediamine  $(k_3 = 1.7 \times 10^5 \text{ M}^{-1} \text{ sec}^{-1})$  (90a). The rate of disappearance of the reducing species, represented by  $e_{\text{sol}}^-$ , can be written as:

$$-\frac{d[e]}{dt} = k_3 [e] [RNH_3^+]$$
 (6)

Using the steady state approximation for RNH3 + gives

$$\frac{d[RNH_3^+]}{dt} = 0 = k_1[H_20][RNH_2] - k_2[RNH_3]_{ss}[OH^-] - k_3[e^-][RNH_3^+]_{ss}$$
(7)

which yields

$$[RNH3]SS = \frac{k_1 [H_2O] [RNH_2]}{k_2 [OH^-] + k_3 [e^-]}$$
(8)

Substituting this result into Equation 6 gives

$$-\frac{d[e]}{dt} = \frac{k_1 k_3 [e] [H_2 O] [RNH_2]}{k_2 [OH] + k_3 [e]}$$
(9)

Measurement of the rate of reaction with water in a ethylenediamine gives approximately

The dev this is

that pre In sec<sup>-1</sup> a

becomes

However

If the re concentra in order

The a in pure et removal of

low. It c . RNH3 + and

be close t

is ≥ 109 M The s

droxides tetrically |

$$-\frac{d[e]}{dt} = k_{e} - [e] [H_{2}0]$$
 (10)

The deviation from pseudo-first-order behavior shows that this is not described by the simple reaction

$$e^- + H_2O \xrightarrow{k_e^-} products$$
 (11)

However, a comparison of the approximate value of  $k_{\rm e}^-$  with that predicted by Equation 9 can be made.

In a typical run [e] =  $10^{-4}$  M. Using  $k_e^- \approx 20$  M<sup>-1</sup> sec<sup>-1</sup> as observed and [H<sub>2</sub>O] = 6 M, the rate of reaction 11 becomes

$$-\frac{d[e^{-}]}{dt} = 1.2 \times 10^{-2} \, \underline{M} \, \text{sec}^{-1} \tag{12}$$

If the reaction were forced to proceed through  $\mathrm{RNH_3}^+$ , the concentration of the hydroxide ion would have to be very low in order for the equilibrium to favor the formation of  $\mathrm{RNH_3}^+$ .

The alkali metal hydroxides are only slightly soluble in pure ethylenediamine with  $K_{\rm sp}=10^{-9}$  (91). Therefore, removal of OH by precipitation could keep its concentration low. It can be assumed that the rate of recombination of RNH<sub>3</sub> and OH according to the reverse of Reaction 3 will be close to the diffusion controlled limit, so that  $k_2 \geq 10^9 \ \text{M}^{-1} \ \text{sec}^{-1}$ .

The solubilities of sodium, potassium and cesium hydroxides in "wet" ethylenediamine were measured conductimetrically as described in Section III. The results are

given in
all of the solute concentrate reached 1 tation was became all increasing solutions hydroxide trations by reacticannot be denominate true, can

If i

Then from

and  $f_{rom}$  E

- d[∈ dt

Solving 14

k<sub>1</sub>

given in Table IV and shown for cesium in Figure 15. With all of the above alkali metal hydroxides, the conductance of the solution increased smoothly with increasing hydroxide concentration. It was not until the hydroxide concentration reached  $10^{-4}$  M ([H<sub>2</sub>O] $\cong$  0.2 M) that any indication of precipitation was observed. At this concentration, the solution became cloudy and the conductance increased more slowly with increasing hydroxide concentration. Therefore, in dilute solutions of water in ethylenediamine, the alkali metal hydroxides are reasonably soluble. Since hydroxide concentrations as high as  $10^{-4}$  M will be attained in these solutions by reaction of the metals with water, and since hydroxide ion cannot be removed by precipitation, the term  $k_2$  [OH $^-$ ] in the denominator of Equation 9 cannot be neglected. That this is true, can be shown by the following argument:

If it is assumed that

$$k_3[e^-] \gg k_2[OH^-]$$

Then from Equation 9

$$-\frac{d[e]}{dt} = \frac{k_1 k_3 [e][H_20][RNH_2]}{k_3 [e]} = k_1 [H_20][RNH_2]$$
 (13)

and from Equation 12

$$-\frac{d[e^{-}]}{dt} = k_1[H_2O][RNH_2] = 1.2 \times 10^{-2} \underline{M} \text{ sec}^{-1}$$
 (14)

Solving 14 for  $k_1$  with  $[RNH_2] = 16 \text{ M}$  and  $[H_2O] = 6 \text{ M}$ , gives

$$k_1 = 1.2 \times 10^{-4} \, \underline{M}^{-1} \, \text{sec}^{-1} \approx 10^{-4} \, \underline{M}^{-1} \, \text{sec}^{-1}$$

[OH

Cesium Hy

[OH-Sodium Hys

TABLE IV

CONDUCTANCE OF CESIUM, SODIUM AND POTASSIUM HYDROXIDES IN "WET" ETHYLENEDIAMINE

[OH <sup>-</sup> ] ( <u>M</u> x 10 <sup>3</sup> )	[H <sub>2</sub> O] <u>M</u>	Specific Conductance (mho x 10 <sup>6</sup> )
Cesium Hydroxide		
0 6.60 10.30 19.86 29.26 33.36 38.92 44.44 50.82 58.10 64.10 72.28	0.26 0.41 0.78 1.14 1.30 1.52 1.73 1.99 2.27 2.51 2.83	0.69 1.97 2.50 3.72 5.64 6.69 8.58 10.90 12.55 15.55 18.28 23.24
[OH <sup>-</sup> ] ( <u>M</u> x 10 <sup>5</sup> ) Sodium Hydroxide	1.00	
0 3.9 5.58 17.30 23.70 30.25 40.56 55.26 63.99 70.86 79.05 86.19 96.12 105.72 116.33 125.73 135.66 145.41	0 0.19 0.47 0.82 1.12 1.42 1.91 2.59 3.00 3.33 3.72 4.04 4.53 4.97 5.47 5.91 6.38 6.84 7.29	0.40 0.58 0.87 1.26 1.57 1.97 3.67 5.63 6.96 7.86 9.22 10.36 12.09 13.42 15.24 16.32 17.90 19.34 21.11

continued

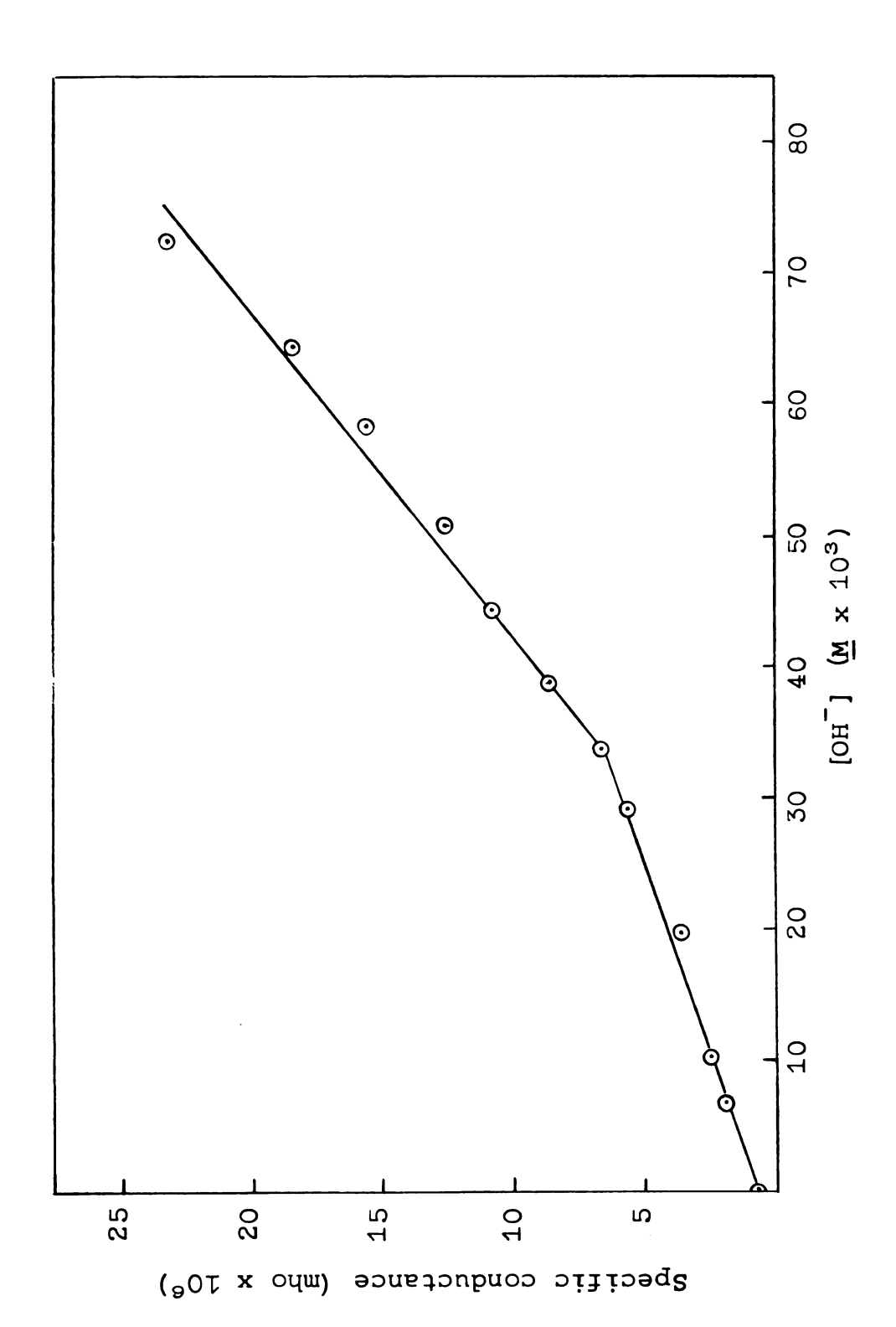
TABLE I

[0

Potassi

TABLE IV--continued

[OH ] ( <u>M</u> x 10 <sup>4</sup> )	[H <sub>2</sub> O] <u>M</u>	Specific Conductance (mho x 10 <sup>6</sup> )
Potassium Hydroxide		
0 1.96 2.41 3.10 4.60 5.43 6.51 7.05 7.90 9.02 9.99	0 0.21 0.36 0.47 0.59 0.75 0.92 0.98 1.07 1.36 1.40	1.01 1.12 3.21 4.79 6.05 7.80 8.22 9.12 10.90 12.51 13.10



Plot of specific conductance vs. hydroxide concentration for cesium hydroxide in "wet" ethylenediamine. Figure 15.

Since  $\frac{k_1}{k_2} = 10^{-12}$  then  $k_2 = 10^8 \, \underline{M}^{-1} \, \text{sec}^{-1}$  and if  $[OH^-] = 10^{-4} \, \underline{M}$  then  $k_2 \, [OH^-] = 10^{+4} \, \text{sec}^{-1}$ 

However in a typical experiment,  $[e^-] = 10^{-4} \, \underline{M}$  and from earlier results  $k_3 = 1.7 \times 10^5 \, \underline{M}^{-1} \, \mathrm{sec}^{-1}$  so that  $k_3 [e^-] = 1.7 \times 10 \, \mathrm{sec}^{-1} = 17 \, \mathrm{sec}^{-1}$ , which is much smaller than the "neglected" term,  $k_2 [\mathrm{OH}^-]$ . Equation 9 therefore takes the form

$$- \frac{d[e^{-}]}{dt} = \frac{k_1}{k_2} k_3 \frac{[RNH_2]}{[OH^{-}]} [e^{-}] [H_2O]$$
 (15)

Since

$$\frac{k_1}{k_2}$$
 [RNH<sub>2</sub>]  $\leq 10^{-12}$  [RNH<sub>2</sub>]  $\leq 1.5 \times 10^{-11} \text{ M}$ 

and with  $k_3 = 1.7 \pm 0.2 \times 10^5 \, \underline{\text{M}}^{-1} \, \text{sec}^{-1}$ , the rate of disappearance of the reducing species according to this mechanism becomes for these concentrations

$$-\frac{d[e^{-1}]}{dt} \le \frac{1.5 \times 10^{-11} \times 1.7 \times 10^{5} \times 10^{-4} \times 6}{10^{-4}} \quad \underline{M} \text{ sec}^{-1}$$
(16)

or

$$\frac{d[e^-]}{dt} \le 1.53 \times 10^{-5} \, \underline{M} \, \text{sec}^{-1}$$

This is to be compared with the observed value

$$\frac{d[e^{-}]}{dt} = 1.2 \times 10^{-2} \, \underline{M} \, \text{sec}^{-1}$$

Therefore the observed rate of reaction is three orders of magnitude larger than that predicted on the basis of the mechanism presumed applicable in metal-ammonia solutions.

Even if the concentration of hydroxide ion were as low as

 $10^{-5}$   $\underline{M}$ , this mechanism predicts a rate which is still two orders of magnitude smaller than that observed. It should be noted that in concentrated water solutions (1 to 5  $\underline{M}$ ), the solubility of the metal hydroxides can be expected to be higher, thus making agreement of the predicted rate constant with the observed rate constant even worse. It is therefore clear that a mechanism involving formation of  $RNH_3^+$  as an intermediate is not operative in the reaction of alkali metals with water in ethylenediamine.

It is evident that the reaction of dilute solutions of the alkali metals with water in ethylenediamine cannot be described by simple first or second order kinetics. It is also evident that the reaction is faster than the same reaction in ammonia and apparently proceeds by a different mechanism. The reason for this difference might result from the complex nature of the metal-amine solutions. Recall that in metal-amine solutions, additional species are present which are not present in metal-ammonia solutions. This is best illustrated by the presence of metal dependent optical absorption bands (R-bands) in metal-amine solutions which are not present in metal-ammonia solutions. The presence of -CH<sub>2</sub>-groups in ethylenediamine might also be important.

Solutions of all the alkali metals except sodium in ethylenediamine possess a metal-independent infrared absorption band (IR-band) similar to the optical absorption observed in metal-ammonia solutions. As already noted, only

30

SC

li

If

'nà

ΟĘ

37,

io:

one optical band, at 660 nm, is observed in solutions of sodium in ethylenediamine. Potassium, rubidium and concentrated cesium solutions have an intermediate optical absorption (R-band), the magnitude of which decreases relative to that of IR-band as the solution is diluted or decomposed (56). This, coupled with the fact that the band position is metal dependent, suggests that the species responsible for this absorption is a metal-containing species which can dissociate upon dilution. It appears likely that the species responsible for this band has the stoichiometry M or M2.

For reasons already discussed (Section II, part B), the infrared absorption observed in metal-amine solutions has been assigned to the solvated electron and its "ammonia-like" aggregates.

Since interconversion of the optical bands in ethylene-diamine appears to be fast, and since the magnitude of the R-band decreases relative to that of the IR-band when the solution is diluted, it is reasonable to assume that an equilibrium exists between the R-species and the IR-species.

If such an equilibrium exists, it is not surprising that this equilibrium can complicate the kinetics of the reaction with water.

Conductance and magnetic data (44) indicate the presence of several species in metal-amine solutions even when only an IR-band is present. These species probably result from ion-pair interactions which are expected to be more

pronounced in ethylenediamine than in ammonia because of the lower dielectric constant of ethylenediamine. By analogy with the metal-ammonia case, the expected stoichiometries of these species would be e, M, M and M2. Assuming equilibrium among these species, the expected rates of disappearance would be  $M_2 > M^- > M > e^-$ .

The evidence which has become available since the earlier treatments of the kinetics of the reaction with water is overwhelmingly in favor of the assumption that the species present in alkali metal-amine solutions are in equilibrium with one another. Using this evidence as a starting point, the consequences of the assumption that an equilibrium exists and is maintained during reaction with water will be explored. The details of the following derivation are given in Appendix The major species assumed to be present can be represented by the stoichiometries e, M, M2 and M (see Section II).

If the species responsible for the IR-band observed in metal-amine solutions is the solvated electron and its "ammonia-like" aggregates, then for the case of cesium in ethylenediamine, four equilibria are necessary for the kinetic treatment of the reaction with water. The four necessary equilibria are:

$$M^{-} \xrightarrow{K_{1}} M + e^{-} \tag{17}$$

$$M = \frac{K_1}{K_2} \qquad M + e^- \qquad (17)$$
 $M = \frac{K_2}{K_2} \qquad M^+ + e^- \qquad (18)$ 

$$M^{+} + OH^{-} \xrightarrow{K_{3}} MOH$$
 (19)

$$M^- + M^+ \frac{K_4}{M_2} M_2$$
 (20)

where all species are understood to be solvated.

Since it is not known which, if any, of the above species reacts preferentially with water, the most general case will be assumed in which any of the species listed above (i.e.,  $e^-$ ,  $M^-$ ,  $M_2$ , M) can react with water to form intermediates which ultimately lead to hydrogen as a product. Since the overall reaction of cesium solutions with water appears to be first order in water over a wide range of water concentrations (90a), the slow step in the reaction is probably the bimolecular reaction of the species listed above with water.

$$M + H_2O \xrightarrow{k_M} [Intermediates] \xrightarrow{H_2O} \frac{1}{fast} H_2 + OH^- + M^+ (21)$$

$$e^- + H_2O \xrightarrow{k_e^-} [Intermediates] \xrightarrow{H_2O} \frac{1}{2} H_2 + OH^-$$
 (22)

$$M_2 + H_2O \xrightarrow{\frac{M_2}{\text{slow}}} [Intermediates] \xrightarrow{\frac{H_2O}{\text{fast}}} H_2 + 2 \text{ M}^+ + 2 \text{ OH}^- (23)$$

$$M^- + H_2O \xrightarrow{k_{M^-}} [Intermediates] \xrightarrow{H_2O} H_2 + M^+ + 2 OH^- (24)$$

The total concentration of reducing species

$$[M_{T}] = [M] + [e] + 2[M_2] + 2[M]$$
 (25)

and the rate of hydrogen production is given by

$$\frac{d[H_2]}{dt} = -\frac{1}{2} \frac{d[^MT]}{dt}$$
 (26)

The time rate of change of total metal concentration is

$$-\frac{1}{2}\frac{d[^{M}T]}{dt} = \{k_{M}^{-}[M^{-}] + k_{M_{2}}[M_{2}] + \frac{k_{M}}{2}[M] + \frac{k_{e}^{-}[e^{-}]}{2}\}[H_{2}O] \quad (27)$$

or

$$-\frac{d[^{M}T]}{dt} = 2k_{M}^{\bullet}[M^{-}] + 2k_{M_{2}}^{\bullet}[M_{2}] + k_{M}^{\bullet}[M] + k_{e}^{\bullet}[e^{-}]$$
 (28)

where

$$k_{x}^{\prime} = k_{x} [H_{2}O]$$

Since the time decay of the total absorbance is measured experimentally, the above equations need to be rewritten in terms of the absorbances rather than the concentrations.

The expression for the total absorbance is

$$A_{T} = A_{M^{-}} + A_{M_{2}} + A_{e^{-}} + A_{M} = A_{P} + A_{D}$$
 (29)

where

$$A_{D} = A_{M^{-}} + A_{M_{2}}$$
 (30)

is the absorbance due to diamagnetic species, and

$$A_{\mathbf{p}} = A_{\mathbf{e}^{-}} + A_{\mathbf{M}} \tag{31}$$

is the absorbance due to paramagnetic species. The concentrations of the individual species in Reactions 17 through 20 can be written as

$$[M] = \left(\frac{K_1}{K_2}\right)^{\frac{1}{2}} [M^+]^{\frac{1}{2}} [M^-]^{\frac{1}{2}} \gamma_{\pm}^2$$
 (32a)

$$[M_2] = K_4 [M^+] [M^-] \gamma_{\pm}^2$$
 (32b)

$$[e^{-}] = \left(\frac{K_1 K_2}{[M^{+}]}\right)^{\frac{1}{2}} [M^{-}]^{\frac{1}{2}}$$
 (32c)

in which  $\gamma_{+}$  is the mean molar activity coefficient.

Substitution of Equations 32a, 32b and 32c into Equations 28 and 29 leads to:

$$A_{D} = \{ \epsilon_{M^{-}} + \epsilon_{M_{2}} K_{4} [M^{+}] \gamma_{+}^{2} \} [M^{-}] = r [M^{-}]$$
 (33)

and

$$A_{p} = \{ \epsilon_{e^{-}} + \frac{\epsilon_{M} [M^{+}] \gamma_{+}^{2}}{K_{2}} \} [e^{-}] = q[e^{-}]$$
 (34)

In Equations 33 and 34, r and q are constants at fixed values of  $[M^{+}]$  and ionic strength and

$$\epsilon_{\mathbf{x}} = \epsilon_{\mathbf{x}}^{\,\prime} \quad \ell$$
 (35)

where:

 $\epsilon_{\mathbf{x}}^{\prime}$  = molar extinction coefficient of species  $\mathbf{x}$ 

 $\ell$  = path length.

Using these results, the net rate of disappearance of total metal is then given by

$$-\frac{d[M_T]}{dt} = (\frac{k_{e^-}^! + k_{M^-}^! [M^+] \gamma_{\pm}^2 / K_2}{q}) A_p + \frac{2(k_{M^-}^! + k_{M_2}^! K_4 [M^+] \gamma_{\pm}^2) A_p}{r}$$
(36)

Solving these equations for the time decay of the total absorbance leads to

$$-\frac{dA_{T}}{dt} = \frac{2r (k_{e}^{!} \pm k_{M}^{!} [M^{+}] \gamma_{\pm}^{2} / K_{2}) \frac{A_{P}}{A_{D}} (A_{D}^{+} \pm \frac{A_{P}}{2}) \pm 4q (k_{M}^{!} \pm k_{M}^{!} K_{4}^{*} [M^{+}] \gamma_{\pm}^{2}) (A_{D}^{+} \pm \frac{A_{P}}{2})}{r \frac{A_{P}}{A_{D}} (1 + \frac{[M^{+}] \gamma_{\pm}^{2}}{K_{2}}) + 4q (1 + K_{4} [M^{+}] \gamma_{\pm}^{2})}$$
(37)

as one form of the solution. Unfortunately, neither the equilibrium constants nor the rate constants are known in ethylenediamine.

In order to put Equation 37 into a more usable form, some further simplifications are necessary. If the assignment of the infrared absorption band in metal-amine solutions to the solvated electron and its "ammonia-like" aggregates is valid, then the results of the extensive treatments of metal-ammonia solutions can be used to simplify the kinetic treatment under discussion here.

Recall that the species M and M2, which are thought to exist in metal-ammonia solutions, are probably ion-paired species of the form (M+ e and (M+ M). The species of stoichiometry M is thought to be an ion pair composed of a pair of weakly interacting electrons in the coulomb field of a metal cation  $(e^- \cdot M^+ \cdot e^-)$ . If these same species are responsible for the IR-band in metal ethylenediamine solutions, then several assumptions can be made regarding the rates of reaction of these various species with water. First, the ion pair association constants for Reactions 18 and 20 should be approximately equal. Therefore,  $K_4 \cong 1/K_2$ . Second, since the species of stoichiometry M is probably a loose ion pair between an alkali metal cation and a solvated electron (M + e -), its rate of reaction with water should be nearly the same as that of the solvated electron. By the same argument, one might expect that the rates of reaction of

 $M_2$ ,  $(M^+, M^-)$  and  $M^-$  with water will also be approximately the same. Finally, since the optical absorption band in metal-ammonia solutions appears to obey Beer's Law (17) and is consistent with the assumption of weak interactions, the extinction coefficients of the various species are related by their stoichiometries according to

$$\epsilon_{e}^{-} = \epsilon_{M}^{-} = \frac{\epsilon_{M^{-}}}{2} = \frac{\epsilon_{M_{2}}}{2}$$
 (38)

Using these three assumptions, Equations 32, 33, 34 and 37 can be combined to give

$$-\frac{dA_{P}}{dt} = \frac{k_{e}^{-} A_{P} + \frac{k_{M}^{-}}{2} A_{D}}{1 + 2 \frac{A_{D}}{A_{P}}}$$

and

$$-\frac{dA_{D}}{dt} = \frac{2k_{e}^{2} - A_{D} + k_{M}^{2} - \frac{A_{D}^{2}}{A_{p}^{2}}}{1 + 2 \frac{A_{D}^{2}}{A_{p}^{2}}}$$

subject to the condition given by Equation 29.

Since the previous mechanisms were shown to be invalid, the kinetics data of Dewald and Feldman were re-analyzed by using this mechanism. The results of this re-analysis are listed along with the data obtained in this work and will be so noted.

Of major concern to progress in the study of the reaction of the alkali metals with water has been the improvement in "kinetic control." The major progress in this area has been the improvements made in solvent purification technique. In previous studies and in the early studies in this work, when metal solutions were mixed with "pure ethylenediamine at the

beginning of a run, a slow decay of the absorbance always was observed. This decay was always slower than that observed during reaction with the lowest water concentration. In later runs (particularly studies with sodium and rubidium), no observable decay was observed when the metal solutions were mixed with the solvent at the beginning of a run. It will be apparent from the discussion and the data listed in the following sections that the data obtained from these runs showed better internal consistency than in those cases where a slow decay of the absorbance was observed when the metal solution was mixed with solvent. Also in the runs where no decay was observed when the metal solution was mixed with solvent, the metal absorbance was always fairly reproducible. In runs where the metal solution decomposed when mixed with solvent, the initial absorbance showed a great variation from push to push during the course of the run. A comparison of these two cases is shown in Figure 16 where the metal absorbances are plotted as a function of push number. Inspection of this Figure shows that in those cases (rubidium and sodium) where mixing of the metal solution with "pure" solvent at the beginning of the run produced no detectable decay, consistency of the values of the initial absorbance, over the course of the run, was observed. However, in the case where a decay of the absorbance occurred when the metal solution was mixed with water, the values of initial absorbance during the course of the run were not constant, indicating that some

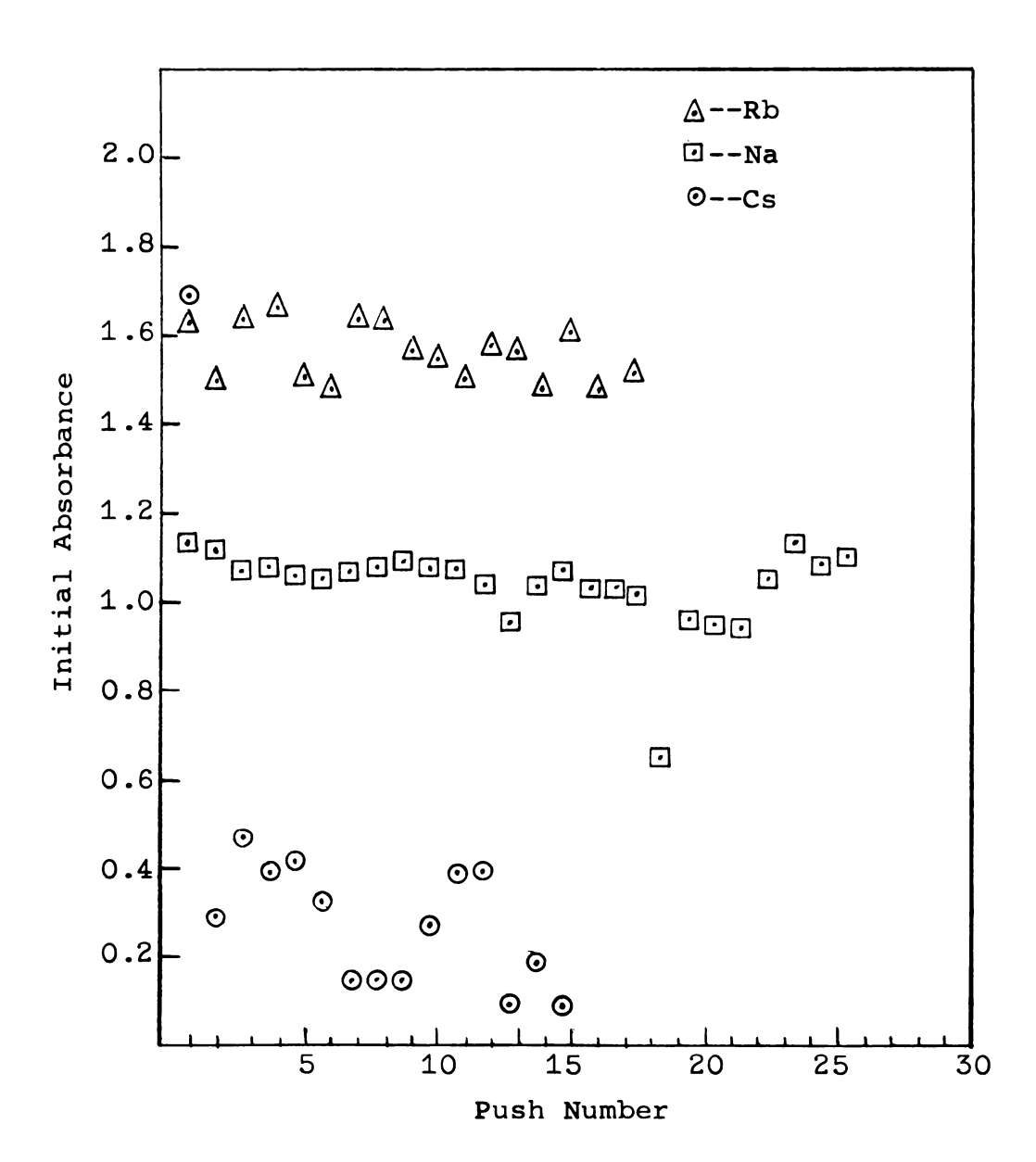


Figure 16. Plot of initial absorbance <u>vs</u>. push number for the reaction of cesium, sodium and rubidium with water, in ethylenediamine.

decomposition of the solution had occurred prior to mixing with water.

The most difficult metal solution to work with, from the point of view of stability, has been cesium. Unfortunately, this was the first metal solution used in the study of the reaction of the metal solutions with water. The reason for using cesium initially (i.e., the fact that it showed only the IR-band) at the time outweighed the disadvantages resulting from the difficulty in preparing a stable solution. However, recently, solutions of cesium in ethylenediamine have been prepared which show the same stability as the rubidium and sodium solutions described above (104). With these thoughts in mind, the results obtained in this work and the significance of the proposed mechanism for the reaction of the alkali metals with water in ethylenediamine can now be discussed.

## B. Alkali Metals Plus Water

## 1. Cesium

The cesium solutions used in this work possessed only one optical band which had a maximum in the infrared at 1280 nm. Since the sensitivity limit of the detectors is only about 1110 nm, the band maximum was never actually observed in these studies. The band shape of the IR-band observed in the cesium solutions is shown in Figure 13. The kinetic data for cesium were initially analyzed by numerical solution

of Equation 39 and the values of the four parameters  $k_e^-$ ,  $k_M^-$ ,  $A_p^-$  and  $A_D^-$  which gave the best fit to the data were calculated. Figure 17 shows a comparison of the observed decay of the total absorbance with that given by the best fit of Equation 39 to this set of data. This fit is typical for those cases where the decay was not complicated by the catalyzed decomposition at long times. A typical fit in the latter case is shown in Figure 18. The tail of the decay curve shown in this Figure is lower than first-order in the absorbance and it can be seen that it does not fit well with the curve calculated using Equation 39.

In spite of the apparently good fit to the decay of the absorbance, the values of the parameters, which gave the best fit, showed a greater than expected variation for pushes within a given run. In all cases, where the four parameter equation (Equation 39) was used to fit the data, the value of  $k_{\rm e}$ — calculated to give the best fit had a very large uncertainty and was for all practical purposes statistically undefined. Inspection of Table V shows this and also shows that in some cases the best fit to the experimental data was accomplished by assigning a negative value to  $k_{\rm e}$ —. These facts suggest that an equally good fit to the data can be obtained using only the three parameters  $k_{\rm M}^{\bullet}$ —,  $A_{\rm p}$  and  $A_{\rm D}$ .

The cesium data were analyzed using a differential equation which involved only the three adjustable parameters  $k_{M}^{+}$ ,  $A_{p}$  and  $A_{D}$ . The derivation of this equation is algebraically equivalent to the derivation of the four parameter equation,

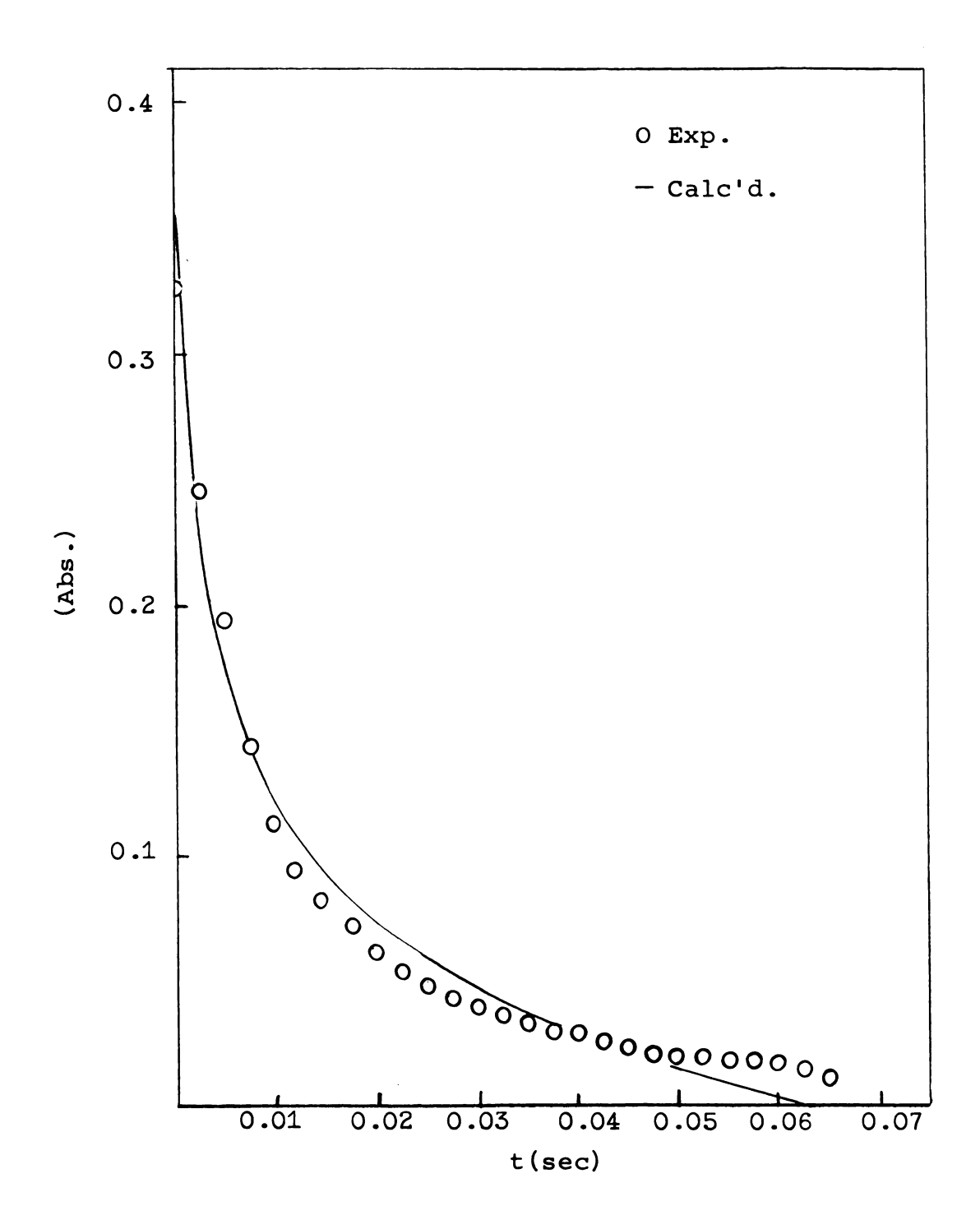


Figure 17. Comparison of observed decay of the absorbance with that given by the best fit of Equation 39 for the reaction of cesium with water in ethylenediamine.

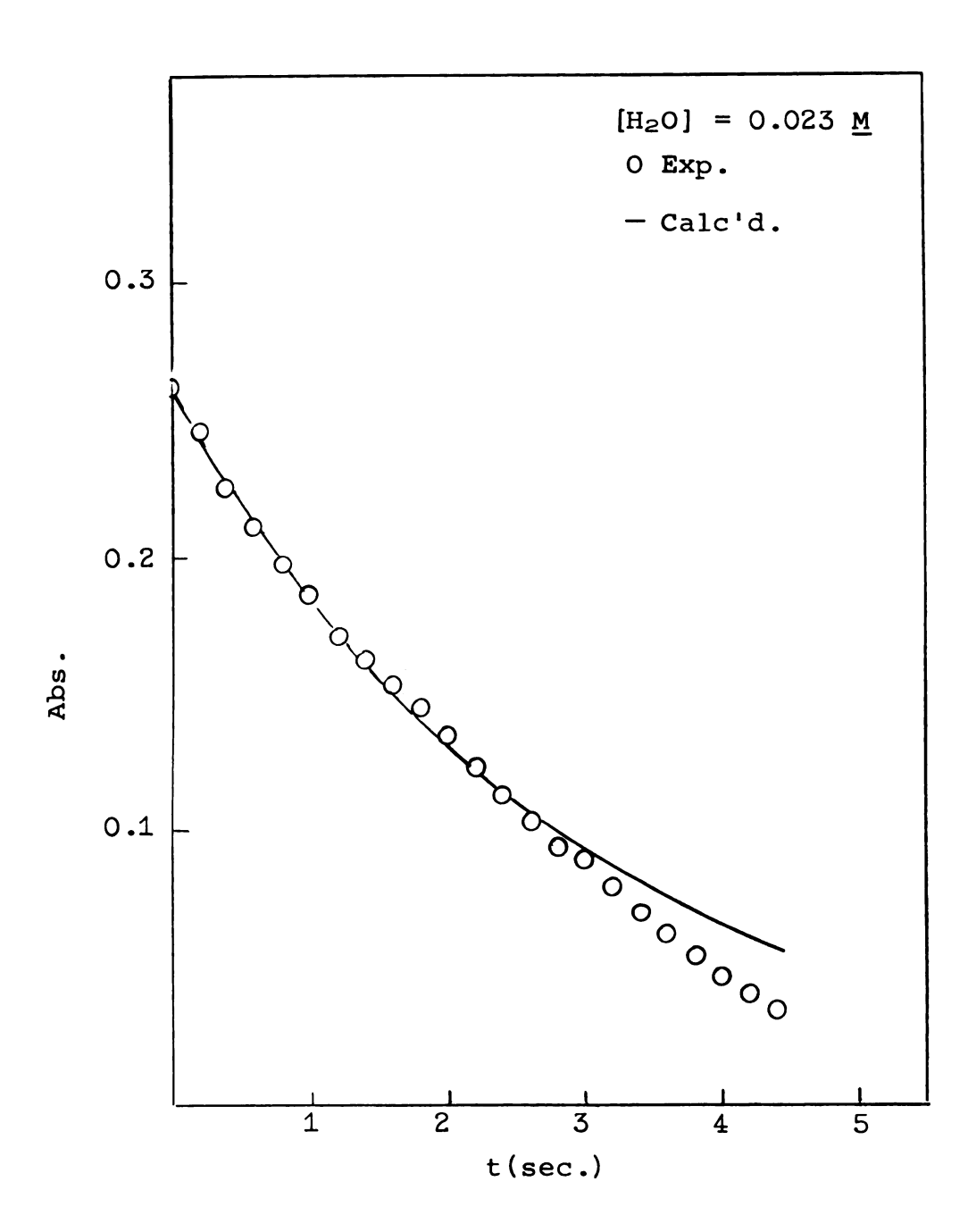


Figure 18. Fit of Equation 39 to observed decay at absorbance for reaction of cesium with water when a long tail is observed.

VALUES OF  $k_{M^-}$  AND  $k_{e^-}$  CALCULATED FROM THE BEST FIT OF EQUATION 39 TO THE DATA OBTAINED FOR THE REACTION OF CESIUM WITH WATER IN ETHYLENEDIAMINE

[H <sub>2</sub> O] ( <u>M</u> )	λ(nm)	k <sub>e</sub> _	<sup>б</sup> k e−	k <sub>M</sub> -	<sup>o</sup> k <sub>M</sub> −
0.0244	1100	12.95	14.061	6.983	4.100
0.0244	1100	5.225	6.910	6.937	4.933
0.0244	950	0.254	0.844	7.799	
0.0244	750	3.197	9.847	7.184	4.871
0.0728	1100	3.342	7.165	2.170	
0.341	1100	41.35	150.840	2.372	1.212
0.341	950	30.65	106.486	28.57	16.890
0.928	1100	-4.565		5.240	
0.928	1100	-4.864		6.380	
1.7755	1100	-3.291		3.89	
1.7755	1100	3.42	8.744	0.823	0.461
1.7755	1100	1.656		1.23	
6.11	1100	-32.83		26.44	
6.11	1100	53.89		18.68	
6.11	1100	-230.51		19.81	

with the exception that no direct reaction is assumed to take place between  $e^-$  or M and water so that  $k_{e^-}^{\prime}=k_{M}^{\prime}=0$ . The resulting differential equations have the form:

$$-\frac{dA_{P}}{dt} = \frac{k_{M}' - A_{D}/2}{1 + 2A_{D}/A_{P}} ; -\frac{dA_{D}}{dt} = \frac{k_{M}' - A_{D}^{2}/A_{P}}{1 + 2 A_{D}/A_{P}}$$
(40)

The results obtained by using these equations to fit the data are given in Table VI. A comparison of the values of  $k_{M^-}$  calculated from Equation 40 above and those from Equation 39 show that they have about the same values. The consistency of the calculated values of  $k_{M^-}$  within a given run is, however, not improved. As might be expected, the uncertainties on the individual values of  $k_{M^-}$  have decreased somewhat. Figure 19 shows that in spite of this improvement it is impossible to tell whether  $k_{M^-}$  has any dependence on the water concentration.

The possible factors involving the non-reproducibility of the values of  $k_{M^-}$  will be discussed later, since the same factors affecting the kinetics of the reaction of cesium with water also will affect the reaction of the other metals with water.

### 2. Sodium

The sodium solution used in this work was more stable than any other metal solution used. When a sample of the sodium solution was mixed with ethylenediamine at the beginning

TABLE VI

VALUES OF k<sub>M</sub>- CALCULATED FROM THE BEST FIT OF EQUATION 40

TO THE DATA OBTAINED FOR THE REACTION OF CESIUM

WITH WATER IN ETHYLENEDIAMINE

[H <sub>2</sub> O] ( <u>M</u> )	λ <b>(nm)</b>	k <sub>M</sub> -	<sup>6</sup> k <sub>M</sub> −
$[Cs] = 1.5 \times 10$	)-4 <u>M</u> (a)		
0.0244 0.0244 0.0244 0.0244 0.341 6.11 6.11 6.11 6.11 6.11	1100 1100 950 750 1100 1100 950 750 750 750	8.907 6.195 8.626 12.251 2.35 26.455 18.655 20.396 19.082	0.913 0.730 0.112 0.357 0.016 4.05 1.062 2.85 2.21
0.023 0.023 0.023 0.023 0.023 5.60	1100 1100 1100 1100 950 950 750	20.076 19.171 16.991 16.181 16.772 33.344 49.387	4.98 0.577 0.538 0.434 1.656 2.20 3.91
[Cs] = 3 x 10- 0.073 0.073 0.928 0.928 1.7755 1.7755 1.7755 1.7755	1100 1100 1100 1100 1100 1100 1100 110	10.022 2.534 15.007 39.090 8.425 8.723 9.338 2.476 4.230	0.631 0.518 8.155 9.061 1.69 2.02 1.32 0.21 6.58

continued

TABLE VI--continued

[H <sub>2</sub> O] ( <u>M</u> )	λ(nm)	k <sub>M</sub> -	<sup>6</sup> k <sub>M</sub> −
$[Cs] = 3.3 \times 10^{-4}$	<u>M</u>		
0.84 0.84 0.84 1.016 1.016 1.667 1.667 1.667	1052 1052 1052 1052 1052 1052 1052 1052	11.631 3.966 8.713 9.161 29.743 15.811 5.733 13.614 30.704 9.220	2.911 0.344 2.281 2.740 7.648 3.617 0.677 3.215 11.738 2.871

<sup>(</sup>a) Reanalyzed data of LHF (90).

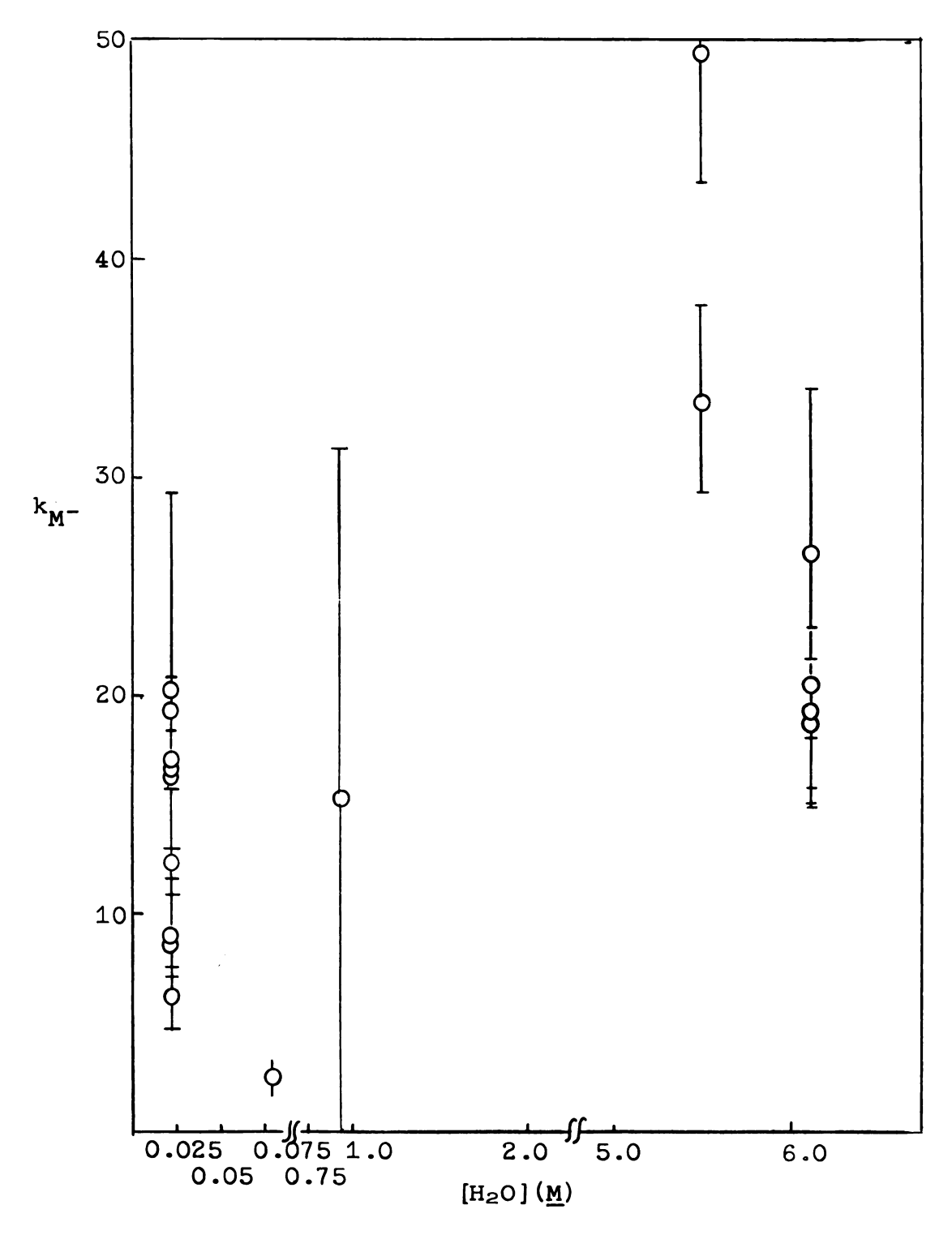


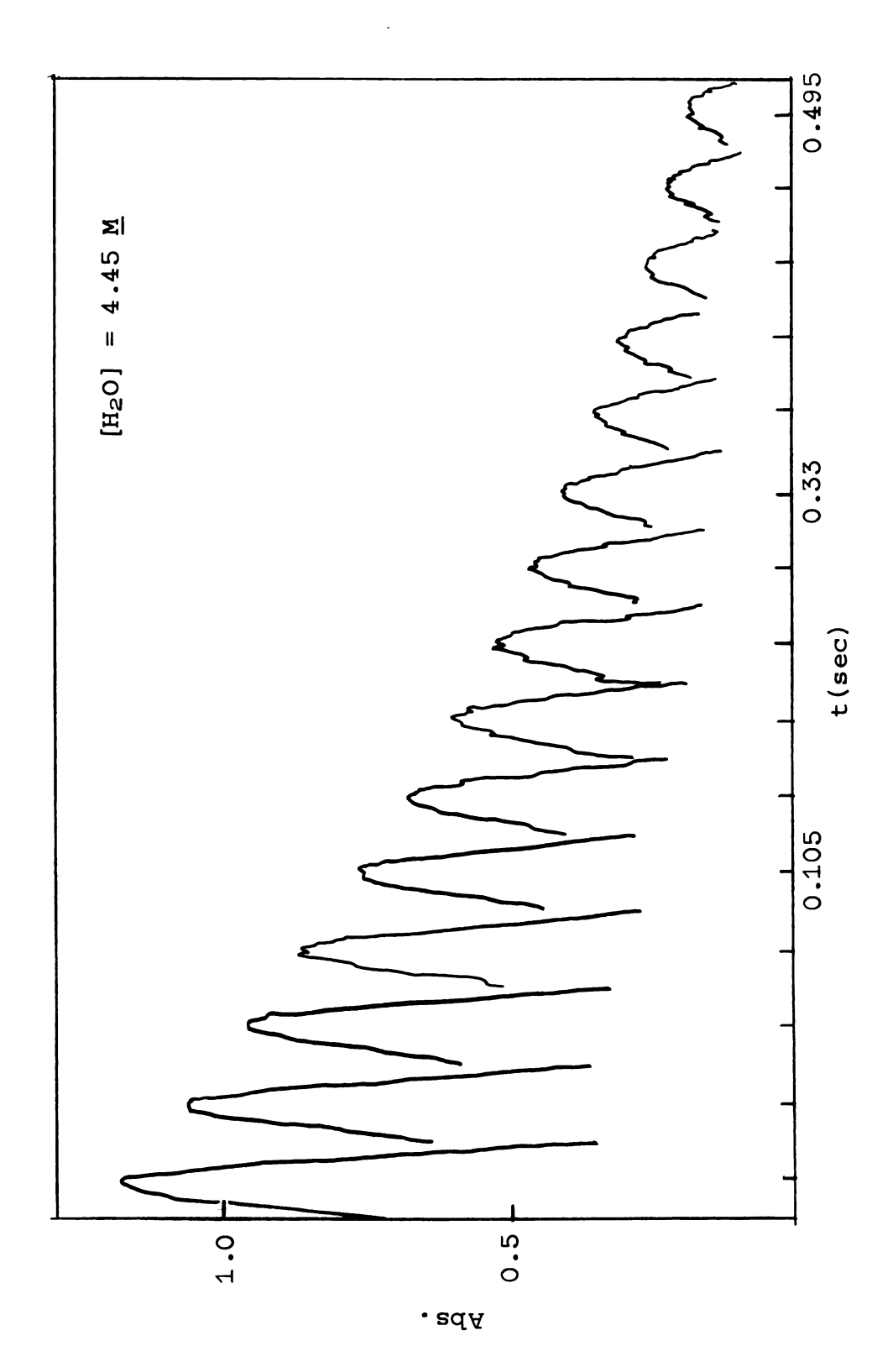
Figure 19. Plot of  $k_{M^-}$ , calculated from Equation 40, versus water concentration for the reaction of cesium with water in ethylenediamine.

of this run, no detectable decay of the 660 nm band occurred. In general, other metal solutions always showed a slow decay of the absorbance when mixed with ethylenediamine. Also, considerable difficulty was encountered in dissolving the sodium. This difficulty was not encountered in the preparation of any of the other metals.

A typical decay of the 660 nm band during the reaction of sodium with water is shown in Figure 20. Figure 21 shows a plot of  $\log \chi$  versus  $\log [H_2O]$ .  $\chi$  is the pseudo-first-order rate constant and is defined by:

Least squares treatment of the data shown in Figure 21 yields a slope of  $1.86 \pm 0.1$ . The line drawn in Figure 21 has a slope of two. Only reactions which had half lives of 3 seconds or less were used in constructing this plot. The reasons for this will be discussed later. Inspection of Figure 22 reveals that no change in the shape of the 660 nm band occurs during the reaction with water and that there is no apparent band shift during the reaction.

The values of the specific rate constants for the reaction of sodium with water are listed in Table VII. Inspection of this Table shows that there is good agreement among the rate constants for this run. Comparison of these rate constants with those obtained by Feldman also shows good agreement. The reasons for the apparently good agreement here will be discussed later.



Decay of 660 nm band of sodium during the reaction with water. Figure 20.

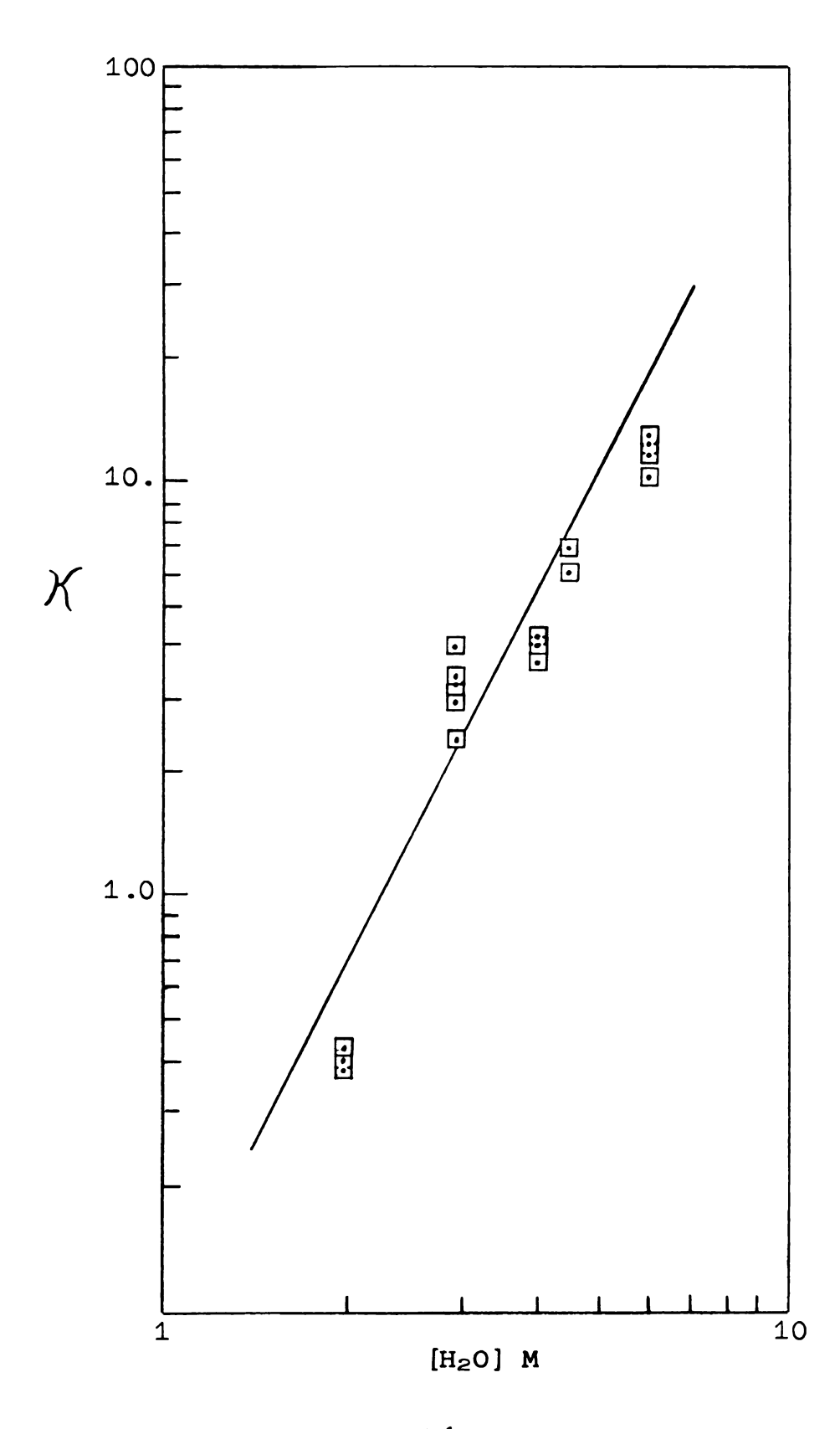
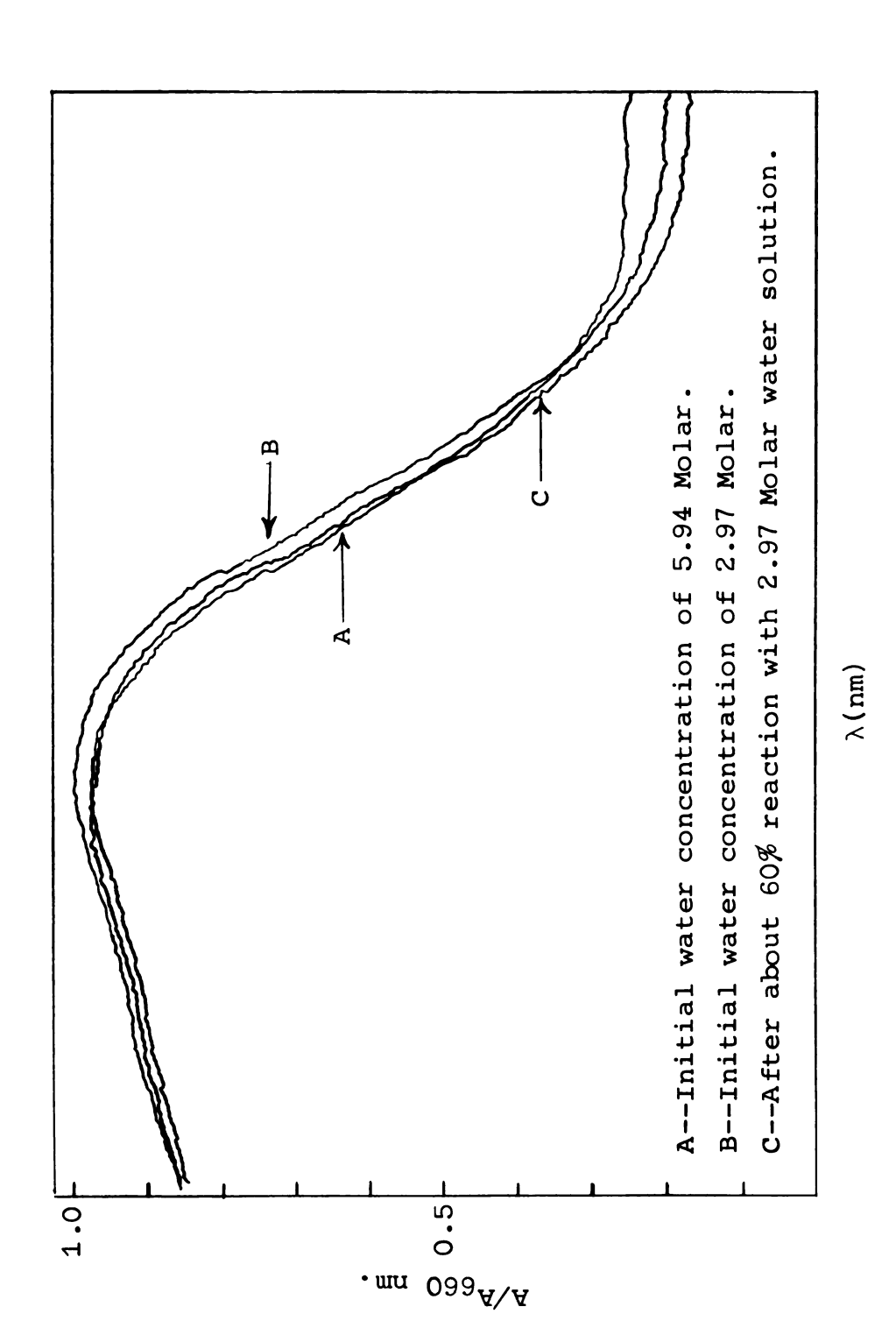


Figure 21. Plot of  $\log \chi_{vs}$  log (water concentration) for the reaction of sodium with water in ethylenediamine. The line drawn has a slope of two.



Band shape and position of the 660 nm band of sodium as a function of the initial water concentration and the extent of reaction. Figure 22.

TABLE VII

VALUES OF THE RATE CONSTANT FOR THE REACTION OF SODIUM
WITH WATER IN ETHYLENEDIAMINE

[H <sub>2</sub> O] [ <u>M</u> )	λ(nm)	X(sec <sup>-1</sup> )	$\chi_{(\underline{M}^{-2} \text{sec}^{-1})}$
5.94	660	<b>1</b> 2.13	0.344
5.94	660	10.64	0.302
5.94	660	12.31	0.349
5.94	660	13.33	0.378
5.94	660	13.27	0.376
5.94	660	13.14	0.372
4.45	660	6.7	0.338
4.45	660	7.47	0.377
3.96	660	4.29	0.273
3.96	660	4.35	0.277
3.96	660	3.72	0.237
2.97	660	3.04	0.344
2.97	660	4.06	0.460
2.97	660	2.55	0.289
2.97	660	3.43	0.389
2.97	660	3.42	0.388
2.97	660	3.29	0.373
1.96	660	0.44	0.114
1.96	660	0.40	0.104
1.96	660	0.42	0.109

Recall that sodium solutions possess only an absorption band at 650-700 nm and show little or no infrared absorption. Since this indicates a low concentration of solvated electrons and "ammonia-like" aggregates, reaction of the V-species with water via intermediate formation of the IR-species is not favored. The following calculation shows that the reaction involving prior formation of the IR-species is too slow to account for the observed rate.

A possible mechanism for the reaction of the V-species with water is

$$V \stackrel{K}{\longleftarrow} IR \stackrel{H_2O}{\longleftarrow} Products \qquad (42)$$

in which "V" represents Na and/or Na<sub>2</sub> and "IR" represents the solvated electron and its "ammonia-like" aggregates. Absorption spectra of sodium-ethylenediamine solutions show only the V-band and indicate that K  $\leq 10^{-2}$  (89). This is confirmed by the reaction of cesium solutions with sodium bromide in ethylenediamine in which the IR-band completely disappears and the V-band appears unless there is an excess of cesium present.

These results would require that the reaction with water through prior formation of the IR-species has a second order rate constant of less than  $0.2 \, \underline{\text{M}}^{-1} \, \text{sec}^{-1}$ . Even at water concentrations as high as  $6 \, \underline{\text{M}}$ , the contribution of this mechanism to the observed pseudo-first-order rate constant  $(12 \, \underline{\text{M}}^{-1} \, \text{sec}^{-1})$  could not exceed 10%. It may, however, become

important at lower water concentrations. Therefore, the reaction of sodium with water probably involves the V-species directly, and this direct reaction leads to the observed second order dependence on water.

At water concentrations below 1  $\underline{M}$ , the reaction is very slow and in some cases is zero-order in the absorbance. This behavior probably occurs because the catalyzed decomposition reaction becomes important at these low water concentrations. It is for this reason that only data with half-lives of 3 seconds or less were used in constructing the log  $\chi$  versus log [H<sub>2</sub>O] plot which is shown in Figure 21.

The mechanism for the reaction of sodium with water is still unknown. Any proposed mechanism must account for the observed second order dependence on water. The species responsible for the V-band is probably the same species responsible for the R-band in other metal-amine solutions and for reasons already mentioned is probably a two electron species which is not a simple ion pair.

One mechanism which could account for the available data and also lends itself to future testing is the following:

$$Na^{-} + H_{2}O \xrightarrow{K_{1}} Na^{-} \cdot H^{+} + OH^{-}$$
 (43)

followed by

$$Na^- \cdot H^+ + H_2O \xrightarrow{k_1} Na^+ + OH^- + H_2$$
 (44)

so that

$$\frac{d[H_2]}{dt} = k_1[Na^- \cdot H^+][H_20]$$
 (45)

Assuming that equilibrium is maintained in the first step gives:

$$[Na^- \cdot H^+] = \frac{K_1 [Na^-] [H_2O]}{[OH^-]}$$
 (46)

which when substituted into equation 45 yields

$$\frac{d[H_2]}{dt} = \frac{k_1 K_1 [Na^-] [H_2O]^2}{[OH^-]}$$
 (47)

The validity of Equation 47 can be tested by observing the effect of added hydroxide on the rate of reaction of sodium with water. If this mechanism is correct, then the reaction should be slower in the presence of added hydroxide. It is also possible that the first step involves equilibrium formation of the hydrated ion, Na<sup>-</sup> · H<sub>2</sub>O, followed by the rate-controlling reaction with H<sub>2</sub>O to produce H<sub>2</sub>. In this case the reaction rate would not decrease when hydroxide ion is added to the solution. The effect of hydroxide ion on the rate of reaction of sodium with water is currently being tested (104). However no conclusive results have yet been obtained.

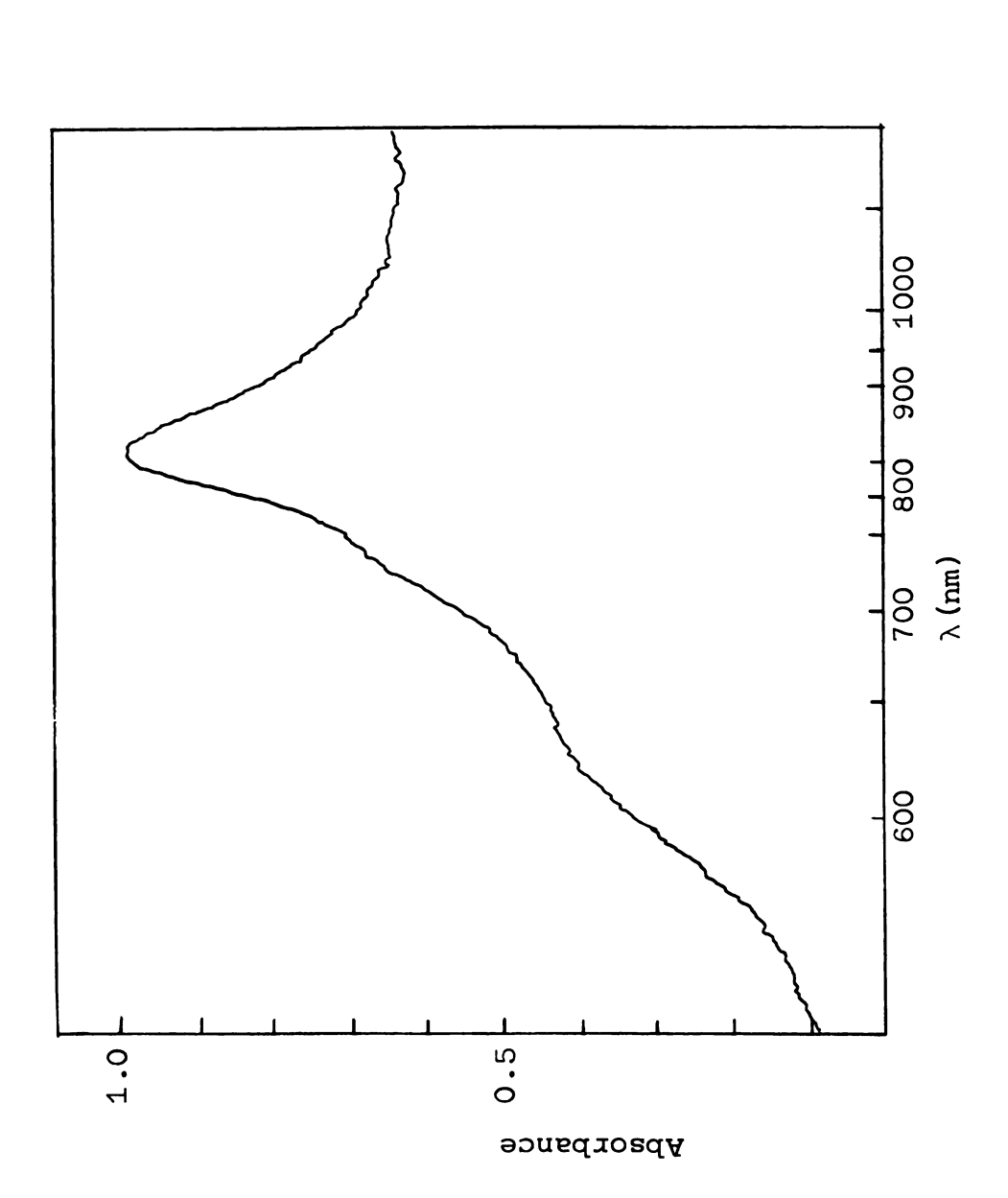
### 3. Rubidium and Potassium

In all the runs using potassium solutions, the kinetics were complicated by the presence of two optical absorption bands in addition to the infrared absorption. One of these

bands was located at 850 nm and the other at 650 nm. In light of Tuttle's results (54) concerning the nature of the 650 nm band, the 650 nm band observed in these solutions was probably due to sodium contamination. Figure 23 shows a typical spectrum of a potassium solution used in these studies. Figure 24 shows that the decay of the absorbance during the reaction with water is not first-order in the absorbance. The kinetic data were analyzed by the methods discussed in the introduction to this Section. The results of these analyses are shown in Table VIII.

The rubidium solutions used to study the reaction with water showed two optical absorptions. One was located at 890 nm (R-band) and the other in the infrared (IR-band). A typical optical spectrum of the rubidium solutions used in this work is shown in Figure 25. It is clear from Figure 26 that both optical bands disappear during the reaction with water but that the R-band disappears faster than the IR-band. Inspection of Figure 14 shows that the decay of the absorbance during the reaction with water does not obey simple first or second order kinetics. It should be noted that the rubidium solutions used in this work showed stability similar to that of the sodium solutions used.

The kinetics of the reaction of rubidium and potassium with water are complicated by the fact that in addition to the presence of the IR-band, the intermediate optical absorption (R-band) is also present. In view of previous arguments



Typical spectrum observed for potassium in ethylenediamine, showing the presence of a V-band in addition to the R- and IR-bands. Figure 23.

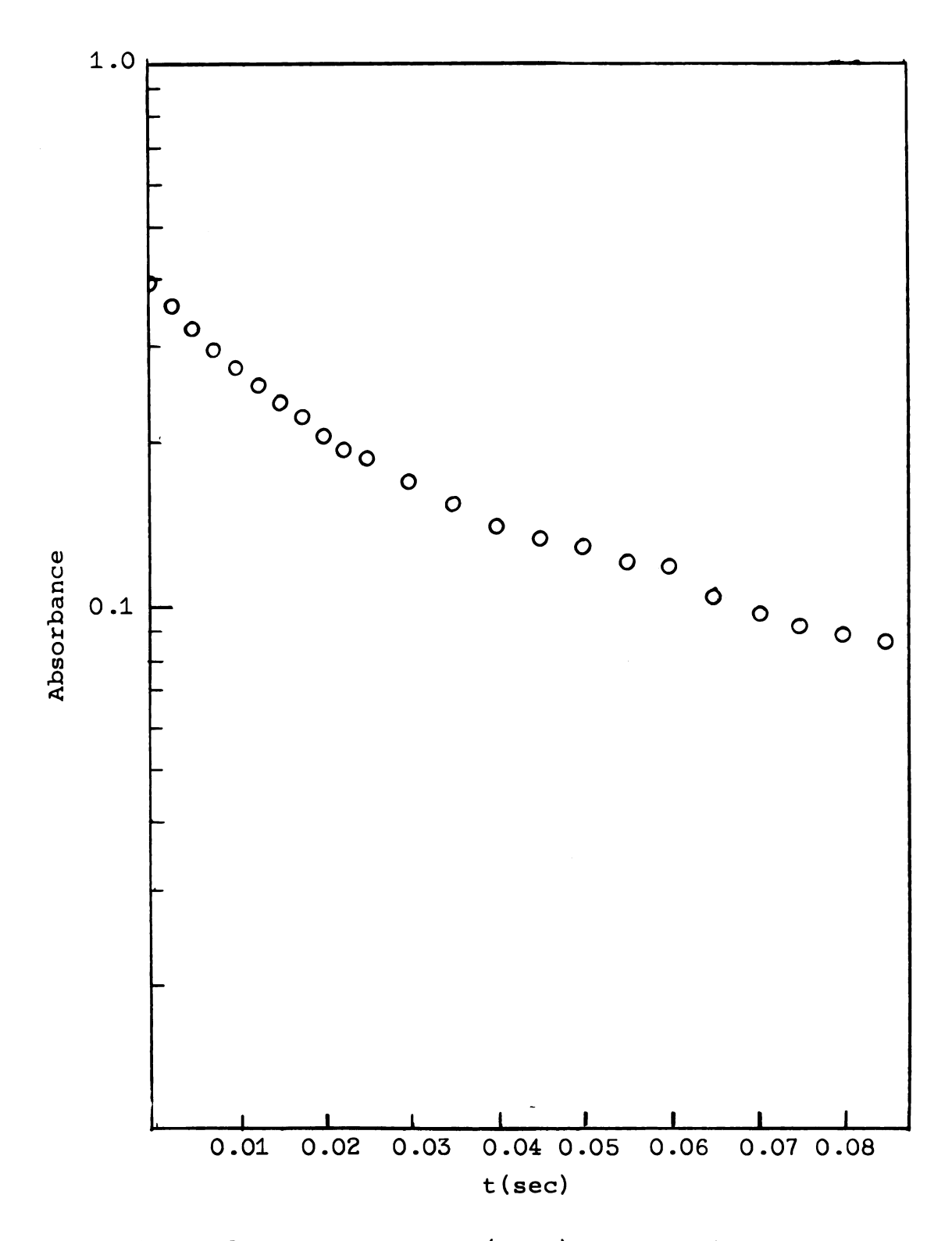


Figure 24. Plot of log (Abs.) versus time for the reaction of potassium with water in ethylenediamine.

TABLE VIII  $\begin{tabular}{llll} \textbf{VALUES OF $k_{\dot{M}}^{\perp}$- CALCULATED FOR THE REACTION OF POTASSIUM WITH } \\ \textbf{WATER IN ETHYLENEDIAMINE CALCULATED USING EQUATION 39} \\ \end{tabular}$ 

		<del></del>	
[H <sub>2</sub> O] ( <u>M</u> )	λ <b>(nm)</b>	k <sub>M</sub> -	<sup>б</sup> к <sub>м</sub> −
[K] = 1.15 x	10 <sup>-4</sup> <u>M</u> (a)		
0.0238 0.0238 0.0238 0.0238 0.0238 0.0238 0.5895 0.5895 0.5895 0.5895 0.5895 0.5895 4.057 4.057 4.057 4.057	1110 1110 950 850 700 700 1110 1110 1110 800 800 800 700 1100 950 950 950 950	12.897 7.534 9.555 10.102 8.904 9.771 16.630 11.683 25.470 37.897 35.336 26.986 7.003 42.391 39.904 27.481 18.395 58.922 39.822	6.492 2.103 2.011 2.531 4.889 4.301 6.466 2.314 14.434 10.355 6.491 3.085 8.361 5.49 2.344 2.179 16.389 4.934
$[K] = 3.03 \times$	10-4 <u>M</u> (b)		
4.45 4.45 4.45 4.45 4.45 0.378 0.378 0.378 0.378	1052 1052 1052 850 850 850 850 850 850 1052	16.231 10.046 7.633 24.613 8.922 9.167 14.613 8.221 6.337 43.612 10.361	4.861 2.897 1.876 6.486 2.310 3.344 4.614 2.380 3.166 8.497 2.865

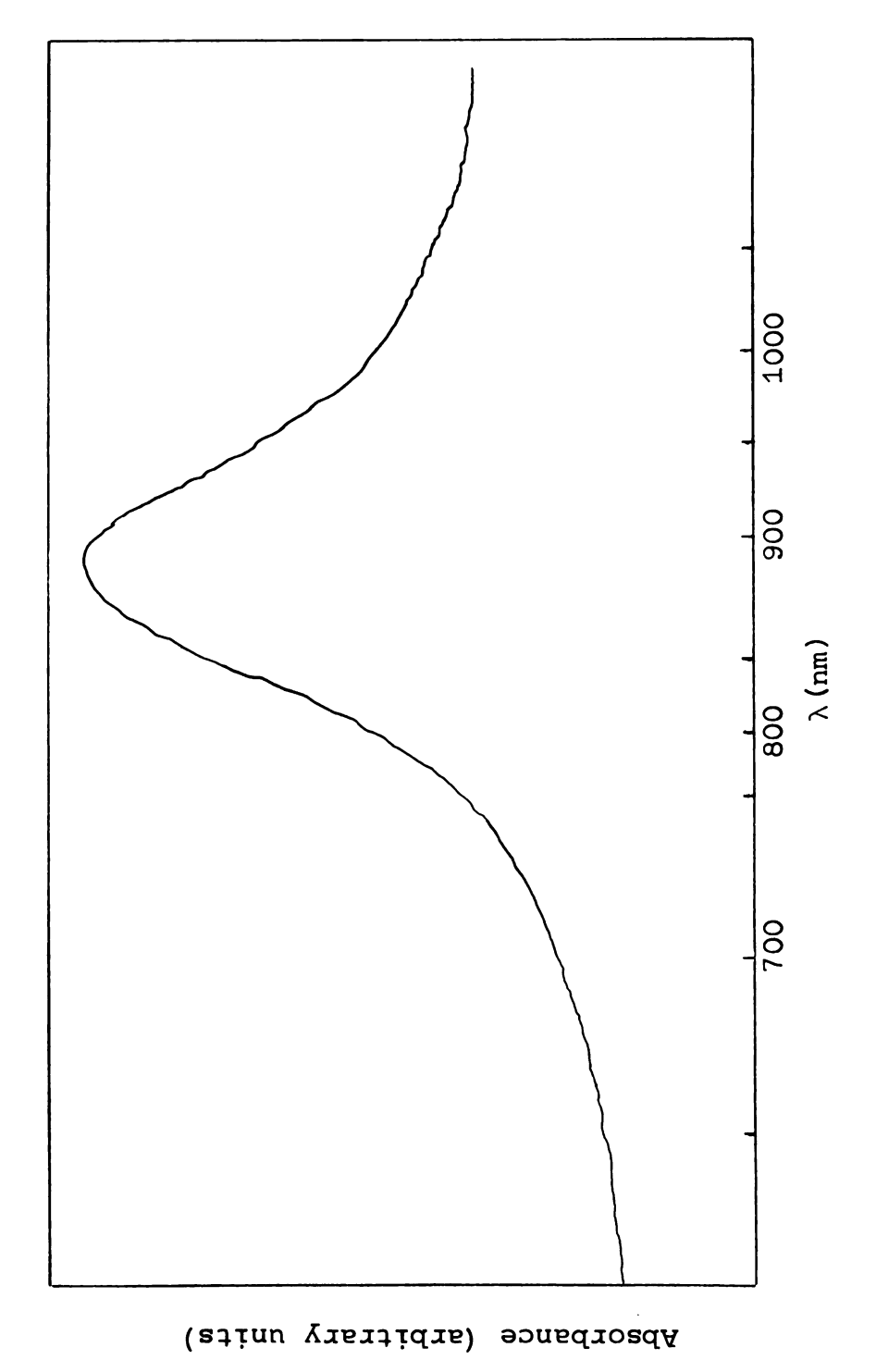
continued

TABLE VIII--continued

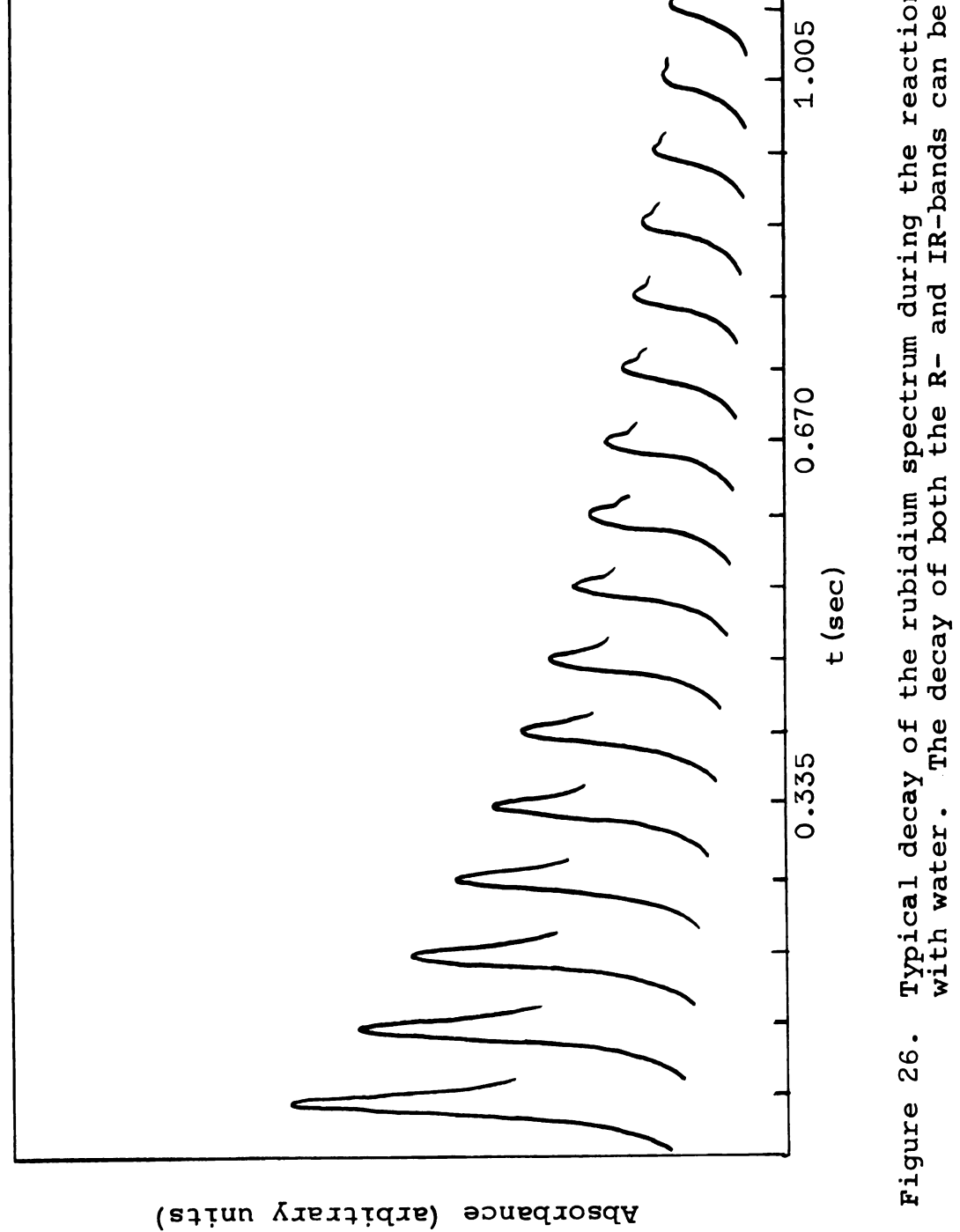
[H <sub>2</sub> O] ( <u>M</u> )	λ <b>(</b> nm)	k <sub>M</sub> -	<sup>6</sup> k <sub>M</sub> −
$[K] = 2.2 \times 1$	.0-4 <u>M</u> b		
0.137	850	10.161	2.316
0.137 0.137	850 1052	24.301 8.937	5.861 2.466
3.03	1052	10.733	3.015
3.03	1052	26.437	7.484
3.03	850	30.817	5.386
3.03	850	8.641	6.971
2.16	850	21.697	4.612
2.16	850	37 <b>.4</b> 11	9.866
2.16	850	42.136	8.194
2.16	850	18.117	3.791

aReanalyzed data of LHF (90).

b Data of this work.



Typical spectrum of rubidium solutions used in this work. Figure 25.



Typical decay of the rubidium spectrum during the reaction with water. The decay of both the R- and IR-bands can be seen.

(c.f. Section II and the Introduction to this Section), the R-species is probably in equilibrium with the IR-species, as:

$$R \xrightarrow{K_5} IR \tag{48}$$

and this further complicates the kinetics of the reaction with water. Since in all cases, the studies of the reaction of potassium solutions with water were further complicated by the presence of a V-band, presumably due to sodium contamination, the following discussion will be focussed primarily on the reaction of rubidium solutions with water. However, it should be remembered that anything which is said about rubidium solutions should, in principle, also apply to those of potassium.

The derivation of the expression for the rate of decay of the total absorbance during the reaction of rubidium with water is algebraically equivalent to the expression derived for the reaction of cesium with water (see Appendix A). The general form of the rate expression is also similar to that derived for the cesium case, but the additional equilibrium between the R- and IR-species makes the final expression more complex for the reaction of rubidium (and potassium) with water. The expression has the form:

$$-\frac{dA_{T}}{dt} = \left\{ k_{M}^{i} - \left[ \frac{1 + K_{4} [M^{+}] \gamma_{\pm}^{2} + k_{R}^{i} / k_{M}^{i} - K_{5}}{1 + K_{4} [M^{+}] \gamma_{\pm}^{2} + 1 / K_{5}} \right] \right\} \frac{A_{p}^{i} + \frac{1}{2} A_{D}^{i}}{1 + \frac{A_{p}}{2A_{D}^{i}}}$$
(49)

where the definitions of the terms are given in Appendix A.

This expression is derived assuming <u>no direct</u> reaction between e or M and water. The reasons for this assumption have already been discussed (c.f. Introduction to this Section).

Equation 49 can be simplified somewhat. It will be shown later that if the process is similar to that involving sodium, then the direct reaction of the R-species with water cannot compete with the dissociative reaction through the IR-species. This implies that

$$k_R^* \ll k_{M^-}^*$$

Since in the case of rubidium,  $K_5 \cong 1$ , the term  $k_R^*/k_M^*-K_5$  is small and can be neglected so that:

$$-\frac{dA_{T}}{dt} = \left\{ k'_{M} - \left[ \frac{1 + K_{4} [M^{+}] \gamma_{\pm}^{2}}{1 + K_{4} [M^{+}] \gamma_{\pm}^{2} + \frac{1}{K_{5}}} \right] \right\} \frac{A_{p} + \frac{1}{2} A_{D}^{i}}{1 + \frac{A_{p}}{2A_{D}^{i}}}$$
(50)

Inspection of Equation 50 shows that it is difficult, at best, to sort out a specific rate constant for the reaction with water without knowledge of the values of  $K_4$ ,  $K_5$ , and  $[M^+]$ . Numerical solution of Equation 50 gives only the value of  $K_4$  given by

$$\chi = \left\{ k_{M}^{-} \left[ \frac{1 + K_{4} [M^{+}] \gamma_{\pm}^{2}}{1 + K_{4} [M^{+}] \gamma_{\pm}^{2} + \frac{1}{K_{5}}} \right] \right\}$$
(51)

The values listed in Tables VIII and IX for potassium and rubidium are values of "Kappa" for the reaction of these metals with water.

TABLE IX values of  $k_{M^-}$  calculated from the best fit of equation 39 TO THE DATA OBTAINED FOR THE REACTION OF RUBIDIUM WITH WATER IN ETHYLENEDIAMINE

[H <sub>2</sub> O] ( <u>M</u> )	λ <b>(n</b> m)	k <sub>M</sub> -	<sup>♂</sup> k <sub>M</sub> −
[Rb] = $1.3 \times 10^{-3}$	a <u>M</u>		
0.023 0.023 0.5895 0.5895 0.5895 5.60 5.60 5.60 [Rb] = 5 x 10 <sup>-4</sup> M	750 750 1100 1100 750 1100 950 750	21.304 21.445 5.342 12.169 11.499 18.772 18.467 26.495	7.638 7.107 2.316 3.914 4.067 4.713 4.258 6.838
0.124 0.124 0.124 0.229 0.229 0.229 0.229 1.05	900 900 900 900 900 900 900 900 900 1052 1052 1052 1052 1052 1052 1052 10	22.056 26.371 24.170 16.494 13.886 17.129 19.899 12.369 19.585 18.689 15.533 21.683 22.901 20.051 17.552 18.882 13.513 26.881 27.995 24.668 14.821 21.443 18.511	5.514 7.252 4.906 4.701 4.735 3.374 4.696 4.589 4.446 4.205 4.401 6.374 3.259 5.334 3.194 4.815 3.932 5.672 7.587 5.822 4.594 4.374 5.257

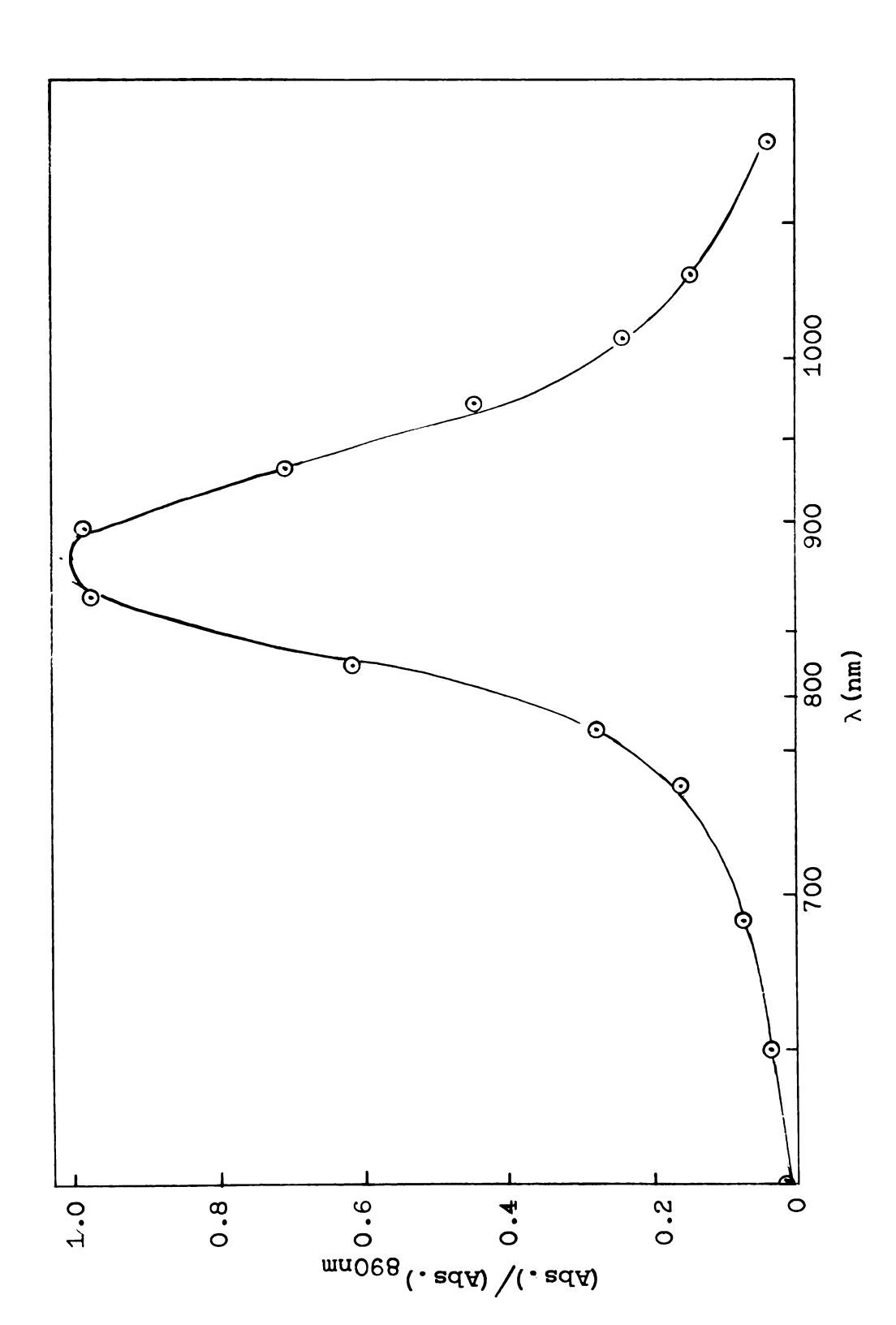
a--Reanalyzed data of LHF. b--Data of this work.

<sup>\*--</sup>Fixed wavelength.

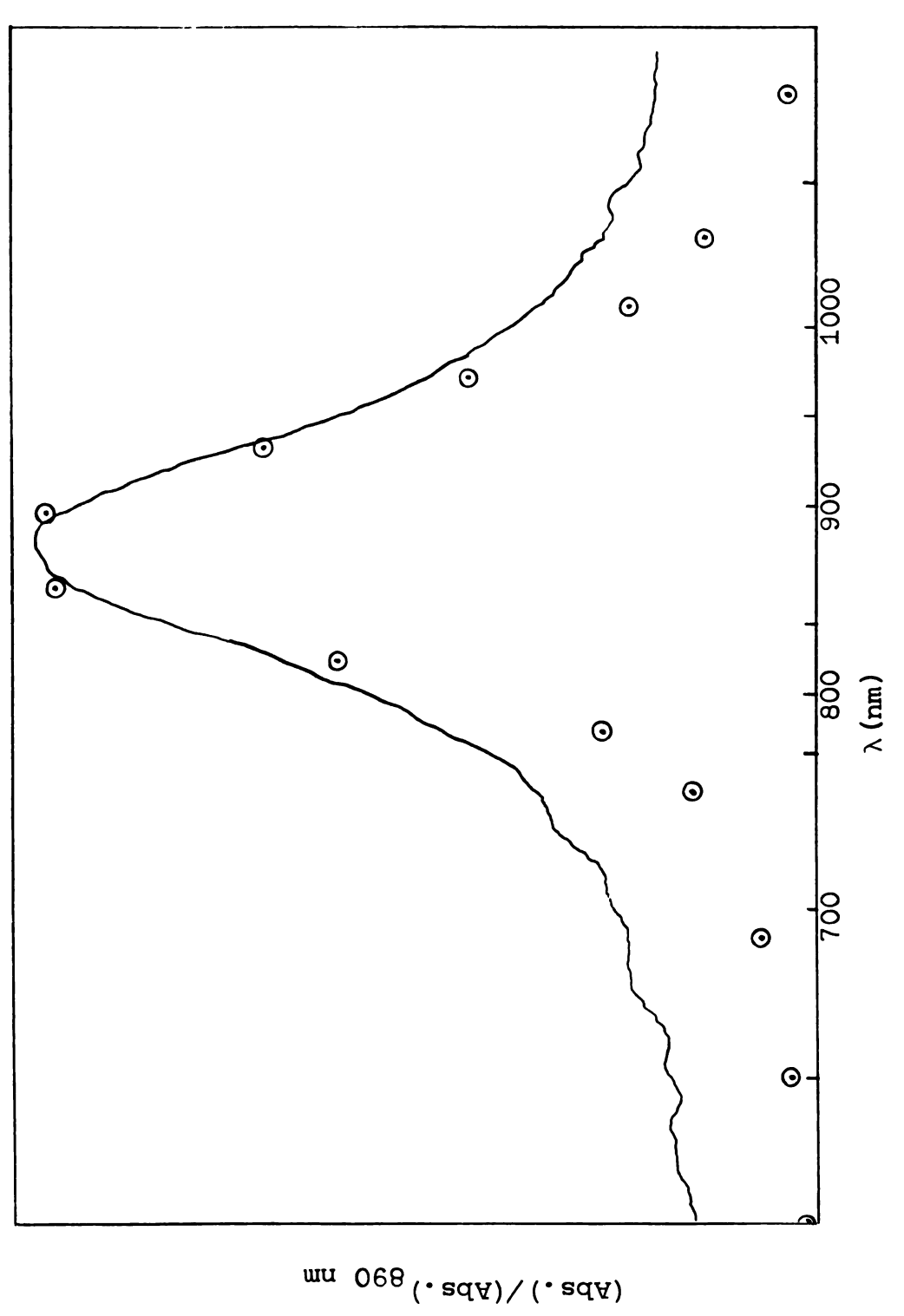
As mentioned above, the calculation of the specific rate constant,  $k_{M^-}$ , can only be carried out by determination of the values of  $K_4$ ,  $K_5$  and  $[M^+]$ . At present these values are not known. In spite of these complexities, several important observations are worth noting.

First, the values of the calculated parameter K, in the analysis of the rubidium show better consistency from push to push than the data for cesium or potassium. However, the magnitudes of the uncertainties in the values of the parameters for a given push are about the same for all metals.

Secondly, as has been mentioned, both the R- and IR-bands decay together during the reaction with water. However, the individual decay rates are probably determined by the stoichiometric requirements of the equilibria among the species. The spectrum of the R-band alone during reaction can be obtained in two different ways. If the shape of the spectrum observed in cesium-ethylenediamine solutions (IR-band only) is normalized at 1100 nm and then subtracted from the spectral decay observed during the reaction of rubidium with water, the decay of the R-band with time is obtained. This is illustrated in Figure 27. That this shape corresponds to that of the R-band can be seen by the comparisons made in Figure 28. Here a spectrum of the R-band was obtained using CAT. The spectrum near the end of a push (after about 80% reaction) was subtracted from the spectrum at the beginning



R-band obtained by subtraction of cesium, IR-band from the rubidium spectrum observed in the kinetic studies. Before the subtraction was performed, the absorbances of the two spectra were normalized at 1100 nm. Figure 27.



Comparison of the R-band shape from Figure 27 with that obtained by subtraction of spectrum near the end of the reaction with water from the spectrum observed at the beginning of the reaction. Figure 28.

of the push. The resulting R-band shape is compared to that which was obtained by subtraction of the cesium spectrum in Figure 28. It can be seen that the band shapes are the same.

#### C. Band Interconversion Reactions

# 1. Cesium plus N<sup>+</sup>

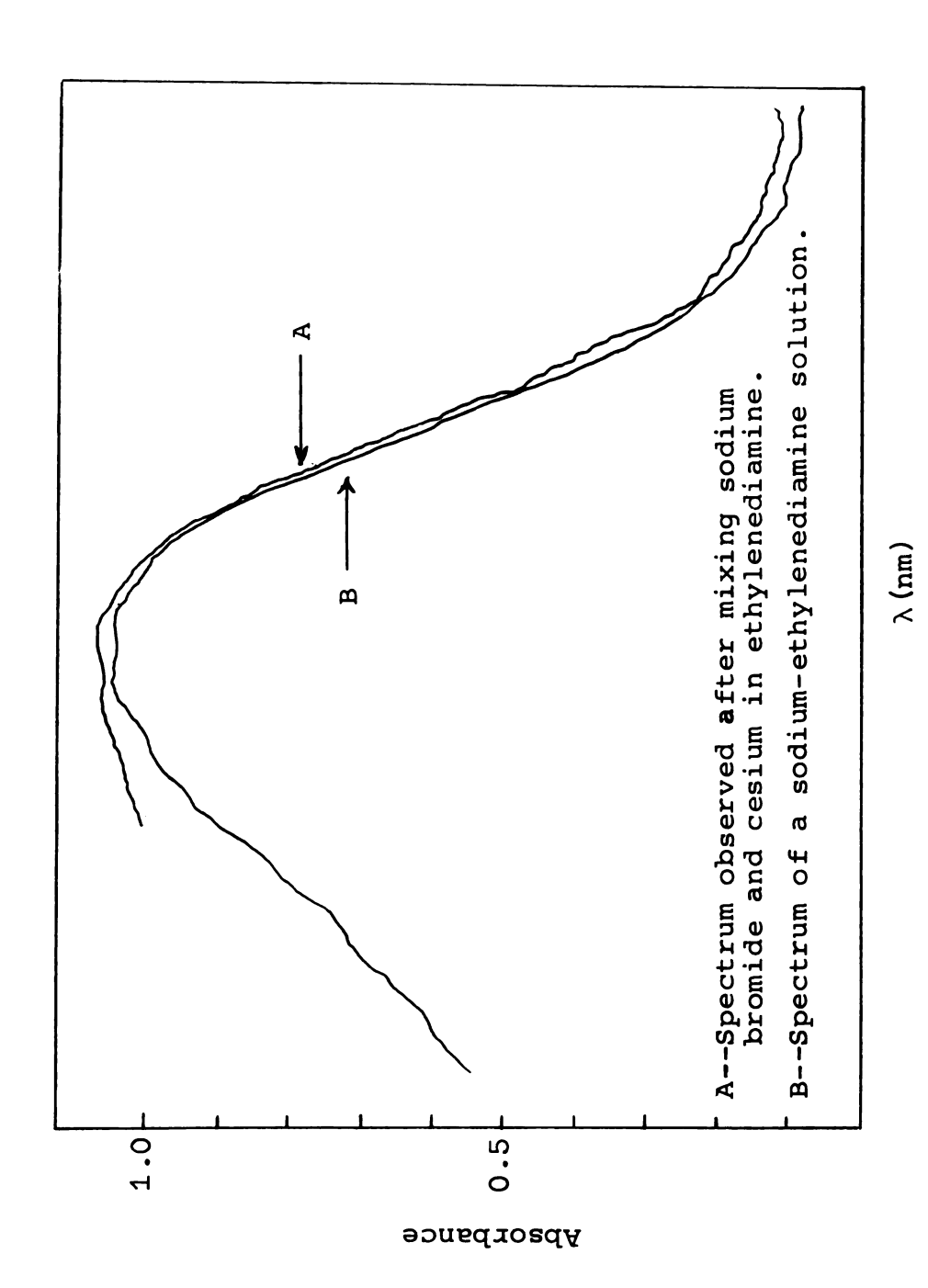
Several studies were made of the reaction of cesium with sodium ions in ethylenediamine. The cesium solutions used in these studies possessed only an infrared absorption. Although the reaction

Cs solution (IR) + Na<sup>+</sup>  $\longrightarrow$  "V-species" (660 nm) + Cs<sup>+</sup> (52)

appears to be too fast to be studied quantitatively ( $t_{\frac{1}{2}} < 10^{-3}$  sec.) using the stopped-flow technique, a few qualitative observations are worth noting.

In those cases where the concentration of Na<sup>+</sup> was in excess, the cesium infrared band decayed completely during, or shortly after, mixing, leaving only the 660 nm band.

A typical spectrum after mixing is shown in Figure 29. Also shown in this Figure is the spectrum observed in solutions of sodium in ethylenediamine. It is evident from Figure 29 that the shapes and positions of these two absorption bands are the same, indicating that the species responsible for the V-band in sodium solutions is the same as that formed by Reaction 52. Also, it can be seen from this Figure that



Spectrum observed after mixing a solution of sodium bromide and cesium in ethylenediamine. Figure 29.

there is no detectable infrared band remaining after reaction of cesium solutions with an excess of sodium ions.

## 2. Rubidium plus K

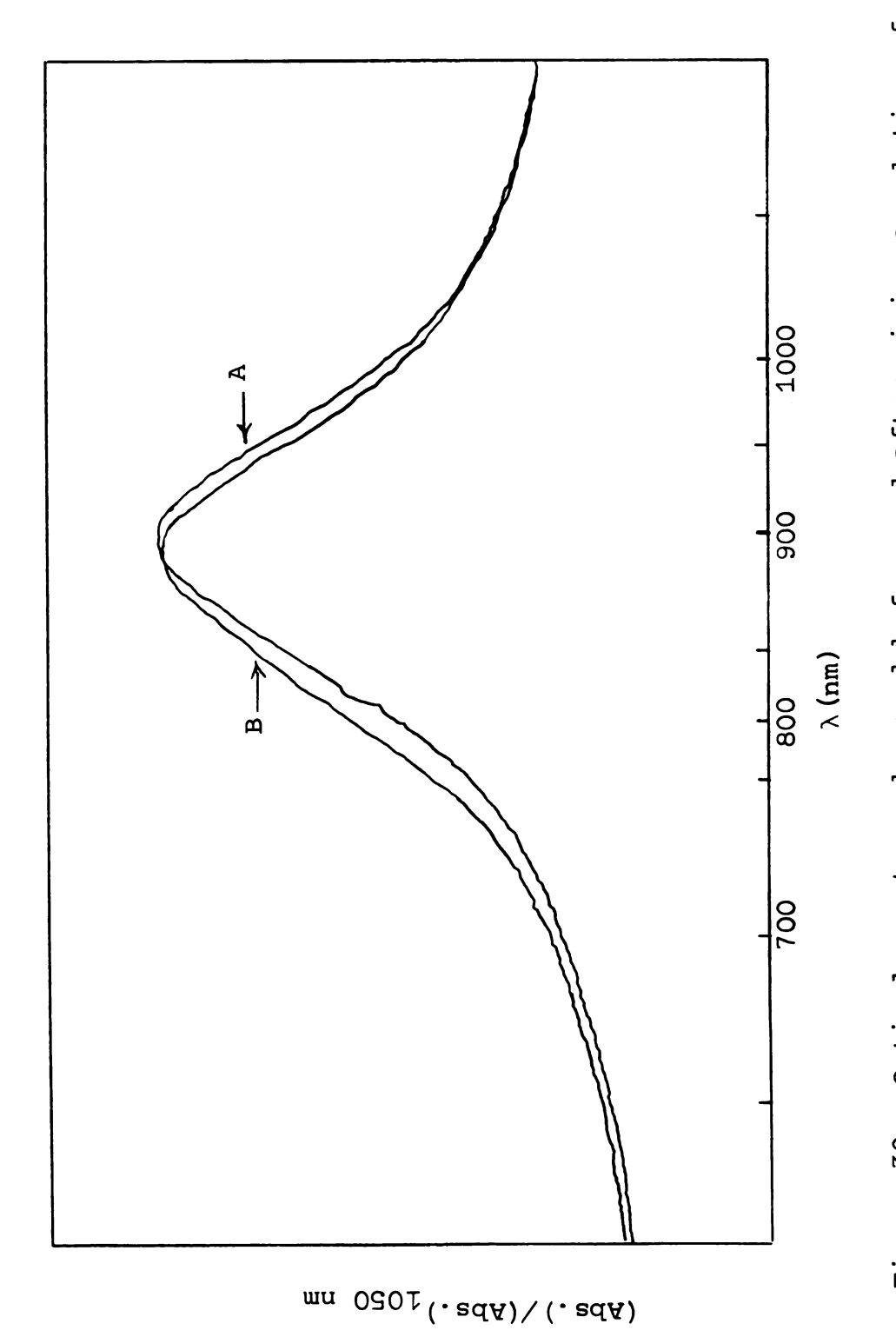
The fact that no 660 nm absorption (V-band) was observed after the reaction:

Rb solution (IR, 890 nm) + 
$$K^+ \longrightarrow K$$
 solution (IR,850 nm)  
+  $Rb^+$  (53)

tends to confirm Tuttle's observation that the V-band sometimes observed in potassium, rubidium and cesium solutions is due to sodium contamination.

Since the R-bands of potassium (850 nm) and rubidium (890 nm) are so close together, no decay of the rubidium R-band with concomitant formation of the potassium R-band was observed. However, Figure 30 gives a comparison of the optical spectrum before and after mixing. It can be seen that the spectrum after mixing shows a slight asymmetry and an apparent shift of the band maximum toward the visible. This indicates the presence of an additional absorption band at shorter wavelengths. Since in all cases, the concentration of rubidium was in excess, this result is the expected one if Reaction 53 proceeds as written.

An important question needs to be considered at this point. If the V-species observed in sodium solutions is indeed of the same type as the R-species observed in rubidium and potassium solutions, how can we ignore direct reaction



Optical spectrum observed before and after mixing a solution of rubidium and potassium bromide in ethylenediamine. Curve A is the spectrum observed before mixing and Curve B that observed after the push. Figure 30.

of the R-species with water as has been proposed for the case of sodium?

Since, with sodium solutions there is no detectable IR-band, the V-species must react with water directly, as previously described. In sodium solutions then, the process may be described by,

$$\begin{array}{c|c}
V & \overline{K_5} & \text{IR} \\
k_1 & H_2O \\
\text{products}
\end{array} (54)$$

However, with rubidium and potassium solutions which show both R- and TR-bands, the following scheme is possible:

with

$$K_5 = [IR]/[R] \approx 1$$

Assuming that the R-band could react directly with water at a rate comparable to the V-band in sodium solutions, and that the IR-band reacts at a rate comparable to the IR-band in cesium solutions, then:

$$\frac{d[H_2]}{dt} = k_1[R][H_2O]^2 + k_2K_5[R][H_2O]$$
 (56)

$$\frac{d[H_2]}{dt} = R[H_2O] \left\{ k_1[H_2O] + k_2K_5 \right\}$$
 (57)

Of course this equation should also be valid for sodium solutions. However, in this case, the optical spectrum shows that  $K_5 \lesssim 0.02$ . Therefore, for the case of sodium, at a water concentration of 1.5 M

$$k_1 \cong 0.41 \, M^{-1} sec^{-1}$$

Taking  $k_2 \approx 20 \, \underline{M}^{-1} \text{sec}^{-1}$  for cesium, then for sodium

$$k_2 K_5 = 0.04$$

and

$$K_5 = 0.002$$

so that there is very little competition of the direct reaction with the dissociative mechanism in the reaction of sodium with water since the equilibrium heavily favors the V-species.

In the case of rubidium and potassium however, there are about equal amounts of R and IR-bands (see Figures 24 and 26), so that  $K_5 \cong 1$ . Taking  $k_2 \cong 20 \ \underline{M}^{-1} \mathrm{sec}^{-1}$ , then

$$k_2 K_5 = 20$$

in the case of rubidium (and potassium). If  $k_1$  has the same value as for sodium (i.e.,  $k_1 = 0.41 \ \underline{M}^{-1} sec^{-1}$  at  $[H_2O] = 1.5 \ \underline{M}$ ) then

$$k_1 = 0.41 \le 0.10 k_2 K_5$$

So that in the reaction of rubidium with water, the direct reaction of the R-species cannot compete with the dissociative mechanism. This is true of all water concentrations up to 4 M. Thus it can be seen that although the V- and R-species might indeed be the same, the reaction of these species with water can proceed by different mechanisms, depending upon the metal used.

An understanding of the mechanism by which molecular hydrogen is produced in the reaction of the alkali metals with water in ethylenediamine is necessary for a detailed understanding of the nature of these reactions. The results of pulse radiolytic studies in water (71,72) have shown that the reaction

$$H + OH^{-} \xrightarrow{k_{H} + OH^{-}} e_{aq}^{-} + H_{2}O$$
 (58)

is relatively fast  $(k_{(H + OH^-)} = 1.8 \times 10^7 \, \underline{\text{M}}^{-1} \, \text{sec}^{-1})$ . However, the addition of hydroxide ion has no apparent effect on the rate of reduction of water by cesium in ethylenediamine (90). This suggests that although hydrogen atoms may be formed in these systems by the direct reaction of the reducing species with water, they are probably short lived in ethylenediamine and that molecular hydrogen is produced by a reaction other than

$$H + H \longrightarrow H_2$$
 (59)

In light of these facts, a plausible alternative mechanism

for molecular hydrogen formation is necessary. One possible mechanism involves the production of hydrogen atoms by the direct reaction of the reducing species with water with subsequent abstraction of a hydrogen atom from the solvent. Since the overall reaction produces one-half mole of hydrogen for every mole of metal consumed, the solvent radicals formed by hydrogen atom abstraction probably react further with the reducing species to form other products. It has been suggested (90) that the  $\alpha$ -hydrogen atoms of the solvent are abstracted to form molecular hydrogen according to

$$(e^{-}) + H_2O \longrightarrow H + OH^{-}$$
 (60)

followed by

$$H + H_2N-CH_2-CH_2-NH_2 \longrightarrow H_2 + H_2N-\dot{C}H-CH_2-NH_2$$
 (61) and

$$(e^{-}) + H_2N - \dot{C}H - CH_2 - NH_2 \longrightarrow H_2N - CH_2 - CH_2 - NH^{-}$$
 (62)

The validity of this mechanism and any other involving  $\alpha$ -hydrogen atom abstraction was tested using as the solvent, ethylenediamine which was labelled at the  $\alpha$  position with tritium. A cesium solution was prepared using the labelled ethylenediamine and was mixed with a water solution of known concentration. The hydrogen formed was collected and burned to water by the reaction

$$AgO + H_2 \xrightarrow{100^{\circ}C} H_2O + Ag.$$
 (63)

If the mechanism of molecular hydrogen production indeed proceeds through abstraction of an  $\alpha$ -hydrogen from the solvent, then the water collected as a result of Reaction 63 should contain tritium and therefore show activity. The results of three such experiments showed that not more than 2% of the hydrogen formed in the reduction of water by metal solution could originate from the  $\alpha$ -positions of the solvent.

The exact mechanism of molecular hydrogen formation is not yet clear. However, it is evident at this point that the abstraction of  $\alpha$ -hydrogen atoms of the solvent plays only a minor role in the mechanism.

#### D. Summary

The reactions of the alkali metals with water in ethylene-diamine are faster and proceed by a different mechanism than the same reactions in liquid ammonia. In the case of sodium, the principal absorbing species (V-species) apparently reacts directly with water by a process which is second order in water. In the case of rubidium, potassium and cesium, the preferred reaction seems to be through dissociation of the R-species to the IR-species. The rate-determining reaction apparently involves "ammonia-like" diamagnetic species rather than isolated solvated electrons.

The stability of the metal solutions used is critical to reliable rate studies in these systems. Only when the metal solutions used showed no decomposition when mixed with

pure solvent were the observed reaction rates with other solutes reproducible. Finally, the mechanism described for the reaction of the alkali metals with water in ethylenediamine is not only consistent with the observed rates but is also consistent with the current models for metal-amine solutions. However, further experimentation is necessary to fully validate this mechanism.

## E. Suggestions for Future Work

The study of the effect of added alkali metal cation and also added hydroxide on the rate of reaction of metal solutions with water should be investigated. These studies are particularly important in determining the extent of the validity of the mechanism described in this work. Also of importance for further work is the investigation of the equilibria which apparently exist in metal-amine solutions. Hopefully these studies would permit measurement of equilibrium constants which then would allow a more exact kinetic treatment of the reaction of the metal solutions with water. Both of these studies involve a great deal of effort, but are necessary if the exact mechanism of the reaction of metal solutions with water is to be understood.

Of secondary importance in further studies are the elucidation of the origin of molecular hydrogen in the reaction with water and also the factors contributing to the

formation of pyrazine in metal solutions in ethylenediamine.

Hopefully, the present study can be extended to the investigation of the kinetics of other reactions of the solvated electron.



#### LIST OF REFERENCES

- 1. W. Weyl, Ann. Physik., 121, 601 (1864); 123, 350 (1864).
- 2. E. J. Kirschke and W. L. Jolly, Science, 147, 45 (1965).
- 3. U. Schindewolf, R. Vogelsgesang and K. W. Bödekker, Agnew. chemie, 6, 1076 (1967).
- 4. G. LePoutre and M. J. Sienko, eds. "Metal Ammonia Solutions: Physico-Chemical Properties," W. A. Benjamin, Inc., New York, 1964.
- 5. C. A. Kraus, J. Chem. Ed., 30, 83 (1953).
- 6. M. C. R. Symons, Quart. Rev., 13, 99 (1959).
- 7. W. L. Jolly, <u>Progr. Inorg. Chem.</u>, <u>1</u>, 235 (1959).
- 8. T. P. Das, Advances in Chemical Physics, 4, 303 (1962).
- 9. D. C. Walker, Quart. Rev., 21, 79 (1967).
- 10. U. Schindewolf, Angew Chem. Internat. Ed., 7, 190 (1968).
- 11. J. K. Thomas, Rad. Res. Rev., 1, 183 (1968).
- 12. E. C. Evers, C. W. Orgeel, A. M. Filbert, p. 67 in Ref. 4.
- 13. S. Gunn, <u>ibid</u>., p. 76.
- 14. W. H. Brendley, Jr., and E. C. Evers, <u>Advances in Chemistry Series</u>, <u>50</u>, "Solvated Electron," R. F. Gould, Ed., American Chemical Society, Washington, D. C., 1965, p. 111.
- 15. S. Gunn, J. Chem. Phys., 47, 1174 (1967).
- 16. R. C. Douthit and J. L. Dye, <u>J. Am. Chem. Soc.</u>, <u>82</u>, 4472 (1960).
- 17. M. Gold and W. L. Jolly, <u>Inorq. Chem</u>., 1, 818 (1962).
- 18. D. F. Burow and J. J. Lagowski, p. 125 in Ref. 14.

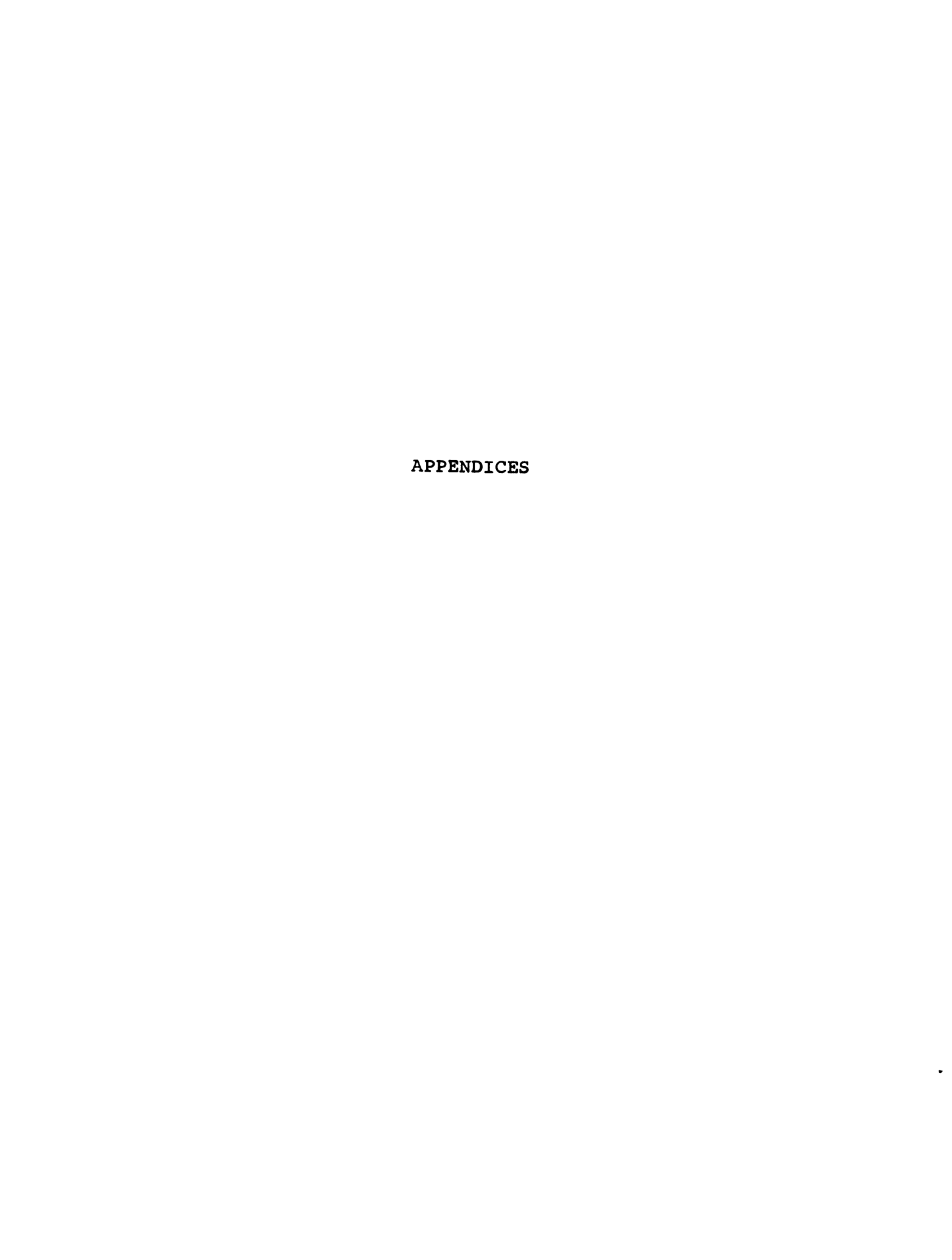
- 19. E. Huster, Ann. Physik., 33, 477 (1938).
- 20. S. Freed and N. Sugarman, J. Chem. Phys., 11, 354 (1943).
- 21. C. A. Hutchison, Jr., and R. C. Pastor, <u>ibid.</u>, <u>21</u>, 1959 (1953).
- 22. (a) J. L. Dye, R. F. Sankuer and G. E. Smith, <u>J. Am.</u>
  <u>Chem. Soc.</u>, <u>82</u>, 4797 (1960); (b) C. A. Kraus, <u>J. Am. Chem.</u>
  <u>Soc.</u>, <u>36</u>, 864 (1914).
- 23. T. P. Das, op. cit.,  $\underline{4}$ , 303 (1962).
- 24. T. R. Hughes, <u>J. Chem. Phys.</u>, <u>38</u>, 202 (1963).
- 25. D. E. O'Reilly, ibid., 41, 3729 (1964).
- 26. M. Gold, W. L. Jolly and K. S. Pitzer, <u>J. Am. Chem. Soc.</u>, 84, 2264 (1962).
- 27. C. A. Kraus, <u>J. Am. Chem. Soc.</u>, <u>30</u>, 1323 (1908).
- 28. R. A. Ogg, Phys. Rev., 69, 668 (1946).
- 29. W. N. Lipscomb, J. Chem. Phys., 21, 52 (1953).
- 30. H. A. Stairs, <u>ibid</u>., <u>27</u>, 1431 (1957).
- 31. A. S. Davydov, <u>J. Expt. Theoret. Phys. U.S.S.R.</u>, <u>18</u>, 913 (1948).
- 32. M. F. Deigen, <u>Trudy Inst. Fiz.</u>, <u>Akad. Nauk. Ukr. SSR.</u>, <u>5</u>, 119 (1954).
- 33. J. Jortner, <u>J. Chem. Phys.</u>, <u>30</u>, 839 (1959).
- 34. L. Landau, Physik. Z. Sowjetunion, 3, 664 (1953).
- 35. J. Jortner, S. A. Rice and E. G. Wilson, p. 222 in Ref. 4.
- 36. E. Becker, R. H. Lindquist and B. J. Alder, <u>J. Chem. Phys.</u>, <u>25</u>, 971 (1956).
- 37. L. Coulter, ibid., 19, 1326 (1951).
- 38. J. L. Dye, G. E. Smith and R. F. Sankuer, <u>J. Am. Chem.</u>
  <u>Soc.</u>, <u>82</u>, 4803 (1960).
- 39. E. Arnold and A. Patterson, Jr., <u>J. Chem. Phys.</u>, <u>41</u>, 3089 (1964).

- 40. E. Arnold and A. Patterson, Jr., p. 285 in Ref. 4.
- 41. S. Golden, C. Guttman, and T. R. Tuttle, Jr., <u>J. Am. Chem.</u> Soc., <u>87</u>, 135 (1965).
- 42. W. L. Jolly, p. 27 in Ref. 14.
- 43. R. H. Land and D. E. O'Reilly, <u>J. Chem. Phys.</u>, <u>46</u>, 4496 (1967).
- 44. R. R. Dewald and J. L. Dye, J. Phys. Chem., 68, 121 (1964).
- 45. K. D. Vos and J. L. Dye, <u>J. Chem. Phys.</u>, <u>38</u>, 2053 (1963).
- 46. K. Bar-Eli and T. R. Tuttle, Jr., <u>Bull. Am. Phys. Soc.</u>, 8, 352 (1963).
- 47. K. Bar-Eli and T. R. Tuttle, Jr., <u>J. Chem. Phys.</u>, <u>40</u>, 2508 (1964).
- 48. L. R. Dalton, J. D. Rynbrandt, E. M. Hansen and J. L. Dye, J. Chem. Phys., 44, 3969 (1966).
- 49. L. R. Dalton, J. L. Dye, E. M. Fielden and E. J. Hart, J. Phys. Chem., 70, 3358 (1966).
- 50. R. R. Dewald and J. L. Dye, <u>J. Phys. Chem.</u>, <u>68</u>, 128 (1964).
- 51. M. Ottolenghi, K. Bar-Eli, H. Linshitz, and T. R. Tuttle, Jr., J. Chem. Phys., 40, 3729 (1964).
- 52. M. Ottolenghi and H. Linshitz, p. 149 in Ref. 14.
- 53. J. L. Dye, L. R. Dalton, and E. M. Hansen, Abstracts, 149th National Meeting of the American Chemical Society (April 1965), p. 455.
- 54. Ian Hurley, T. R. Tuttle, Jr. and Sidney Golden, J. Chem. Phys., 48, 2818 (1968).
- 55. Marc G. DeBacker, personal communication.
- 56. J. L. Dye and R. R. Dewald, <u>J. Phys. Chem.</u>, <u>68</u>, 135 (1968).
- 57. A. Debierne, <u>Ann. Physique (Paris)</u>, <u>2</u>, 97 (1914).
- 58. D. E. Lea, "Actions of Radiation on Living Cells," The Macmillan Co., New York, p. 47 (1947).
- 59. G. Stein, <u>Disc. Fara. Soc.</u>, <u>12</u>, 227 (1952).

- 60. R. L. Platzman, "Physical and Chemical Aspects of Basic Mechanisms in Radiobiology," U. S. Nat. Research Council, Pub. No. 305, pp. 22-50 (1953).
- 61. A. O. Allen, "The Radiation Chemistry of Water and Aqueous Solutions," Van Nostrand, Princeton, 1961.
- 62. N. F. Barr and A. O. Allen, J. Phys. Chem., 63, 928 (1959).
- 63. E. Hayon and J. J. Weiss, J. Chem. Soc., 5091 (1960).
- 64. J. H. Baxendale and G. Hughes, Z. Phys. Chem. (Frankfurt), 14, 306 (1958).
- 65. G. Czapski and H. A. Schwartz, <u>J. Phys. Chem.</u>, <u>66</u>, 471 (1962).
- 66. F. S. Dainton, E. Collinson, D. R. Smith, S. Tazuké, Proc. Chem. Soc., 140 (1962).
- 67. E. J. Hart and J. Boag, <u>J. Am. Chem. Soc.</u>, <u>84</u>, 4090 (1962).
- 68. J. Boag and E. J. Hart, Nature (London), 197, 45 (1963).
- 69. M. Anbar and P. Neta, <u>Int. J. Appl. Radiat. Isotopes</u>, <u>18</u>, 493 (1967).
- 70. E. J. Hart, S. Gordon and E. M. Fielden, <u>J. Phys. Chem.</u>, 70, 150 (1966).
- 71. M. S. Matheson and J. Rabani, <u>J. Phys. Chem.</u>, <u>69</u>, 1324 (1965).
- 72. J. Rabani, p. 242 in Ref. 14.
- 73. M. Anbar, p. 64, in Ref. 14.
- 74. L. M. Dorfman and I. A. Taub, <u>J. Am. Chem. Soc.</u>, <u>85</u>, 2370 (1963).
- 75. E. A. Shaede and D. C. Walker, "The Alkali Metals," Spec. Pub. No. 22, The Chemical Society, London (1967).
- 76. D. C. Walker, Can. J. Chem., 45, 807 (1967).
- 77. R. W. Ahrens, B. Suryanarayana and J. E. Willard, <u>J. Phys.</u> Chem., <u>68</u>, 2947 (1964).
- 78. D. M. Compton, J. F. Bryant, R. A. Cesena and B. L. Gehman, in "Pulse Radiolysis," M. Ebert, J. P. Keene, A. J. Swallow and J. H. Baxendale, Ed., Academic Press, London and New York, 1965, p. 43.

- 79. B. Ward, Advances in Chemistry Series, 81, "Radiation Chemistry," Vol. I, R. F. Gould, Ed., American Chemical Society, Washington, D. C., 1968, p. 601.
- 80. M. C. Sauer, Jr., S. Arai and L. M. Dorfman, <u>J. Chem.</u> Phys., <u>42</u>, 708 (1965).
- 81. L. M. Dorfman, p. 36 in Ref. 14.
- 82. J. P. Keene, Rad. Res., 22, 1 (1964).
- 83. M. S. Matheson, p. 47 in Ref. 14.
- 84. J. H. Baxendale, Rad. Res. Suppl., 4, 139 (1964).
- 85. K. H. Schmidt and W. L. Buck, Science, 151, 70 (1966).
- 86. R. R. Hentz, Farhataziz, D. J. Milner and M. J. Burton, J. Chem. Phys., 47, 374 (1967).
- 87. J. Rabani, W. A. Mulac and M. S. Matheson, <u>J. Phys. Chem.</u>, 69, 53 (1965).
- 88. J. Jortner, Rad. Res. Suppl., 4, 24 (1964).
- 89. R. R. Dewald, Ph. D. Thesis, Michigan State University, 1963.
- 90. (a) L. H. Feldman, Ph. D. Thesis, Michigan State University, 1966; (b) L. H. Feldman, R. R. Dewald, and J. L. Dye, p. 163 in Ref. 14.
- 91. K. Keskey, S. Spleet and J. L. Dye, unpublished results.
- 92. M. A. Elfroymson in "Mathematical Methods for Digital Computers," A. Ralston and Herbert S. Wilf, Eds., John Wiley and Sons, Inc., 1964.
- 93. R. N. Jones, Can. J. Chem., 44, 3031 (1966).
- 94. W. E. Wentworth, <u>J. Chem. Ed.</u>, <u>42</u>, 96, 162 (1965).
- 95. W. C. Hamilton, "Statistics in Physical Science," Ronald Press Co., New York, N. Y., 19, ch. 4.
- 96. Kuo, "Numerical Methods and Computers," Academic Press, New York, N. Y., 1965.
- 97. R. R. Dewald, J. L. Dye, M. Eigen, L. DeMaeyer, J. Chem. Phys., 39, 2388 (1963).

- 98. R. Catterall, personal communication, 1968.
- 99. J. S. Waugh, Ed., "Advances in Magnetic Resonance," Vol. 1, Academic Press, New York, N. Y., 1965.
- 100. J. L. Dye, Weyl Collogium II, Cornell University, June 1969, Ithaca, New York.
- 101. R. R. Dewald and J. H. Roberts, <u>J. Phys. Chem.</u>, <u>72</u>, 4224 (1968).
- 102. S. Matalon, S. Golden and M. Ottolenghi, <u>J. Phys. Chem.</u>, <u>73</u>, 3098 (1969).
- 103. R. R. Dewald and J. H. Roberts, <u>J. Phys. Chem.</u>, <u>72</u>, 4224 (1968).
- 104. M. DeBacker, personal communication.
- 105. I. A. Taub, D. A. Harter, M. C. Sauer, Jr., and L. M. Dorfman, <u>J. Chem. Phys.</u>, <u>41</u>, 979 (1964).



#### APPENDIX A

# A DETAILED DERIVATION OF THE RATE EQUATION FOR THE MECHANISM DESCRIBED IN SECTION IV

Any assumptions made in this derivation will be so noted. The derivation will be divided into two parts, one for the rate expression for the case of the reaction of cesium with water and the other for the reaction of rubidium or potassium with water. Although the two cases differ in principle, it will be seen that the general form of the rate expression in each case is the same.

## Case I: Cesium and water. The necessary equilibria are:

$$M^{-} \xrightarrow{K_{1}} M + e^{-}$$
 (1A)

$$M \stackrel{K_2}{\longrightarrow} M^+ + e^- \tag{2A}$$

$$M^{+} + OH^{-} \xrightarrow{K_{3}} MOH$$
 (3A)

$$M^- + M^+ \xrightarrow{K_4} M_2 \tag{4A}$$

In the above equations, all species are understood to be solvated. For reasons discussed in Section IV, the slow step in the reaction is assumed to be the bimolecular reaction of the reducing species with water, which may be represented

by the following reaction.

$$M^- + H_2O \xrightarrow{k_{M^-}} [Intermediates] \xrightarrow{H_2O} H_2 + M^+ + OH^-$$
 (5A)

$$M_2 + H_2O \xrightarrow{k_{M_2}} [Intermediates] \xrightarrow{H_2O} H_2 + 2M^+ + 2OH^-$$
 (6A)

$$M + H_2O \xrightarrow{k_M} [Intermediates] \xrightarrow{H_2O} \frac{1}{2} H_2 + M^+ + OH^-$$
 (7A)

$$e^- + H_2O \xrightarrow{k_{e^-}} [Intermediates] \xrightarrow{H_2O} \frac{1}{fast} + OH^-$$
 (8A)

The concentration of total metal is

$$[M_{T}] = [e^{-}] + [M] + 2[M^{-}] + 2[M_{2}]$$
 (9A)

and the rate of hydrogen formation is

$$\frac{d[H_2]}{dt} = -\frac{1}{2} \frac{d[^MT]}{dt} = \left\{ k_M - [M^-] + k_{M_2} [M_2] + \frac{k_M}{2} [M] + \frac{k_{e^-}}{2} [e^-] \right\} [H_2O] \quad (10A)$$

The concentrations of  $e^-$ ,  $M_2$  and M are obtained from inspection of the equilibria listed above, and are given by

$$[e^{-}] = (\frac{K_1 K_2}{[M^{+}]})^{\frac{1}{2}} [M^{-}]^{\frac{1}{2}}$$
 (11A)

$$[M_2] = K_4 [M^+] [M^-] \gamma_+^2$$
 (12A)

and

$$[M] = \left(\frac{K_1}{K_2}\right)^{\frac{1}{2}} [M^+]^{\frac{1}{2}} [M^-]^{\frac{1}{2}} \gamma_{\pm}^2 \qquad (13A)$$

Since the total absorbance,  $A_{\overline{\mathbf{T}}}$ , is measured as a function of time, it is defined as

$$A_{T} = A_{M} + A_{e^{-}} + A_{M^{-}} + A_{M_{2}}$$
 (14A)

and for convenience let

$$A_{M} + A_{e^{-}} = A_{p} \tag{15A}$$

and

$$A_{M_2} + A_{M^-} = A_D \tag{16A}$$

Where  $A_p$  is the absorbance due to the paramagnetic species M and  $e^-$  and  $A_D$  is the absorbance due to the diamagnetic species  $M_2$  and  $M^-$ . Equation 14A now becomes

$$A_{T} = A_{P} + A_{D} \tag{17A}$$

Expressing the total absorbance in terms of the extinction coefficients and concentrations of the species gives

$$A_{T} = \epsilon_{e^{-}}[e^{-}] + \epsilon_{M}[M] + \epsilon_{M^{-}}[M^{-}] + \epsilon_{M_{2}}[M_{2}]$$
(18A)

and substituting the expression for [M] and  $[M_2]$  into Equation 18A yields,

$$A_{T} = \{ \epsilon_{e^{-}} + \epsilon_{M} [M^{+}] \gamma_{\pm}^{2} / K_{2} \} [e^{-}] + \{ \epsilon_{M^{-}} + \epsilon_{M_{2}} K_{4} [M^{+}] \gamma_{\pm}^{2} \} [M^{-}]$$
 (19A)

Identification of terms in Equation 19A with those in Equation 17A above shows that

$$A_{p} = \{ \epsilon_{p} + \epsilon_{M} [M^{+}] \gamma_{+}^{2} / K_{2} \} [e^{-}] = q [e^{-}]$$
 (20A)

and

$$A_{D} = \{ \epsilon_{M^{-}} + \epsilon_{M_{0}} K_{4} [M^{+}] \gamma_{+}^{2} \} [M^{-}] = r [M^{-}]$$
 (21A)

where q and r are constants at fixed values of  $[M^+]$  and ionic strength and have obvious definitions. The time

derivatives of  $A_{\mathbf{p}}$  and  $A_{\mathbf{D}}$  are

$$\frac{dA_p}{dt} = q \frac{d[e]}{dt}$$
 (22A)

and

$$\frac{dA_D}{dt} = r \frac{d[M^-]}{dt}$$
 (23A)

subject to the condition that

$$\frac{dA_{T}}{dt} = \frac{dA_{P}}{dt} + \frac{dA_{D}}{dt}$$
 (24A)

Note that in taking the time derivatives of  $A_p$  and  $A_D$ , the time derivatives of q and r are assumed to be zero. Inspection of the definitions of q and r show that the quantity  $\frac{d[M^+]}{dt}$  is taken to be zero. Substitution of the values of [e<sup>-</sup>] and [M<sup>-</sup>] from Equations 20A and 21A into Equation 11A gives a relationship between  $A_p$  and  $A_D$ , which after simplification is

$$A_{D} = \left\{ \frac{r \left[M^{+}\right] \gamma_{\pm}^{2}}{K_{\perp} K_{2} q^{2}} \right\} A_{P}^{2}$$
 (25A)

The derivation from this point on is concerned with deriving an explicit expression for the decay of the total absorbance with time.

The rate of disappearance of total metal is

$$\frac{d[M_T]}{dt} = \frac{d[e^-]}{dt} + \frac{d[M]}{dt} + 2\frac{d[M^-]}{dt} + 2\frac{d[M_2]}{dt}$$
 (26A)

Substitution of the expressions for  $\frac{d[M_2]}{dt}$  and  $\frac{d[M]}{dt}$ ,

obtained from differentiation of Equations 11A, 12A and 13A, into Equation 26A gives

$$\frac{d[M_T]}{dt} = \{1 + [M^+] \gamma_{\pm}^2 / K_2\} \frac{d[e^-]}{dt} + 2 \{1 + K_4 [M^+] \gamma_{\pm}^2\} \frac{d[M^-]}{dt}$$
(27A)

Upon substitution of the expressions for  $\frac{d[e^-]}{dt}$  and  $\frac{d[M^-]}{dt}$  from Equations 22A and 23A, Equation 27A becomes

$$\frac{d[M_T]}{dt} = \left\{ \frac{1 + [M^+] \gamma_{\pm}^2 / K_2}{q} + \frac{4[M^+] \gamma_{\pm}^2 (1 + K_4[M^+] \gamma_{\pm}^2) A_P}{K_1 K_2 q^2} \right\} \frac{dA_P}{dt}$$
(28A)

Now, the rate of disappearance of total metal may also be written

$$-\frac{d[M_T]}{dt} = k'_{e} - [e^-] + k'_{M}[M] + 2k'_{M} - [M^-] + 2k'_{M_2}[M_2]$$
 (10A)

where for convenience

$$k_x' = k_x [H_2O]$$

Substitution of the expressions for [M] and [M2] (Equations 11A, 12A, 13A) into Equation 10A yields

$$-\frac{d[M_T]}{dt} = \{k_{e^-} + k_{M}^{\dagger}[M^{\dagger}]\gamma_{\pm}^2/K_2\} \quad [e^-] + 2\{k_{M^-}^{\dagger} + k_{M_2}^{\dagger}K_4[M^{\dagger}]\gamma_{\pm}^2\} \quad [M^-]$$
(29A)

which upon substitution of the expressions for [e] and [M] (Equations 20A and 21A) becomes

$$\frac{d [M_T]}{dt} = -\left\{ \frac{(k_e^{\dagger} - + k_M^{\dagger} [M^{\dagger}] \gamma_{\pm}^2 / K_2)}{q} A_P + 2 \frac{(k_M^{\dagger} - + k_M^{\dagger} K_4 [M^{\dagger}] \gamma_{\pm}^2)}{r} A_D \right\}$$
(30A)

The expression for  $\frac{d^Ap}{dt}$  is obtained by equating 28A and 30A and solving for  $\frac{d^Ap}{dt}$  . The result, after

simplification, is

$$-\frac{dA_{p}}{dt} = \frac{\frac{(k_{e}^{1} + k_{M}^{1} [M^{+}] \gamma_{\pm}^{2} / K_{2})}{q} A_{p} + 2 \frac{(k_{M}^{1} - k_{M}^{1} K_{4} [M^{+}] \gamma_{\pm}^{2})}{r} A_{p}}{\left\{\frac{1 + [M^{+}] \gamma_{\pm}^{2} / K_{2}}{q} + 4 \frac{[M^{+}] \gamma_{\pm}^{2} (1 + K_{4} [M^{+}] \gamma_{\pm}^{2})}{K_{1} K_{2} q^{2}} A_{p}\right\}} (31A)$$

The time derivative of Equation 25A is

$$\frac{dA_D}{dt} = 2 \frac{A_D}{A_D} \frac{dA_P}{dt} = \frac{2 A_P r [M^{\dagger}] \gamma_{\pm}^2}{K_1 K_2 q^2} \frac{dA_P}{dt}$$
(32A)

Substitution of the expression for  $\frac{dAp}{dt}$  from Equation 31A into Equation 32A gives the expression for  $\frac{dA_D}{dt}$ , which after simplification is

$$-\frac{dA_{D}}{dt} = \frac{2r \left[M^{+}\right] \gamma_{\pm}^{2}}{K_{1}K_{2}q^{3}} \frac{(k_{e}^{+} + k_{M}^{+} \left[M^{+}\right] \gamma_{\pm}^{2} / K_{2}) A_{p}^{2} + 4 \left[M^{+}\right] \gamma_{\pm}^{2} (k_{M}^{+} + k_{M}^{+} K_{4})}{\left[M^{+}\right] \gamma_{\pm}^{2} / A_{p}^{A} A_{D}}$$

$$-\frac{\left[M^{+}\right] \gamma_{\pm}^{2} / A_{p}^{A} A_{D}}{K_{1}K_{2}q^{2}}$$

$$\frac{1 + \left[M^{+}\right] \gamma_{\pm}^{2} / K_{2}}{q} + \frac{4 \left[M^{+}\right] \gamma_{\pm}^{2} (1 + K_{4} \left[M^{+}\right] \gamma_{\pm}^{2})}{K_{1}K_{2}q^{2}} A_{p}$$
(33A)

Recalling that

$$\frac{dA_{T}}{dt} = \frac{dA_{p}}{dt} + \frac{dA_{D}}{dt}$$
 (24A)

and using the expression for  $\frac{dA_D}{dt}$  and  $\frac{dA_p}{dt}$  derived above, one form of the expression for the rate of decay of the total absorbance is, after simplification,

$$-\frac{dA_{T}}{dt} = \frac{\left\{2r\left(k_{e}^{+} + k_{M}^{+}\left[M^{+}\right]\gamma_{\pm}^{2}/K_{2}\right)\frac{A_{P}}{A_{D}} + 4q\left(k_{M}^{+} + k_{M2}^{+}K_{4}\left[M^{+}\right]\gamma_{\pm}^{2}\right)\right\}\left(A_{D} + \frac{A_{P}}{2}\right)}{r\frac{A_{P}}{A_{D}}\left(1 + \left[M^{+}\right]\gamma_{\pm}^{2}/K_{2}\right) + 4q\left(1 + K_{4}\left[M^{+}\right]\gamma_{\pm}^{2}\right)}$$
(34A)

Equations 31A and 33A can be further simplified by using the three assumptions discussed in Section IV. These assumptions are:

(i) The rate of reaction of e with water is assumed to be approximately equal to that of M\_with water. Similarly the rate of reaction of M with water is assumed to be approximately equal to that of M<sub>2</sub> with water. The results of these assumptions are

$$k_{e}^{\prime} = k_{M}^{\prime}$$

and

$$k_{\mathbf{M}}^{\mathbf{I}} \cong k_{\mathbf{M}_{2}}^{\mathbf{I}}$$

(ii) The ion pair association constants  $K_2$  and  $K_4$  are assumed to be approximately equal, so that

$$K_2 \cong 1/K_4$$

(iii) The extinction coefficients of the various species are assumed to be related by the stoichiometries of the species, thus

$$\epsilon_{e}^- = \epsilon_{M} = \frac{1}{2} \epsilon_{M}^- = \frac{1}{2} \epsilon_{M_2}$$

The simplification gives

$$-\frac{dA_{D}}{dt} = \frac{2k_{e}^{!} - A_{D} + k_{M}^{!} - A_{D}^{2}/A_{P}}{1 + 2 A_{D}/A_{P}}; -\frac{dA_{P}}{dt} = \frac{k_{e}^{!} - A_{P} + k_{M}^{!} - A_{D}/2}{1 + 2 A_{D}/A_{P}}$$
(35A)

These coupled differential equations were used to fit the cesium data subject to Equation 17A by a non-linear least squares procedure. <u>Case II</u>: As discussed in Section IV, when Equation 35A was used to attempt fitting the cesium data, it was apparent that a better fit of the data could be obtained using only the three parameters  $k_{M}^{I}$ ,  $A_{P}^{O}$  and  $A_{D}^{O}$ . This corresponds to the case where there is no direct reaction of  $e^{-}$  or M with water (i.e.,  $k_{e^{-}}^{I} = k_{M}^{I} = 0$ ). The derivation of the rate equation for this case is the same as that for Case I but with  $k_{e^{-}}^{I} = k_{M}^{I} = 0$ . The resulting differential equations now have the form

$$-\frac{dA_{D}}{dt} = \frac{k_{M}^{1} - A_{D}^{2}/A_{P}}{1 + 2 A_{D}/A_{P}}; -\frac{dA_{P}}{dt} = \frac{k_{M}^{1} - A_{D}/2}{1 + 2 A_{D}/A_{P}}$$
(36A)

Case III: Rubidium (or potassium) with water. This is the case of the reaction of metal solutions which possess an intermediate R-band in addition to the IR-band. This fact necessitates the inclusion of one additional equilibrium. This equilibrium has the form

$$R \stackrel{K_5}{\longrightarrow} IR \tag{37A}$$

Since experimental evidence points to the fact that the R species is a two electron species (see Sections I and IV), it is assumed to be in direct equilibrium with the two electron "aggregate" species of the IR-band. That is

$$R \stackrel{K_5}{\longleftarrow} M^- (\text{or } M_2) \tag{38A}$$

so that

$$r = \frac{[M^-]}{K_5} \tag{39A}$$

The following discussion will assume that the R species is in direct equilibrium with  $M^-$  although the derivation is the same if the R species is in equilibrium with  $M_2$ .

The expression for the total absorbance now becomes

$$A_{T} = A_{P} + A_{D} + A_{R}$$
 (40A)

where  $A_p$  and  $A_D$  have the same meanings as before and  $A_R$  is the absorbance due to the R species. For convenience let

$$A_{D} + A_{R} = A_{D}^{\prime} \tag{41A}$$

So that

$$A_{\mathbf{T}} = A_{\mathbf{p}} + A_{\mathbf{D}} \tag{42A}$$

also

$$A_{D}^{\prime} = r^{\prime} [M^{-}] \tag{43A}$$

where r' has the definition

$$\mathbf{r'} = \mathbf{r} + \frac{\epsilon_{\mathbf{R}}}{\kappa_{5}} = \epsilon_{\mathbf{M}^{\perp}} + \epsilon_{\mathbf{M}_{2}} \kappa_{4} \left[\mathbf{M}^{+}\right] \gamma_{\pm}^{2} + \frac{\epsilon_{\mathbf{R}}}{\kappa_{5}} \tag{44A}$$

The expression for the rate of disappearance of total metal is

$$-\frac{d[M_T]}{dt} = 2 k_{M-}^{'}[M^{-}] + 2 k_{M_2}^{'}[M_2] + 2k_{R}^{'}[R] + k_{e-}^{'}[e^{-}] + k_{M}^{'}[M]$$
(45A)

and also

$$\frac{d\left[M_{T}\right]}{dt} = \frac{2d\left[M\right]}{dt} + \frac{2d\left[M\right]}{dt} + \frac{2d\left[R\right]}{dt} + \frac{d\left[e\right]}{dt} + \frac{d\left[M\right]}{dt}$$
(46A)

From this point on, the derivation is algebraically equivalent to that for Case I. The final expression for the rate of decay of the total absorbance is similar in form to that for Case I. It is

$$-\frac{dA_{T}}{dt} = \left\{ k_{e}^{i} - \frac{A_{P}}{A_{D}^{i}} + k_{M}^{i} - \left\{ \frac{1 + K_{4} [M^{+}] \gamma_{\pm}^{2} + k_{R}^{i} / k_{M}^{i} - K_{5}}{1 + K_{4} [M^{+}] \gamma_{\pm}^{2} + 1 / K_{5}} \right\} \right\} \frac{A_{P} + \frac{1}{2} A_{D}^{i}}{1 + \frac{A_{P}}{2A_{D}^{i}}}$$

$$(47A)$$

For the case that  $k_{e^-}^{\, \prime} = k_M^{\, \prime} = 0$ , the above equation has the form

$$-\frac{dA_{T}}{dt} = \left\{k_{M}^{\dagger} - \frac{\left[1 + K_{4} \left[M^{\dagger}\right] \gamma_{\pm}^{2} + k_{R}^{\dagger} / k_{M}^{\dagger} - K_{5}\right]}{1 + K_{4} \left[M^{\dagger}\right] \gamma_{\pm}^{2} + 1 / K_{5}}\right\} \frac{A_{P} + \frac{1}{2} A_{D}^{\dagger}}{1 + \frac{A_{P}}{2A_{D}^{\dagger}}}$$
(48A)

#### APPENDIX B

#### DESCRIPTION OF COMPUTER PROGRAM FOR ANALYZING DATA

The computer program used to analyze data in this research was designed primarily to handle kinetic data punched on IBM cards using a Varian C-1024 Time Averaging Computer (CAT). However, the program was written with enough flexibility to accept manually punched kinetic data of the appropriate format.

The principle advantage of this program is its ability to test a number of possible mechanisms. The user has the option of comparing any kinetic mechanism to any set of kinetic data. The best least squares fit of the data of the mechanism can be obtained provided that the necessary information about the mechanism has been supplied to the program.

A block diagram of the general sequence of operation of the Program Kenanal is given in Figure 31. A description of the necessary subroutines and the function of each is given at the end of this Appendix.

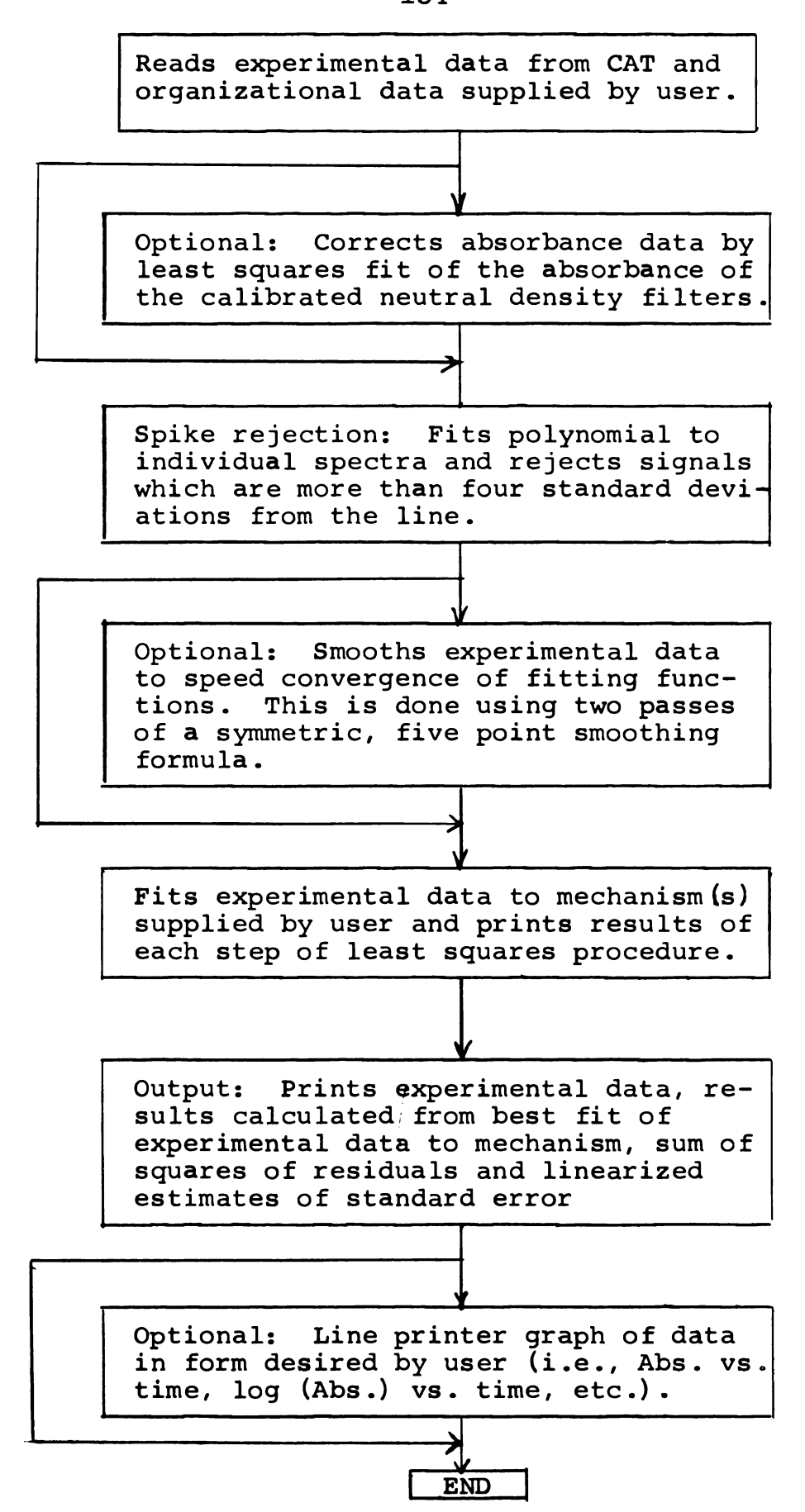


Figure 31. Operational block diagram of program KENANAL.

The following is a functional description of the subroutines used with Program KENANAL.

#### KENANAL

This is the main program from which all of the subroutines are called. The principal function of the main program is the reading and organization of the data necessary
for the subroutines.

#### **ABSCOR**

This is a subroutine for calibration of the neutral density filter data. A polynomial fit of the neutral density filter is performed. This polynomial has the form:

$$\frac{\text{(Abs.)}}{\text{(Abs.)}} = f(\text{Abs.)}$$

where (Abs.) obs. is the absorbance read from CAT and Abs. is the calibrated absorbance of the neutral density filter. This polynomial is then used later in the program to correct the experimental absorbances. (The use of this absorbance correction is optional.)

#### **MEKANISM**

This subroutine contains the information about the mechanism or mechanisms to be used in analyzing the kinetic data. At present, the program can be expanded to analyze up to twenty-five different mechanisms for a given set of experimental data. A control card supplied by the user

selects the mechanisms to be used. Also contained in MEKANISM are the initial values of the parameters used in fitting a particular mechanism to a set of data. Mechanisms may be added by the user as needed.

#### MULTREG

This is a subroutine which performs linear multiple regression analysis (92). It can only be used when the equation is linear in the adjustable parameters. This subroutine was programmed by John Bartelt.

### CURVEFIT

This is a non-linear least squares subroutine which will fit an equation to a set of experimental data. This routine was written by Vince Nicely, using the ideas found in papers by Jones (93) and Wentworth (94). This subroutine also calculates the relevant statistics for estimating the goodness of the fit of given equation to a set of experimental data. The basis for the statistics used in this subroutine can be found in Hamilton (95). To use this subroutine, the user must also supply subroutines FN and SIMUL3.

#### SIMUL3

This is a subroutine which inverts matrices using the Gauss elimination method. It was written by Duane Knirk.

#### FN

This subroutine contains the functional form of the equations to be used by CURVEFIT for least squares analysis.

### RUNGE

This subroutine performs Runge-Kutta integrations and is necessary only when the rate equations cannot be integrated analytically. This subroutine is essentially that described by Kuo (96).

#### APPENDIX C

# OBSERVATION OF PYRAZINE ANION IN DECOMPOSED RUBIDIUM-ETHYLENEDIAMINE SOLUTIONS

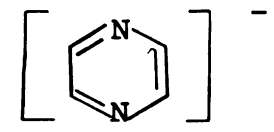
One interesting but annoying experiment was inadvertently performed during the course of this work. In several attempts to prepare solutions of rubidium in ethylenediamine, a competitive reaction was noted. As the solvent was thawed and allowed to come into contact with the rubidium metal, a purple color was observed instead of the usual blue color.

In one of the three observations of this phenomenon, the purple color disappeared or was obscured by the formation of the blue solution. However, when this blue solution was mixed with ethylenediamine in the stopped-flow system, using the rapid scanning monochromator, a fast decay of the 890 nm band resulted and a purple solution formed. This purple solution had an optical absorption in the visible at 520 nm. The absorbance at the maximum grew from 0.2 to 0.85 over a period of twenty-five minutes.

In two other attempted solution preparations using rubidium metal, only a transient blue color was observed in the solution, which was not stabilized by further dissolution of the metal. The resulting solution had a deep purple color.

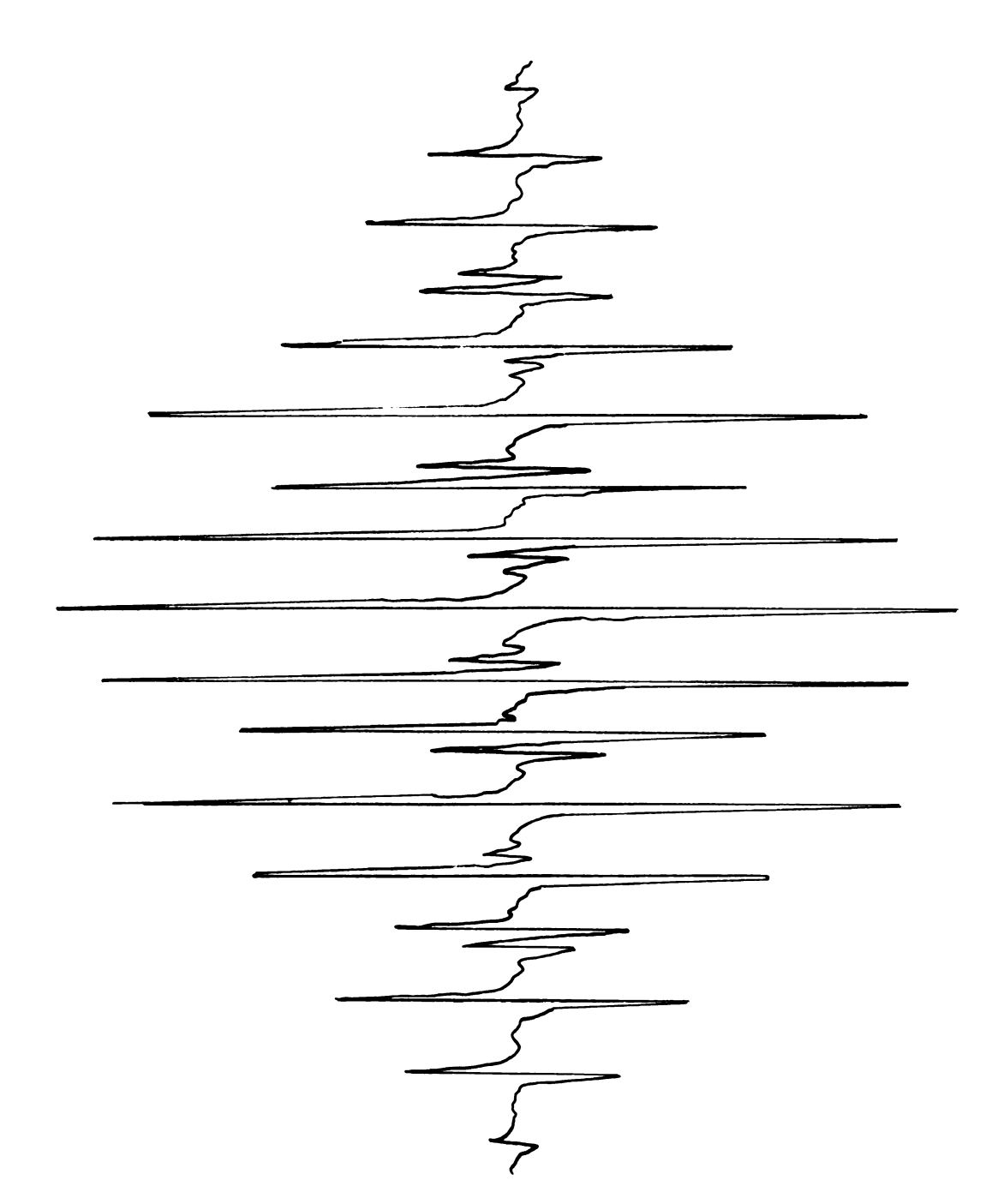
A small amount of this purple solution was poured, in vacuo, into an ESR tube and the X-band EPR spectrum of the solution was examined using a Varian V4500 EPR spectrometer. The solution was found to be paramagnetic. Its EPR spectrum is shown in Figure 32. This spectrum yields splitting values of 2.6 and 6.9 gauss. An optical spectrum was taken on a Cary 14 spectrophotometer and one peak was observed at 525 nm.

It was suggested that the EPR spectrum resembled that of an aromatic negative ion such as anthracene or naphthalene negative ion (98), but the splitting values were not in agreement. A search of the literature, revealed that the spectrum agreed well with that observed for pyrazine negative ion,



The two splitting values given in the literature for the negative ion are 2.66 and 7.1 gauss (99). No data on the optical spectrum of the pyrazine negative ion were available in the literature.

The vapor above the purple solution was found to consist of two major components. This was determined by vapor phase chromatography, using an Aerograph Model A-90-P gas chromatograph. A five foot column, packed with 15% Tetraethylenepentamine and 5% THEED (Tetra-hydroxy-ethyl ethylenediamine)



EPR spectrum of the pyrazine anion formed in decomposed rubidium-ethylenediamine solutions. Figure 32.

was used for this determination. The two components were identified as ammonia and ethylenediamine. It is likely that the reaction by which the pyrazine is formed has ammonia as one of its products.

The exact mechanism for the formation of pyrazine is not clear although it probably results from ring condensation of 2 species having the carbon skeleton of ethylenediamine. The first step in the overall process probably involves the formation of an abla-free radical of the solvent,

$$NH_2$$
 -  $CH_2$  -  $\dot{C}H$  -  $NH_2$ 

The actual ring condensation, mentioned above, also would produce ammonia. After the pyrazine is formed, it then attaches an electron as  $e_{sol}^- + \left( \begin{array}{c} N \\ N \end{array} \right) \longrightarrow \left( \begin{array}{c} N \\ N \end{array} \right)$  to form the ammonia which was identified as a product. The mechanism of this reaction bears further investigation since it seems to be important to the chemistry of metal-amine solutions.

HICHIGAN STATE UNIV. LIBRARIES
31293101561607